DEXTROMETHORPHAN AND ITS METABOLITES IN RAT BONE TISSUES BY GAS CHROMATOGRAPHY-MASS SPECTROMETRY ANALYSIS FOLLOWING DIFFERENTIAL MICROCLIMATE DECOMPOSITION

Author: Kirk Unger

Submitted in Partial Fulfillment of the Course FORS 4095

Department of Forensic Science

Laurentian University

Sudbury, ON P3E 2C6

Kirk A. Unger and James H. Watterson

Dextromethorphan and its Metabolites in Rat Bone Tissues by Gas Chromatography Mass Spectrometry Analysis Following Differential Microclimate Decomposition

ABSTRACT:

The effect of microclimate on dextromethorphan (DXM) and dextrorphan (DXT) responses in skeletonized rat remains was examined. Animals (n=10) received dextromethorphan at 75 mg/kg by i.p. injection for comparison against drug-free controls (n=4), and across different decomposition sites. Rats were divided equally into two groups and placed at different sites for decomposition immediately following euthanasia (30 minutes post dose). Rats at Site A decomposed in a shaded forest microenvironment on a grass-covered soil substrate. Site B animals rested on rock and gravel substrate exposed to open air and direct sunlight. Site A and Site B are approximately 600 m apart. Ambient temperature and relative humidity measurements recorded by data loggers mounted 3 cm above rats at each site established microclimate differences. Bone elements (vertebrae, ribs, pelvic girdles, femora, tibiae, humeri and scapulae) were harvested, cleaned and pulverized for Microwave Assisted Extraction in methanol. Drug and metabolite extractions were isolated by solid phase extraction prior to GC/MS analyses. Mass normalized DXM and DXT levels and metabolite/drug ratios were compared across different bone elements (within and between animals) and microclimate sites. Concentrations calculated from drug responses and standard curve plots gave estimated concentrations of 399 to 10,474 ng/g for DXM and 132 to 3,668 ng/g for DXT. Max/min values across animals and bone elements examined response variation. No significant differences in DXT levels or metabolite/parent ratios were observed between sites or across different bone elements. The only significant difference for DXM levels were found in femurs compared across microclimate sites. Microclimate showed no significant influence on observed DXM or DXT values, indicating bone as a drug reservoir may behave uniformly for certain drugs across different environments of decomposition. The results of this study show limited agreement with previous work from our laboratory on drug recoveries from decomposed bone tissues.

KEYWORDS: Blood, Decomposed Bone, Dextromethorphan, Dextrorphan, Forensic Toxicology, GC/MS, Microclimate, MAE, SPE.

ACKNOWLEDGEMENTS

The author is grateful to the Natural Sciences Engineering Research Council of Canada for their financial support of this work and would like to thank Dr. Gerard Courtin and Dr. Jackie Litzgus for the use of their environmental instruments. Heather Cornthwaite and Courtney Campbell are acknowledged for their collaboration during the study. Above all, many thanks are owed to Dr. James Watterson for his instruction throughout this research.

TABLE OF CONTENTS

LIST OF TABLES

LIST OF FIGURES

GLOSSARY

ACU	Acute Dose
AH	Absolute Humidity
CV%	Coefficient of Variance
CYP	Cytochrome Enzymes
DXM	Dextromethorphan
DXT	Dextrorphan
dmDXT	3-hydroxymorphinan
GC	Gas Chromatography
GC/MS	Gas Chromatography/Mass Spectrometry
i.p.	Intraperitoneal Injection
LOD	Limit of Detection
LOQ	Limit of Quantification
MAE	Microwave Assisted Extraction
RH%	Relative Humidity
RR/m	Mass Normalized Response Ratio
SIM	Selected Ion Monitoring
SPE	Solid Phase Extraction
V_d	Volume of Distribution

CHAPTER 1

INTRODUCTION AND BACKGROUND

1.1 Introduction

Toxicological analysis of bone tissue may be considered in cases of advanced decomposition or post-mortem manipulation of remains where blood or other tissues and fluids are not present or degraded beyond toxicological use. Toxicological analysis of human bone has been performed in cases of work-place or environmental exposure to toxins (1–4) and for drugs in a number of forensic cases (5–8) using a variety of bone tissues and analyses. Though drug detection in post-mortem bone tissues is possible, interpretation of drug-in-bone analysis is difficult given the number of factors that determine drug deposition in bone and dearth of research and casework (8). Recent studies from our laboratory and others have measured drug exposure in bone using animal models and have established differences in drug distributions within bone elements, between acute vs. repeated doses and by environment of decomposition (9–18). Only one study has compared drug responses in bone after surficial decomposition across different microclimate environments (18) by gas chromatography-mass spectrometry (GC/MS) analysis for ketamine and metabolites. Environmental conditions have been shown to control the rate and degree of decomposition which influences and is reflected by the degree of insect activity , the production of putrefaction products (19) and extent of bioerosion of bone tissues by microorganisms (20), the effects of climate on drugs in bone following advanced surficial decomposition is largely unknown.

1.2 Drug Detection in Skeletal Tissues

Drugs and their metabolites have been detected in human bone tissues using various methods of extraction. Amitriptyline (5) was detected by GC/MS analysis in vertebral marrow following extraction by warm ethanol and a series of liquid-liquid extractions (LLE). GC/MS

detection of methamphetamine followed LLE and SPE treatment of ethyl ether extraction from femoral marrow (6). GC/MS instrumentation detected triazolam in femoral marrow following digestion in 2M sodium hydroxide, extraction in tert-butyl methyl ether and a series of LLE (21). Citalopram was extracted from iliac crest sections by soaking the bone in methanol and was isolated by LLE prior to GC/MS analysis (22). A broader study demonstrated a number of forensically relevant drugs and their metabolites (amitriptyline, citalopram, meperidine, oxycodone, diazepam, codeine, cocaine and others) can be detected in bone tissues by GC/MS using a methanolic extraction (8). This study also compared bone responses to blood and found no appreciable relationship, though chronic exposure was speculated to lead to the presence of drug in bone tissues, especially where none was present in blood (8).

The stability of a given drug in post-mortem tissues is an important factor to be considered, and sample selection should be done with this in mind. Though bone tissues offer the potential for qualitative analyses, post-mortem drug redistribution and stability, among a number of other factors, make the interpretation and quantification of post-mortem analyses of drugs in bone complicated and challenging (23). A study in the temporal fate of drugs in pig remains showed drug concentrations in soft tissues increased as tissues decomposed (24); maggots feeding on the remains were shown to have detectable levels of drugs within a few days and remained detectable in soil below the carcass for up to 2 years (24). Though this study did not analyze bone tissues, the results show that lipid or water solubility of the drugs may play important roles in drug distribution within remains that are exposed to surficial decomposition environments (24).

Because no clear relationship between drug-in-bone and blood concentration has been established, controlled experiments using animal models have explored bone tissues as a repository for drugs of forensic interest. Drug-in-bone interpretation is made even less clear because of the

lack of standardized methods used for the analysis of a given drug in bone tissue. The use of animal models allows for comparison of drugs, metabolites, doses, dose-death intervals and the time and environments of decomposition and can be used to establish standardized methods for drug-bone analysis and patterns useful in interpreting post-mortem drug-in-bone toxicological results.

1.3 Drugs in Animal Bone Tissues

Animal studies have shown bone tissues may be useful reservoirs for forensically relevant drugs across a number of bone tissue types, bone elements and ranges of post-mortem environments (10, 11, 13–18, 22). However, as in the above human bone analyses, methods can vary across animal model studies and lack standardization. Part of the work in our laboratory has been to establish consistent methods of analysis going towards a standardized way of analyzing animal bone tissues for drugs and metabolites.

Attempts to correlate drug concentrations in blood or plasma to those in bone have been made using animal studies. Desipramine in femoral and tibial marrow following repeated oral administration in rabbits was shown to be a good indicator of plasma concentration of the drug 90 minutes post-dose by High Performance Liquid Chromatography (HPLC) analysis (25). This study showed the potential of marrow as a suitable matrix for tricyclic antidepressant analysis in the absence of blood, however the timeframe of this study precludes such interpretations in cases of advanced decomposition where drug and marrow stability in bone matrices have serious questions to be addressed.

Morphine from rabbit marrow following intravenous (IV) injection was analyzed by immunoassay following 7 and 14 days of burial post dose for comparison to marrow, blood and urine morphine concentration and showed good correlation with perimortem blood-marrow opioid

levels even as the measured response of the drug in marrow decreased roughly 50% over the 14 day period (13). This study showed drug and/or marrow stability may influence recovered drug in marrow, and though blood-marrow correlation following burial was significant, though the study is limited by immunoassay techniques and further research using statistically valid numbers of samples and quantitative analytical methods is necessary.

In a study analyzing post-mortem morphine by GC/MS in mouse tissues, no such correlation between marrow-blood concentrations could be determined (26). This study compared repeated and acute doses of morphine in a variety of mouse tissues, and showed that the lipophilicity of the drug may influence post-mortem distribution, and that drug levels in bone following chronic vs. acute exposures can vary significantly (26). The stability of morphine in skeletal tissues was also shown to be a problem and was measured only below the Limit of Quantification (LOQ) after storage in soil after 2 months; though a blood-marrow correlation may exist, it was not shown in this study (26). Determining if a given exposure followed repeated morphine dosing could not be determined from the analysis of skeletal tissues, though an acute lethal dose might be detected (23). The results of this study go to illustrating the difficulties of interpreting post-mortem drug analysis from bone tissues. Metabolism can vary across species and individuals (27, 28), which effects the levels of certain metabolites used to quantify drugs in toxicological analyses. The route of administration (27) and chemical properties of the drugs will affect the uptake of the compound by bone tissues (29), the environment and position of the remains during post-mortem decomposition can influence the presence of drugs in individual bone elements (14, 17, 18, 30) and the paucity of research and lack of standardized methods make interpretation of drug-bone levels a risky prospect at best.

The inability to accurately quantify drug in bone tissues to doses or perimortem blood concentrations has led to different methods of toxicological study of bone tissues. In our laboratory, Watterson and colleagues have used mass-normalized response ratios (RR/m) and parent drug-metabolite ratios to investigate relative drug distribution across skeletal elements in order to assess the effects of repeated and acute doses and environments of decomposition (9, 11, 14, 16–18, 31).

A study of amitriptyline, citalopram, diazepam, morphine and pentobarbital in porcine skeletal tissues found that skeletal element type was a main effect of drug levels, with rib, femoral, vertebral and pelvic girdle tissues having the highest RR/m drug levels (16). The use of RR/m addresses the inability to accurately quantify drug concentrations in bone tissues since the sample matrix is a heterogeneous material and analyte recovery cannot be definitively quantified using techniques standard to forensic toxicology. The higher drug level in central cavity bones may indicate post-mortem redistribution from surrounding organs and tissues, illustrating the limits of interpretation of drug levels in bone given varying responses skeletal elements (16).

Ketamine distribution in rats across different sections of bone (marrow, epiphyseal and diaphyseal) by ELISA and GC/MS analysis were compared across burial environments (17). The results of this study indicated the recovery of ketamine is both bone tissue and burial dependent (17). This goes to showing the influence of the local environment on the recovery of drugs in bone tissues.

The value of parent-metabolite ratios was introduced in a study that used SPE and GC/MS to analyze amitriptyline and citalopram in porcine bone tissues following outdoor decomposition (12). A high variability of parent drug levels were again across bone elements, though the ratio of levels of parent drug to those of their metabolites were less variable (12), indicating forensic

potential in investigating the levels of both metabolites and drugs in bone tissues. Another study (14) established the value of parent-metabolite ratios in comparison in rat skeletal tissues by SPE and GC/MS analyses for acute and repeated doses of amitriptyline and citalopram. Ratios between parent and metabolite compounds varied across repeated and acute exposure types, indicating a pattern of drug use may be distinguished in bone analyses following advanced decomposition (14).

The effect of body position and microclimate was explored in rats given acute doses of ketamine in two different microclimate environments (18). Ketamine and its metabolites were analyzed for by GC/MS in different bone elements. The results of the study showed an influence of body position and the surficial microclimate environment during decomposition on the RR/m of the parent drug, metabolites and parent-metabolite ratios in different skeletal elements (18). This study illustrates the difficulty of interpreting toxicological analysis of bone by introducing a new factor to consider.

The work of Watterson and colleagues has continued to develop methods for the analysis of forensically relevant drugs. A recent study investigated DXM and DXT in decomposed rat bone tissues (9) presents a method for assay using MAE, SPE and GC/MS for DXM and DXT analysis and established the stability of the compounds in both microwave extraction and in bone after decomposition. The methods from this paper (9) were used to develop the extraction and analytical techniques used in the current study.

1.4 Dextromethorphan and its Metabolites

Dextromethorphan is primarily known for its cough-supressing antitussive effect, and is the "DM" in many brand over the counter cough syrups. Cough supressing effects are present at therapeutic doses of 30 to 60 mg of DXM. Experimental uses of DXM have been to test for the treatment of Huntington's disease (32), Parkinson's disease (33), complex partial seizures (34) as

doses of DXM higher than antitussive treatments has shown to have neuroprotective and anticonvulsant properties (35–37). Blood concentrations associated with abuse for DXM are in excess of 200 mg with dissociative hallucinogenic effects similar to phencyclidine (PCP), which may seriously limit therapeutic use (27). Reported effects of DXM abuse are euphoria, hallucinations, perceptual alterations, aggressive behavior, nausea and drunkenness (27, 38). Abuse of DXM has been reported in the literature as early as 1964 (39) and fatal overdoses have been reported (40–42). Post-mortem blood concentrations of DXM associated fatalities ranged from 950 to 3230 ng/mL in 5 deaths, well above reported therapeutic plasma concentrations of 10 to 40 ng/ mL (42, 43). Post-mortem redistribution of DXM in blood is reported, the interpretation of toxic levels of DXM should take the location of post-mortem blood samples into account. Central to peripheral blood ratios of DXM levels from 5 post-mortem cases ranged from 1.0 to 3.5, with volumes of distribution (V_d) of 5.0 to 6.4 L/kg (44). Post-mortem redistribution of drugs may be a factor influencing the degree drugs partition into bone tissues and should be considered when investigating drug in bone concentrations.

The major metabolite of DXM, dextrorphan (DXT), has been shown to have pharmacological effects similar to PCP at high doses and may be a prodrug that produces dissociative hallucination effects. The prodrug nature of DXM and has been indicated by a number of studies in animals (45–47), some indicating DXM offers no PCP-like effects (48). The route of administration and the metabolic rates of individuals will therefore influence the degree of DXM to DXT conversion and the desired effects of DXM abuse (27). Since DXM is primarily metabolized by the cytochrome enzyme CYP2D6 (27), phenotypic discrimination between fast and slow metabolizers has been investigated using post-mortem ratios of DXM and DXT (28). The metabolic pathway of DXM is presented in Figure 1.1.

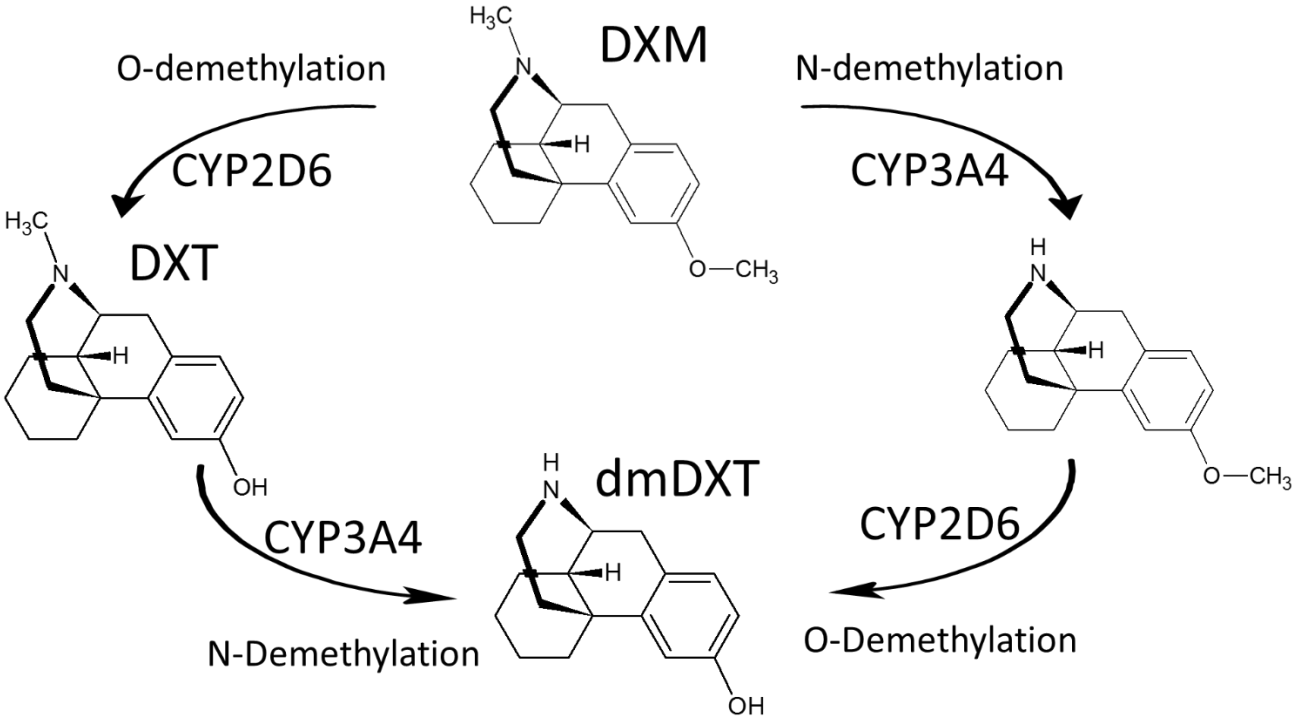

Figure 1.1: Metabolic pathway of dextromethorphan to secondary metabolite 3-hydroxymorphinan (dmDXT) from first metabolites dextrorphan (DXT) or 3-methoxymorphinan from demethylation by liver cytochrome (CYP) enzyme action.

Dextrorphan shares similar antitussive and neuroprotective effects with DXM (27). Unlike its parent drug, DXT has been shown to have a high affinity for PCP receptor cites in rat brains, which may account for the PCP-like behaviours in animals given DXT (48–50). DXT, like PCP and ketamine, acts as a non-competitive antagonist on N-methyl-D-aspartate (NMDA) receptors, inhibiting ion-channel protein function in nerve cells (51). A corresponding rise in extracellular glutamate concentrations in the prefrontal cortex of rat brains has been seen at sub-anesthetic doses of non-competitive NMDA antagonists like ketamine (52). The rise in prefrontal glutamate concentrations and prefrontal activity in humans has also been seen in other more widely used hallucinogens like psilocybin, along with ketamine and with high doses of DXM (52, 53), the NMDA antagonist function of the latter may largely be due to its active metabolite DXT (27, 45, 48, 50).

Because of the active metabolite nature of DXT and extensive first pass metabolism of DXM by CYP liver enzymes (27), the route of administration (RoA) of DXM will affect the time course and free DXT concentrations. DXM and DXT in rat plasma and brain tissues following different routes of administration were compared using HPLC methods; maximum concentrations (C_{max}) of DXT in brain tissues and plasma were 5 and 12 times higher in intraperitoneal injection than for subcutaneous (SC) injections (27). Free DXM concentrations were higher following SC, the differences in DXM and DXT concentrations in plasma and brain tissues is attributed to the extensive first pass metabolism afforded to IP injections (27). Along with route of administration, the CYP2D6 phenotype should also be considered when investigating DXM or DXT concentrations in human samples. Given the C_{max} of DXT will favor a RoA that allows for first pass metabolism of DXM, the minority of humans with CYP2D6 gene deletions or mutations will have lower DXT concentrations and higher DXM levels following administration of DXM (27,

28). Studies looking into DXM metabolism and behavioral effects should consider CYP2D6 phenotypes and RoA as they will determine the C_{max} and time course of DXM and the prodrug DXT.

1.5 Microwave Assisted Extraction

Microwave Assisted Extraction (MAE) is an efficient, effective and rapid way of extracting a number of compounds from a variety of matrices, including drug from bone (9, 15, 54–59). Microwave energy is non-ionizing electromagnetic radiation that at 2450 MHz, heats the irradiated materials by the rotation and agitation of polar molecules (59). Microwave heating is also volumic, heating the entire mass of reactant and the solvent even above theoretical solvent boiling points under closed systems, the latter better facilitates analyte extraction (57, 59). Microwave energy can selectively heat chemical species while simultaneously breaking down microstructures of sample matrices to release targeted analytes, and since many organic solvents absorb microwave energy to lesser extents than many compounds, organic solvents serve to effectively cool and solvate targeted compounds (54, 58).

Since its inception, MAE has offered a number of advantages over previous extraction methods including significant reduction in extraction time, reduced solvent use, increased number of sample extractions, improved yield of extracted analytes, automation and improved precision, tailored methods for specific compounds and matrices, and constant sample agitation throughout extraction (54, 57, 59). Though MAE methods are useful for extraction of many organic compounds, the stability of desired analytes and the appropriate solvents used must be validated prior to use in toxicological studies. The stability of DXM and DXT under MAE conditions was established in previously published work and the extraction of DXM, DXT and dmDXT in this

study follow those from previously published drug from bone MAE extraction methods (9, 15, 18, 55).

1.6 Gas Chromatography and Mass Spectrometry

Chromatography is a method of separating chemical compounds in a sample; gas chromatography is the separation of organic volatile compounds (VOCs) (60). Compounds are separated by chemical interactions with immiscible stationary and mobile phases. Different compounds will react differently with the stationary phase. Compounds with a high affinity for stationary phase interactions will lag behind compounds with lower affinity for the stationary phase. The degree a compound interacts with the stationary phase compared to its concentration in the mobile phase is known as the distribution coefficient, or K_d. For a given compound, different mobile and stationary phases will affect the compounds K_d, so for compounds of interest, the choices of stationary and mobile phases used in chromatography should be made with optimal analyte separation in mind.

Gas chromatography uses the above principles of distribution to achieve analyte resolution. A mixture of a number of compounds is carried in a gas mobile phase over a stationary liquid film or gel phase lining the inside of a column which separates the compounds by differing K_d (61). The GC method has proven to be an accurate method of compositional analyses for a number of fields including petroleum, pharmaceutical and chemical industries, biochemical research, forensic sciences and even food and flavour studies (61). The heart of the GC method is the column. The degree of compound separation, and thereby the full resolution of endogenous compounds and analytes, can be determined solely the column used (61). Today fused-silica columns are the standard capillaries used in GC methods (60). Silica lining the inside of capillaries is treated by high temperature silylation, a method that renders active silica sites chemically inert and allows

for more uniform lining by stationary phase films (62). Analyte resolution can also be helped by narrowing the capillary used in GC and increasing the temperature through the run to improve compound volatility, especially for those eluting later (61).

Some compounds are not amenable to GC as reactive groups can impair volatility and increase interactions with the stationary phase. Polar groups with active hydrogen sites, like amine and hydroxyl groups, will perform poorly in the column and peak width spreading and tailing may be seen, reducing compound resolution impairing interpretation of GC analysis (63). An additional step during sample preparation replaces active sites with an unreactive group that will improve volatility, and therefore GC performance, especially for small molecules with inter-molecule polar interactions, such as carboxyl acids, phenols, alcohols and other reactive groups (64). Derivatization can be completed with acylation and alkylation, but most commonly silylation, where the active hydrogen on the substrate is replaced by a silyl group, generally trimethylsilyl (64). A generalized silylation derivatization reaction of DXT is presented in Figure 1.2. Silylation proceeds by S_N2 mechanism (64) where the analyte acts as the nucleophile. Derivatization agents are manufactured with the derivatizing group are bound to a good leaving group. The resulting product is a new "derivatized" compound with improved GC performance that is amenable in a variety of column types and analytical conditions (63).

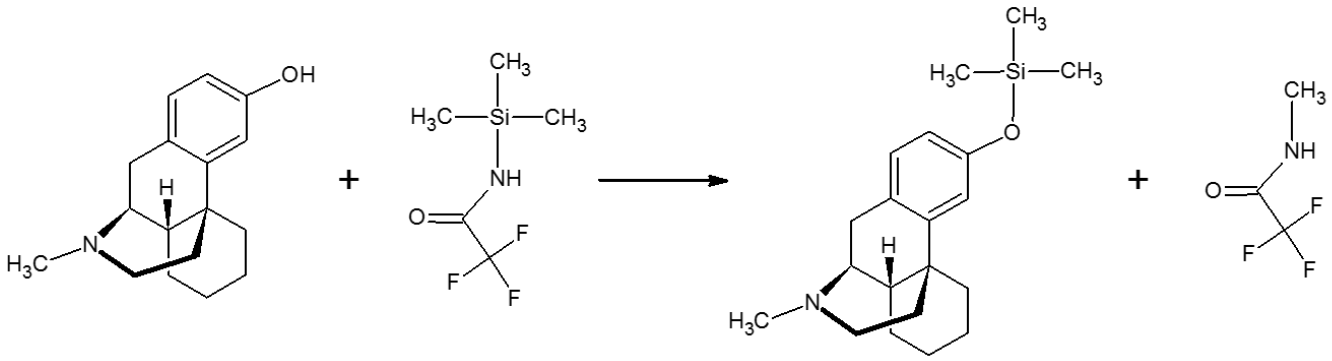

Figure 1.2: Reactants and products of the derivatization reaction of DXT with N-methyl-N-(trimethylsilyl)trifluoroacetamide (MSTFA). The active hydrogen of the 3-hydroxyl group on DXT is silylated to improve resolution in GC capillaries by reducing capillary wall interactions.

The separation of compounds within a mixture by GC is well established, but separation of an analyte from a sample mixture is not enough for compound identification. A detector instrument must be used to identify compounds as they elute from the GC column. Mass spectrometry (MS) is a useful tool in forensic toxicology as MS methods generate reproducible, standardized results for a given compound across a wide variety of analytical conditions (63). Compounds separated by GC elute from the column into a MS instrument that can provide qualitative and quantitative detection of analytes (63). In GC/MS, compounds that elute from the capillary are ionized and fragmented by electron bombardment. The ionized molecules and fragments are sorted by molecular weight, or "mass to charge ratio" (m/z) by (quadrupole) mass analyzer instrumentation (61). For a given ionization energy, a molecule will ionize and fragment, creating a diagnostic mass spectrum, allowing for identification of the resolved analyte eluting from the GC capillary (63). The quadrupole instrument can isolate ions of specific m/z by changing voltages across the four poles of the instrument which generates oscillating radio frequency currents that permit all (full scan, or FS) or desired (selected ion monitoring, or SIM) ions to be detected (63) by the MS instrument. Using SIM mode for MS analysis allows for the user to measure specific diagnostic ions which imparts greater sensitivity by increasing the detection time for diagnostic ions and reducing signal noise from undesired ions that reach the detector (61). Mass spectra of an analyte, be it from FS or SIM modes, can be compared to known standards or a library of mass spectra for identification (61, 63).

1.7 Environmental Factors and Microclimate Conditions during Decomposition

The environment of decomposition has been shown to influence drug stability and therefore recovery in animal bone tissues (17, 18), though environmental data has not been collected during these studies. Microclimate conditions have been shown to influence the rate of putrefaction

product formation during decomposition of human remains, with temperature as a driving factor in chemical reaction rates (19). Temperature is thought to be the predominant factor in determining the rate of decomposition and several methods using accumulated degree-days are used to estimate post-mortem intervals, or PMI, where intervals are corrected to an average temperature interval period (65, 66). Moisture levels are also important controls in the rates and degrees of decomposition, as extremely dry conditions will lead to the desiccation of tissues, inhibit microbial action and exclude important insect or other carrion activity. When water is present, attributes associated with water that influence decomposition are "(a) a high specific heat that stabilizes temperatures; (b) buffering capacity that moderates the effects of local pH changes; (c) sources of hydrogen required for numerous biochemical reactions; (d) its effect as a diluent; and (e) its ability to act as a solvent for polar molecules (67)". Environment pH, partial pressure of oxygen and temperature are also important factors that influence the rate of decay (67). Significant variation in environmental data has been observed across microclimatic sites, even over small distances, and the use of regional weather data for PMI calculations should be done so with caution (68).

Energy exchange in the environment is has largely been overlooked in forensic research of decomposing bodies. A body in direct sunlight can receive in excess of 2 calories per cm^2 per minute of energy (a value that will change with increasing or decreasing latitude) and upwards of 0.76 $cal/cm^2/min$ from surface substrate radiating as a black body, even at night (69). This energy flux will affect chemical and molecular rates and stability, evaporation of water and volatiles and other biological processes that may influence drug and metabolite stability in decomposing tissues across a variety of environments and shelters. Clearly, there are a number of factors that will influence the stability and therefore recovery of drug from bone tissues. There is a lack of research investigating the role of microclimate on post-mortem drug stability. Microclimatic factors, if

established as an influence on post-mortem drug stability and differential tissue compartmentalization shouldn't be solely related to outdoor environments of decomposition. Cases of advanced decomposition from outdoor environs are not the typical workload of forensic toxicologists, advanced putrefaction can be found in cases of advanced decay within dwellings where a person has been dead for a number of days or weeks prior to discovery. The temperature and moisture surrounding the deceased, regardless of environment will play a role in the rates of putrefaction products, entomological activity, rates of decay and analyte stability. To date no catalog of these factors on bone tissue analyses has been developed.

1.8 Goals of Study

Dextromethorphan (DXM) and metabolites dextrorphan (DXT) and 3-hydroxymorphinan (dmDXT) were recovered from bone elements from rats given acute doses of DXM following differential microclimate decomposition using Microwave Assisted Extraction (MAE), Solid Phase Extraction (SPE) and GC/MS. Rats were divided into two groups to compare observed drug levels across different microclimate sites to investigate climate effects on DXM and metabolite levels following decomposition as little is known about environmental effects on drug stability and the effect on bone as a matrix for drug retention, and that differences were observed following a similar study using ketamine (18). Temperature and relative humidity (RH%) data was recorded at each site throughout the study to establish different microclimatic conditions.

The objective of this study is to determine if microclimatic conditions during decomposition can be discriminated in dextromethorphan and its metabolites in post-mortem bone tissues. Patterns of parent-metabolite ratios have been shown to be different in ketamine analyses across different microclimates (18), aid in the discrimination of repeated or acute drug doses (12, 14) and may reflect drug-metabolite stability across microclimates. In this study, unlike the

ketamine study, environmental data was logged remotely at both decomposition sites and compared to regional climate data. Dextromethorphan was administered by i.p. injection to rats at a dose of 75mg/kg and were euthanized by CO_2 asphyxiation. Rats (n=10) were divided across two microclimate sites, 5 rats were placed outside in a temperate forest with grass and soil substrate, the other 5 were placed on an exposed rock barren with gravel substrate; both sites are located on the Laurentian University campus in Sudbury, Ontario. Levels of DXM and DXT were measured using GC/MS with silylation derivatization and corrected for sample masses. Parent to metabolite ratios were calculated to determine possible site discrimination for individual elements or pooled bone results.

CHAPTER 2

MATERIALS AND METHODS

2.1 Drug Standards

Dextromethorphan and dextrorphan drug standards, and corresponding deuterated internal standards were obtained from Cerilliant Corporation (Round Rock, TX). DXM and DXT drug standards were diluted from 1 mL methanolic solutions at concentrations of 1 mg/mL. Deuterated internal drug standards d3-DXM and d3-DXT were diluted from 100 ug/mL methanolic solutions. 3-methoxymorphinan (dmDXT) was provided by Toronto Research Chemicals (Toronto, ON) in 1 mg powder form and was diluted as needed. No deuterated internal standard for dmDXT was available at the time of study.

2.2 Chemicals

Reagent grade chemicals were used in this study. Acetonitrile (ACN), isopropanol (ISO), and glacial acetic acid (GAA) were obtained from BDH/VWR Analytical (Radnor, PA). Ammonium hydroxide (NH_4OH) and methanol (MeOH) were supplied by Fisher Chemicals (Pittsburgh, PA). Ethyl acetate (EA) was provided by EMD Chemicals (Gibbstown, NJ). Anhydrous sodium monophosphate was obtained from Amresco LLC (Solon, OH). Selectra-Sil® N-methyl-N-(trimethylsilyl) trifluoroacetamide with 1% trimethylchlorosilane derivatization agent (MSTFA+1%TMCS) was purchased from United Chemical Technologies (Bristol, PA).

2.3 Animal Care and Drug Administration

All procedures during the course of this study were in compliance with the Laurentian University Animal Care Committee. Fourteen adult male Sprague-Dawley® rats were provided by Charles River Laboratories (Saint-Constant, QC). Live rats were housed and handled at the Laurentian University Animal Care Facility on a 12 hour light/dark cycle and supplied water and

Harlan Teklad Laboratory Diet 8640 (Indianapolis, IN) with no set feeding schedule. Ten rats were given single intraperitoneal (i.p.) injections of DXM at 75 mg/kg and 4 remained drug-free to serve as control animals for this study. Animals were euthanized by CO_2 asphyxiation 30 minutes after DXM administration.

Heart blood was taken perimortem from all rats with the exception of Animal ACU A4, which died prior to blood sampling and asphyxiation. Blood was stored in 4 mL BD Vacutainer® tubes with 10 mg sodium fluoride and 8 mg potassium oxalate anticoagulants from BD Diagnostics (Franklin Lakes, NJ). Blood samples were stored at 4°C prior to analysis.

Euthanized animals were divided across two microclimate decomposition sites, 5 drug positive animals were placed at Site A (ACU A1-A5) and 5 drug positive animals were placed at Site B (ACU B1-B5). Site A is a shaded forest site with soil and grassy substrate. Site B is an exposed rock barren site with gravel substrate. Animals were enclosed in wooden framed 1/2" welded wire mesh cages. Wire mesh was purchased from Home Depot (Sudbury, ON) and 1/2" mesh was selected to permit access to the rats by necrophagous insects and to prevent scavenging from larger animals. Ambient microclimate measurements 3 cm above the rats were recorded hourly by HOBO® H08-32-IS data loggers from Onset Computer Corporation (Bourne, MA) on the underside of white plywood panels mounted above animals A3 and B3. Sites A and B both received 2 control animals which were similarly secured with 1/2" wire mesh 3 m away from drug positive animals. Rats decomposed from July 7th to July 30th, 2015. Animal remains were collected individually in aluminum foil wrap prior to dissection. Control animals were collected from both sites first to prevent downstream contamination from drug-positive animals.

2.4 Validation Bone Extract Preparation

Methods used in this study followed those previously published (9). Rat bone extract used in method validation was prepared from the remains of decomposed drug-free animals that were allowed to decompose until skeletonized on the Laurentian University campus in Sudbury, ON. Rats were covered with welded wire mesh to prevent scavenging from animals. Rat remains were collected and dissected for bone tissues. The following bone elements were collected from each animal: skull, vertebrae, ulnae, radii, humeri, ribs, pelvic girdles, femora, scapulae and tibiae. Tweezers and scalpels were used to remove any remaining soft tissues from the bone elements. Bones were washed with a 0.1M phosphate buffer solution at pH of 6 (PBS), MeOH and ACN to remove surface contaminants. PBS was prepared with a SB70P SympHony pH meter (VWR Analytical, Radnor, PA). Washed bone elements dried for a minimum of 24 hours prior to grinding using a Micro-Mill® Grinder from Bel-Art SP Science Ware (Wayne, NJ) followed by pulverization using a 5100 Mixer/Mill® from SPEX® SamplePrep, LLC (Metuchen, NJ).

Pulverized bone tissues underwent microwave assisted extraction (MAE) in MeOH using a MARS6 Microwave Reaction System and MARS Xpress™ 25 mL PTFE reaction vessels from CEM Corporation (Matthews, NC) at 70°C for 30 minutes. The solvent was pipetted from the reaction vessels in 5 mL volumes into 13-100 mm Fisherbrand Borosilicate test tubes (Pittsburgh, PA), and were evaporated to dryness under vacuum using an Acid Resistant CentriVap® Concentrator and -50°C CentriVap® Cold Trap (Labconco, Kansas City, MO). The dried constituents of each test tube were reconstituted and vortexed with 1 mL of PBS using a VX-200 Vortex Mixer from Labnet International (Edison, NJ) and then pooled for method validation analyses.

2.5 Validation Sample Preparation

Standard curves with nine triplicate concentrations of DXM, DXT and dmDXT ranging from 0-2000 ng/ mL were prepared for GC/MS analysis in 1 mL volumes of bone tissue extract prepared as above. All samples received 200 ng of d3-DXM and d3-DXT internal standards. Samples and dilutions were prepared to desired concentrations using 5-50 μL, 20-200 μL and 100-1000 μL Signature Ergonomic High Performance Pipettors from VWR Analytical. This method is used as a best approximation of drug recovery from bone tissues as it is impossible to impregnate a skeleton or single skeletal element, be it from a living or deceased animal, with a known concentration of any drug.

Samples with known drug concentrations for the standard curves were treated with 3 mL of 1:1 MeOH:ACN for lipid-protein precipitation for 12 hours at -20°C. Sample supernatant was isolated from the precipitated solids into clean test tubes following centrifugation at 4000 rpm (1500 x g) for 10 minutes using a Clinical 100 micro-centrifuge from VWR Analytical and then evaporated to a volume of 1 mL using the CentriVap® concentrator and cold trap.

Samples were prepared for mixed-mode solid phase extraction (SPE) to isolate drugs and internal standards from unwanted compounds present in the supernatant. 100 μL of GAA was added to each test tube to increase extraction efficiency by protonating the drugs and internal standards for anion interactions during extraction. All samples were diluted with 1.5 mL of PBS prior to loading on the SPE well plate. Clean Screen® XCEL I 96 well plates from United Chemical Technologies were used for SPE. The Xcel 1sorbent material is a mixed-mode anion material, allowing neutral and positive charged molecules to adsorb to the surfaces of the sorbent. Each well was conditioned for SPE with sequential 1.5 mL volumes of MeOH to wet the SPE resin, distilled water to wash out any residual MeOH, and PBS to promote sample-sorbent

interaction by giving the well environment a pH of 6.0, well below the pKa values for DXM and DXT (8.3 and 9.2, respectively). Samples were loaded by gravity following well conditioning. Wells were sequentially washed with 1.5 mL volumes of PBS, 0.1M acetic acid and MeOH, with a 5 minute drying time using a Rocker 400 vacuum pump from Rocker Scientific (Linkou District, Taiwan) at -50 kPa prior to the latter wash, and again for 10 minutes following the final MeOH wash. Drugs were eluted from the columns with a 3:17:80 solution of NH_4OH:ISO:EA and collected in a dry 96 well elution plate from United Chemical Technologies, which was cleaned prior to each drug elution by 5 minute sonication bath using a FS20D Digital Ultrasonic Cleaner from Fisher Scientific. Eluted drugs were pipetted into clean test tubes using Pasteur pipettes and then evaporated to dryness under vacuum using a CentriVap® Concentrator. Dried samples were reconstituted in 50 μL of EA and received 50 μL of the derivatizing agent MSTFA+1%TCMS using Positive Displacement Microdispensers from Drummond Scientific Company (Broomall, PA). Tubes were capped and vortexed for 30 seconds and the samples were derivatized at 70°C on an Analog Heatblock from VWR Analytical for 60 minutes. Derivatized samples were transferred to 200 μL glass MicroSert Inserts from ThermoScientific (Rockwood, TN) in 1.8 mL amber glass autosampler vials from VWR International for GC/MS analysis.

2.6 Experimental Sample Preparation

Each rat was dissected individually with control animals harvested first to prevent downstream contamination. Bone elements from each animal where cleaned, washed and pulverized individually using the methods presented above. Pulverized bones were stored in clean glass test tubes prior to drug extraction and analysis. Of the bones collected from each animal, the skeletal elements that were prepared for analysis were skull, vertebrae, humerus, scapula, pelvic girdle, femur and tibia. Drugs were extracted by MAE using 0.2 g of pulverized bone from each

element in individual reaction vessels. Blood volumes of 0.25 mL were diluted to 1 mL volumes with PBS and treated with the same methods as bone samples following MAE for SPE and derivatization.

2.7 GC/MS Analysis

Analyses were performed on a Clarus 600C Gas Chromatography-Mass Spectrometry instrument in Selected Ion Monitoring (SIM) and Full Scan (FS) modes with TurboMass v.5.4.2.1617 software from PerkinElmer LAS (Shelton, CT) using a Zebron ZB-Drug-1 column (Phenomenex, Torrance, CA). Extracts of 2 μL from derivatized samples were injected into the instrument's injection port held at 250 °C. Initial oven temperature was held at 100 °C for 3 minutes before ramping for 15 minutes to 220°C at 10°C per minute. Oven ramp rate decreased to 5°C/min for 6 minutes to 250°C to aid in resolution of targeted parent and metabolite peaks from endogenous compounds. Oven temperature ramped at 10°C /min until 300°C was reached and held for 3 minutes to finish the run. The total run time of each analysis was 31 minutes. A retention time standard of 1000 ng of derivatized pure drugs was run at the beginning of each series of analyses to identify the elution times of the targeted compounds. DXM was quantified by m/z ion 271, DXT with ion 150 and dmDXT with ion 315, d3-DXM and d3-DXT were quantified with m/z ions 274 and 153 respectively from peak area integrations calculated by TurboMass software.

2.8 Method Validation

Proficiency and method repeatability was demonstrated by completing 3 standard curves on different days per Scientific Working Group for Forensic Toxicology (SWGTOX) recommendations (70) using the methods presented by Fraser, et al (9). Triplicate samples of 9 concentrations ranging from 0 to 2000 ng of drugs in 1 mL of drug free bone extract were used to produce the standard curves. DXT was quantified with the ion m/z ratio of 329 and ions 272 and

150 were used to qualify DXT. Initial standard curves were validated with these ions. Internal standard d3-DXT was quantified with ion 332 and qualified using ions 275 and 153. DXM was quantified with 271 ion and qualified with 214 and 150 ions, d3-DXM was similarly identified by ions 274, 217 and 153. The secondary metabolite dmDXT was quantified using ion 315 and qualified by 270 and 136 m/z ions. Retention times for DXM, DXT, dmDXT and corresponding internal standards were 18.95, 19.27 and 19.54 minutes, respectively. Drugs and internal standards were identified by their retention times and mass spectra.

During experimental analyses, an endogenous compound with a strong 329 ion response was present in a number of samples and could not be fully resolved from DXT 329 ion peaks. This interferent was present in samples from both sites but was predominant in Site B analyses. The DXT interferent was absent in all samples during validation. Sample and standard curve results were reassessed for DXT quantifying and qualifying ions not present in the interferent. To distinguish DXT from the interferent, with m/z ion 150 was used to quantify and those with m/z 59 and 214 were used as qualifying ions. Figure 2.1 presents an example chromatogram with 329 ion interferent and reassessed 150 ion response. The internal standard was similarly reassessed and ions 153, 62 and 217 were used to identify d3-DXT. All standard curves and experimental results that follow for DXT and d3-DXT were calculated using 150 and 153 as quantifying ions, respectively.

Quantification of drugs was calculated using Response Ratios (RR) where drug quantifying peak areas were divided by quantifying internal standard peak areas; d3-DXM served as the internal standard for dmDXT. Method validation calculations were completed using Excel® 2013 (Microsoft Corporation, Redmond, WA). The response ratio (RR) formula is presented below:

$$RR = \frac{Drug\ Quantifying\ Ion\ Peak\ Area}{Internal\ Standard\ Quantifying\ Peak\ Area}$$

Each set of replicate standard curves were assessed by the coefficient of determination (R^2) and the coefficient of variance (CV%) for DXM, DXT and dmDXT results. Bias was assessed by the inclusion of two samples of unknown concentrations prepared in triplicate for comparison of fit to the linear model from the standard curve results. Variance in DXM and DXT results were within CV% limits 20% down to a limit of quantification (LOQ) 10 ng/mL samples, however the LOQ is more reliably 25 ng/mL, the LOQ used in this study. Results for DXM and DXT linear models showed good fit with R^2 values ranging from 0.9916-0.9991 and from 0.9893-0.9996 respectively. Bias results for DXT and DXM were all satisfactory with no value falling outside ±20% of the linear models. The results of dmDXT analyses were not sufficient for validation. Limit of detection of dmDXT from standards curves was 500 ng/mL and CV% were in excess of accepted limits across all detected concentrations. Though dmDXT can be detected, dmDXT cannot be used for quantification in this study given the poor recovery and the dispersion of standard curve results. Standard curves and validation calculations are presented in the Appendix.

2.9 Experimental Sample Analyses

Drug and metabolite chromatogram peaks were identified from GC/MS analyses using mass spectra of DXM, DXT and dmDXT and comparison to retention time standards. Drug and internal standard responses were calculated from TurboMass peak area integrations for RR values calculated in Excel spreadsheets. All experimental samples were normalized for mass (RR/m) to account for variability in the masses of milled bone tissues used in sample preparation by dividing relative responses by sample mass:

$$RR/_m = \frac{Drug\ Response\ Ratio}{mass\ of\ sample\ tissue}$$

Blood volume was used to normalize results of blood analyses. Whole blood density is approximately 1.05 g/mL, so blood volume and blood mass are essentially equivalent for purposes of this study (71).

Statistical analysis of results was completed using Excel® 2013 and StatPlus:Mac 2009 v 5.8.3.8 (AnalystSoft Inc., Wallnut, CA). Blood correlations across bone types was calculated by the square of Pearson product moment correlation coefficient (R^2). Kolmorov-Smirnov tests determined non-normal distribution of data so nonparametric analyses were used in this study. Drug and metabolite responses were compared across bone elements and decomposition sites by Mann-Witney *U* tests with significant differences acknowledged for *p* values less than 0.05 ($p < 0.05$). Kruskal-Wallis tests compared distributions across bone types with statistical significance at $p < 0.05$. Analytical results are presented in the Appendix.

2.10 Microclimate Measurements and Data Analyses

Environmental measurements were collected throughout the experiment to establish microclimate differences at Sites A and B. Six HOBO® H08-32-IS data loggers and additional environmental instruments were provided for this study by Dr. Jaqueline Litzgus and Dr. Gerard Courtin of the Biology Department at Laurentian University to establish different microclimatic conditions at Sites A and B. Data logger temperature measurements were verified using an Omega HH-25TC Type 1 Thermocouple (Omega Engineering, Inc., Stamford, CT). Relative humidity measurements were verified against a Kestrel® 3000 Pocket Weather Meter (Nielsen-Kellerman, Chester, PA) and against equilibrium relative humidity of different saturated salt solutions and pure water in a sealed vessel (72). Data loggers sat above saturated solutions for 1 hour recording

measurements every 5 minutes to test humidity sensors against known RH values of 33%, 53% and 75% for saturated salt solutions of magnesium chloride, magnesium nitrate and sodium chloride salt, respectively (72). Pure water was used to test for 100% relative humidity. Data logger measurements for temperature and RH% were also compared against a Taylor Precision Products (Oakbrook, IL) 1328 Sling Psychrometer at Sites A and B, and in the Laurentian University forensic toxicology laboratory.

Temperature measurements from all 6 data loggers showed good fit with all other instruments used in verification. Relative humidity testing showed only three data loggers had functioning RH sensors. Data loggers with working RH sensors showed good fit with the Kestrel and sling psychrometer measurements and were within expected instrument error margins of ±2% RH and sensor drift over time for all saturated salt solutions and pure water sealed container tests. Plots of RH% validation are presented in the Appendix.

Ambient microclimate measurements were collected using the three HOBO® data loggers with working RH sensors. Two sensors were mounted 3 cm (lower) above decomposing rats at Sites A and B and the third 1.5 m (upper) above ground at Site A per convention. Temperature and RH% measurements were recorded hourly from July 7th to July 30th, 2016. Absolute Humidity (AH), the mass of water vapor in a parcel of air (g/m^3) was recorded by BoxCar® Pro v. 4.3.1.1 software (Onset Computer Corporation) from each hourly temperature and RH% measurements when data was downloaded from the HOBO® dataloggers. Recorded AH values were verified from calculations using measured temperatures in degrees Celsius (T) and relative humidity ($RH\%$) with the formula:

$$Absolute\ Humidity\ (grams/m^3) = \frac{6.11\ \times 10^{(7.5\ \times T)/(T+273.3)}\ \times RH\%\ \times\ 2.1674}{273.15 + T}$$

The formula is based on the Ideal Gas Law and Tetens saturated vapor pressure equation, the latter used to calculate accurate water vapor pressures over the temperature ranges observed during the study (73, 74). AH was calculated to assess atmospheric moisture content between microclimate sites. Downloaded AH values at each site were compared against calculated AH values by Mann-Whitney *U* tests to check data logger accuracy. Microclimate measurements were downloaded after the first day of the experiment to ensure data logger function, again after 7 days and finally at the end of the experiment. Differences in microclimate parameters between sites was assessed by Mann-Whitney *U* tests. Hourly regional weather data was obtained from Weather Canada (75) at the Greater Sudbury Airport, approximately 22 km from the decomposition sites at Laurentian University if regional comparison with microclimate measurements was warranted.

CHAPTER 3

RESULTS

3.1 Microclimate Analysis

Boxplot distributions of microclimate data are presented in Figure 3.1. Site B (exposed) microclimate data exhibited warmer and drier RH% conditions. Greater variability in Site B microclimatic parameters is evidenced by wider interquartile ranges (IQR) for temperature and RH% measurements relative with those at Site A (forested). Site A distributions for AH showed higher minimum and maximum AH values than at Site B though means and IQRs for Sites A and B appear similar. Average, maximum and minimum recorded values for temperature, RH% and AH (g/m^3) are presented in Table 3.1. Mann-Whitney *U* tests were used to assess differences in Sites A and B microclimates. Significant differences were noted for temperature ($p = 0.006$) and RH% ($p = 0.006$) between Site A and Site B microclimates. Because AH, the amount of water vapor in air (g/m^3) above the animals were not significantly different ($p = 0.27$), differences in decomposition rates were attributed to sunlight and temperature. Downloaded and calculated AH values at Site A and Site B show no significant differences (Site A $p = 0.97$, Site B $p = 0.96$). Animals at Site A were in a shaded forest area with prolonged insect activity that yielded skeletonized remains. Insect activity during the first few days of decomposition at Site B was much higher than at Site A. The initial presence of more insects at Site B is attributed to the rapid onset of bloat, but insect activity at Site B dropped off sharply as the study progressed. Conditions at the Site B led to mummified and partially skeletonized remains with much of the muscle tissues and internal organs preserved in Site B animals. Intestinal chyme was present in the remains of some of the Site B animals, indicating both insect and digestive microbial activity was supressed under the conditions at the exposed microclimate.

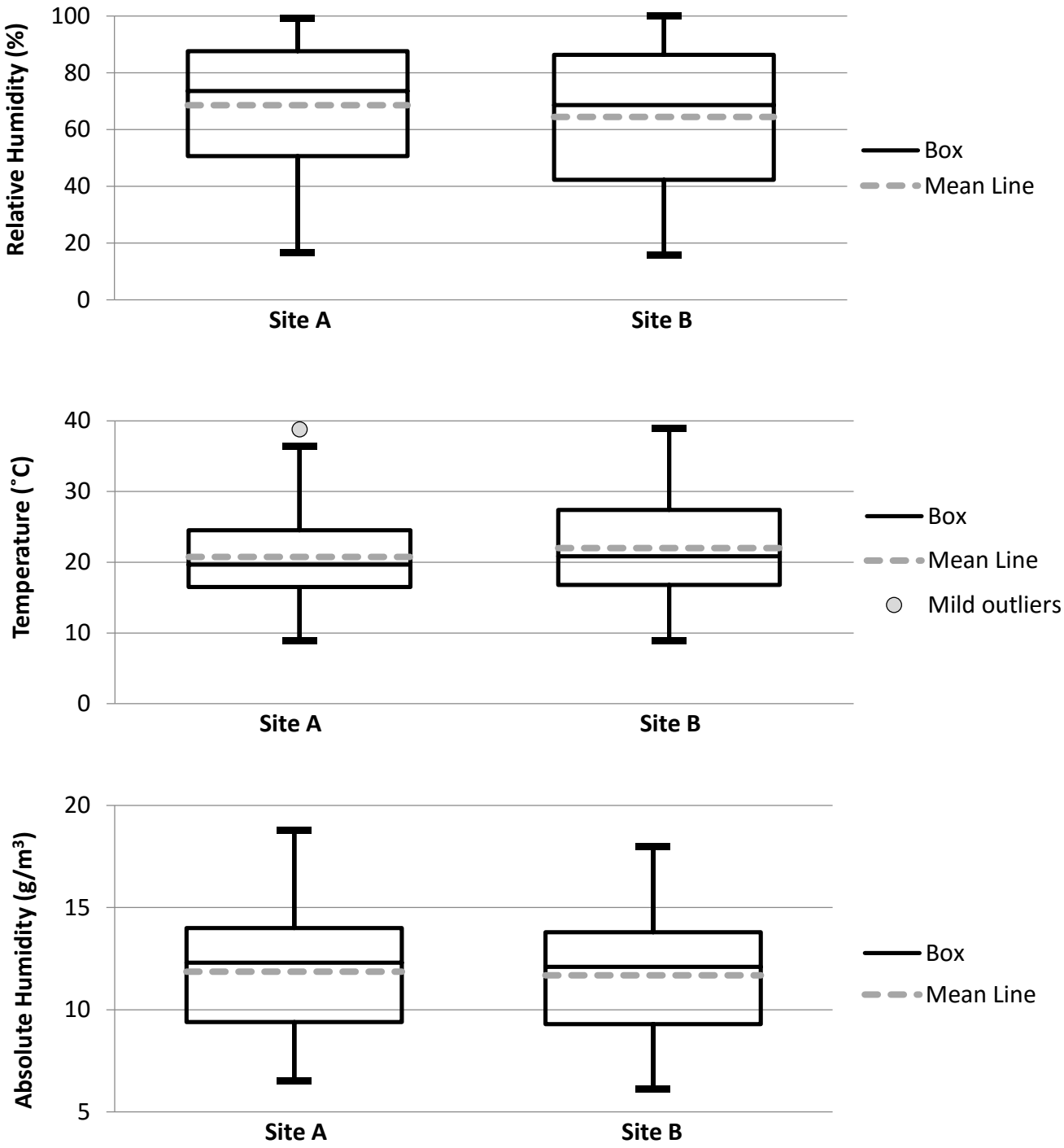

Figure 2.1: Distributions of microclimate parameters at Site A (forested) and Site B (exposed). Relative humidity (RH%) and temperature (°C) were significantly different between sites while absolute humidity (g/m^3) had no significant differences.

Table 3.1: Summary of microclimate parameters temperature (°C), relative humidity (RH%) and absolute humidity (g/m^3) during differential decomposition. Statistical significance ($p < 0.05$) between Sites A and B for microclimate parameters reflect significant differences in temperatures.

Microclimate Variable	**Site A Average (Range)**	**Site B Average (Range)**	***p*-Value**
Temperature (°C)	20.8 (8.9-38.8)	22.0 (9.0-39.1)	0.006
Relative Humidity (%)	68.6 (16.6-100.0)	64.4 (15.8-99.9)	0.006
Absolute Humidity (g/m^3)	11.9 (6.5-19.7)	11.7 (6.1-18.4)	0.27

3.2 Expression of Drug Levels

Mass normalized response ratios (RR/m) for DXM and DXT measurements are presented in this study as in previously published works (12, 14, 18, 31). Proper calibration of analyte recovery from a heterogeneous sample matrix like bone tissue cannot be assessed using conventional techniques as the bone matrix cannot be homogenized with internal drug standards. DXT m/z ion 150 and interferent m/z ion 329 comparisons are summarized in Figure 3.1. Normalizing measured response ratios with the mass of the sample allows the comparison of different drug responses prepared using the same methods as RR/m is proportional to the concentration of drug in bone. These values should be viewed as approximations of bone-drug concentrations only as accurate calibration of an analyte from solid matrices is not possible. Estimated concentrations of DXM and DXT are presented below in Table 3.2.

3.3 Influence of Bone Elements on Drug Distribution

DXM and DXT were detected in all analyzed drug-positive skeletal elements from both microclimate sites, but some DXT (n = 9) responses were below the LOQ and were excluded from quantitative comparison. Mean DXM RR/m responses across bone elements were larger than all corresponding mean DXT values. Mean drug levels in bone elements from Sites A and B for DXM, DXT and metabolite-parent mass normalized ratios (RR_{DXT}/RR_{DXM}) are presented in Figure 3.3. Differences in drug responses across bone elements within animals at each microclimate site were assessed using Kruskal-Wallis tests to test bone element as an effect on drug distribution. No significant statistical differences ($p > 0.05$) for DXM or DXT were seen across bone elements at Site A or Site B. Kruskal-Wallis analysis of the RR_{DXT}/RR_{DXM} ratios at Site A were insignificant. Site B ratios showed statistically significant differences across bone elements ($p = 0.048$) but lacked significant bivariate differences by Dunn's multiple comparison post hoc tests.

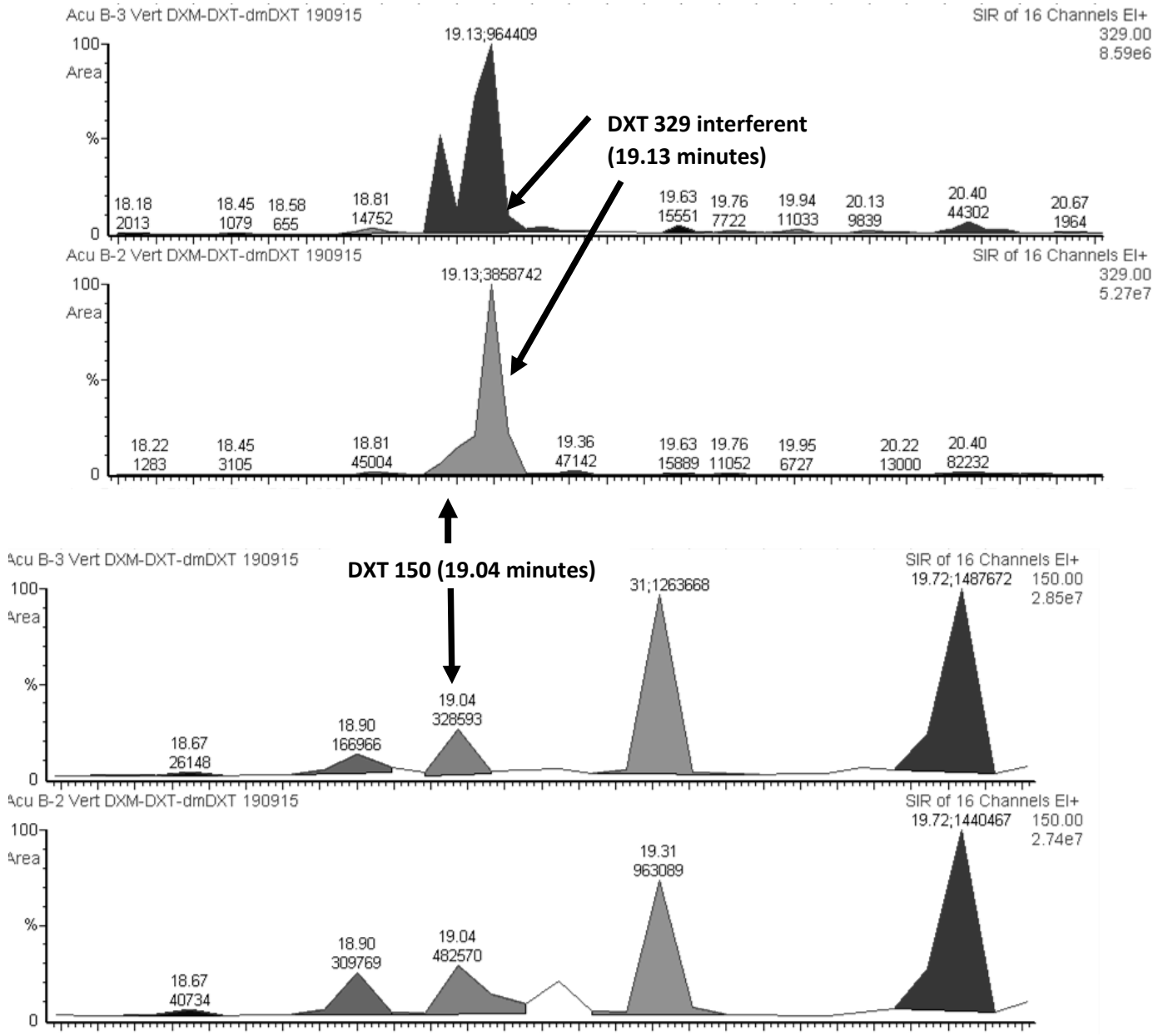

Figure 3.2 Example DXT reassessment of ACU B-2 and B-3 vertebrae samples with ion 150 due to ion 329 endogenous interferent. The predominant 329 interferent elutes 0.09 minutes after DXT and prevents resolution of the metabolite from endogenous compounds using ion 329. DXT was assessed and revalidated using ion 150 (ion 153 for d3-DXT) for all experimental analyses and standard curves used in this work.

Table 3.2: Estimated DXM and DXT concentrations in bone samples between Sites A and B. Estimated drug concentrations were calculated from standard curve plots and drug responses, and corrected for sample bone mass. These concentrations should be viewed with caution and at best, estimates only, as concentrations from solid matrices cannot be validated using standard toxicological methods.

	Site A DXM (ng/g):	**Site B DXM (ng/g):**	**Site A DXT (ng/g):**	**Site B DXT (ng/g):**
Maximum Drug Concentration	10,474	8,726	3,045	3,668
Minimum Drug Concentration	399	3,435	142	133
Range	10,075	5,291	2,903	3,535

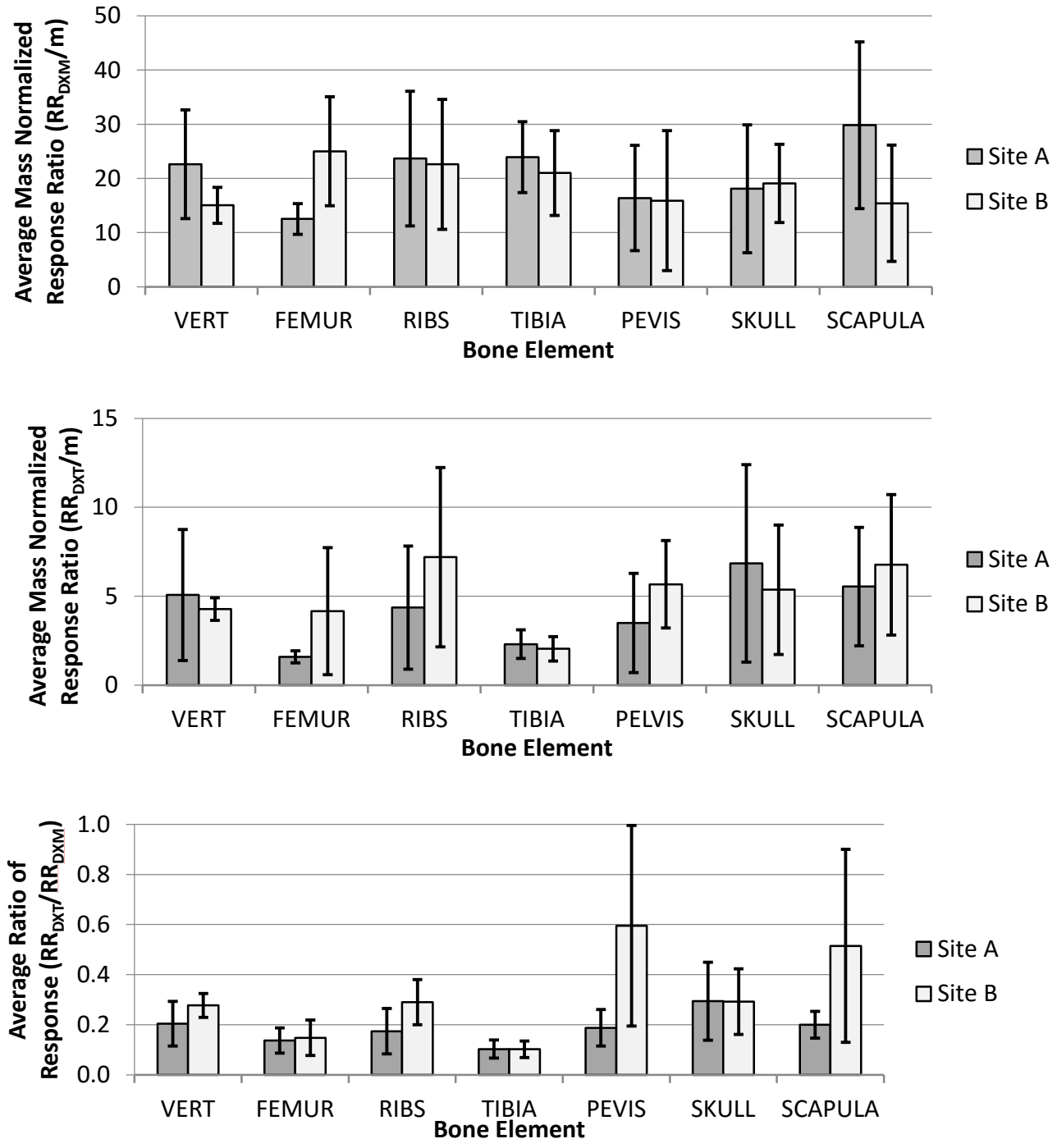

Figure 3.3: Average mass normalized response ratios (RR/m) for DXM and DXT, and ratio of mass normalized response ratios of DXT to DXM (RR_{DXT}/RR_{DXM}) from decomposed bone elements for Site A (forest) and Site B (exposed) microclimates following acute i.p. (75mg/kg) DXM administration.

3.4 Influence of Microclimate on Drug Distribution

Microclimate differences were established in this study and drug responses were tested across the different decomposition environments. Box plot distributions of observed drug levels (RR/m) for DXM, DXT and metabolite-parent ratios (RR_{DXT}/RR_{DXM}) for Sites A and B are presented in Figure 3.3. Site A DXM and DXT levels expressed greater variations in response as larger IQRs vs. Site B DXM and DXT distributions. Site B metabolite/parent ratios skew towards higher values with greater variation than at Site A. Differences in pooled observations for DXM and DXT levels, and RR_{DXT}/RR_{DXM} values between microclimate sites were assessed using Mann-Whitney *U* tests. No statistically significant differences were seen in pooled drug responses or metabolite-parent ratios between microclimate sites. Differences for DXM, DXT and RR_{DXT}/RR_{DXM} levels in each skeletal element between microclimate sites were evaluated by Mann-Whitney *U* tests. Only one significant difference in RR/m (femoral DXM, $p = 0.0472$) was observed between microclimates. DXT responses and metabolite/parent ratios show no significant differences within bone elements between Site A and Site B.

Examination of RR/m shows a higher variability for DXM and DXT levels (expressed as the ratio of maximum to minimum drug levels) at the forested microclimate, Site A. Table 3.2 summarizes the variability in observed drug responses and metabolite-parent ratios for Sites A and B across different bone elements, within animals and for pooled data. DXM and DXT show 22-fold and 52-fold variations, respectively, at Site A, and 10-fold and 18-fold variations for DXM and DXT, respectively, at Site B. The maximum variations for DXM and DXT are both within given bone elements (Table 3.2), indicating skeletal element may be a factor, though below statistical significance, in DXM and DXT distribution. Calculated R^2 values, means, coefficient of variance (CV%) and standard deviations of RR/m values are presented in Table 3.3.

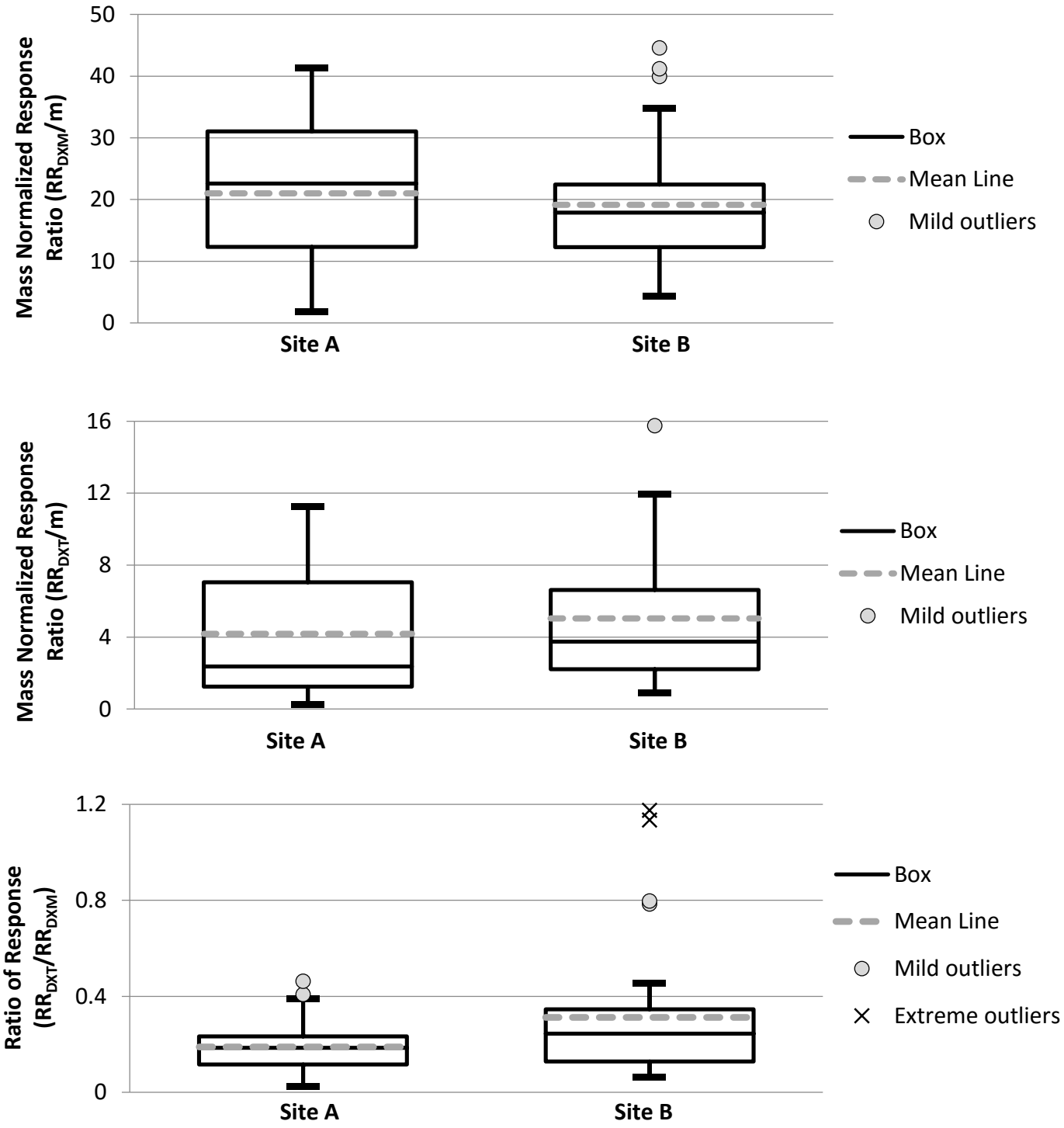

Figure 3.4: Distribution of pooled mass normalized response ratios (RR/m) for DXM and DXT, and ratio of mass normalized response ratios of DXT-to-DXM (RR_{DXT}/RR_{DXM}) for all bone elements from Site A (forest) and Site B (exposed). No significant differences across sites were observed.

Table 3.3: Mean, standard deviation (SD), coefficients of variance (CV%), and Pearson correlation with blood (R^2) of RR/m and metabolite-parent ratios for all analyzed skeletal elements.

Site A:	**Vertebrae**	**Femur**	**Ribs**	**Tibia**	**Pelvis**	**Skull**	**Scapula**
DXM							
Mean:	22.62	12.52	23.68	23.91	16.38	18.11	29.81
SD:	10.04	2.85	12.43	6.55	9.71	11.80	15.39
CV%:	44.4	22.8	52.5	27.4	59.3	65.2	51.6
R^2:	0.03	0.01	0.21	0.17	0.10	0.00	0.12
DXT							
Mean:	5.07	1.59	4.36	2.30	3.50	6.85	5.54
SD:	3.69	0.34	3.47	0.81	2.79	5.55	3.33
CV%:	72.8	21.6	79.5	35.2	79.7	81.0	60.1
R^2:	0.06	0.10	0.15	0.84	0.04	0.34	0.97
RR_{DXT}/RR_{DXM}							
Mean:	0.20	0.14	0.17	0.10	0.19	0.29	0.20
SD:	0.09	0.05	0.09	0.04	0.07	0.16	0.05
CV%:	43.5	36.8	52.3	35.3	38.7	52.9	26.9
R^2:	0.15	0.34	0.02	0.60	0.01	0.29	0.22

Site B:	**Vertebrae**	**Femur**	**Ribs**	**Tibia**	**Pelvis**	**Skull**	**Scapula**
DXM							
Mean:	15.04	25.00	22.60	21.00	15.90	19.09	15.41
SD:	3.32	10.04	11.98	7.82	12.91	7.21	10.75
CV%:	22.1	40.2	53.0	37.3	81.2	37.8	69.7
R^2:	0.30	0.00	0.01	0.89	0.17	0.27	0.08
DXT							
Mean:	4.28	4.16	7.19	2.04	5.67	5.36	6.77
SD:	0.63	3.57	5.04	0.68	2.46	3.64	3.95
CV%:	14.7	85.9	70.0	33.5	43.4	68.0	58.3
R^2:	0.47	0.01	0.15	0.02	0.57	0.49	0.03
RR_{DXT}/RR_{DXM}							
Mean:	0.28	0.15	0.29	0.10	0.60	0.29	0.52
SD:	0.05	0.07	0.09	0.03	0.40	0.13	0.39
CV%:	17.3	48.0	31.1	32.1	67.3	44.9	74.9
R^2:	0.20	0.08	0.11	0.06	0.90	0.08	0.85

Variability in drug responses was examined across different bone elements, within animals and pooled results expressed as the ratio of maximum to minimum RR/m values for DXM, DXT and RR_{DXT}/RR_{DXM}. Table 3.4 presents calculated max/min measures of variability. Variability is highest across different bone elements at both microclimate sites, showing that different bones, as seen in previous studies may be factor in drug distribution (12, 14, 18, 31). Differences in variability across microclimates is shown, indicating potential microclimate influence on recoveries of DXM and DXT. Variability is highest at Site A with factors of 22 and 52 for DXM levels and DXT levels, respectively, versus 10 fold for DXM levels and 18 fold for DXT levels at Site B.

Table 3.4: Ratio of maximum to minimum (Max/Min) response for DXM and DXT, and metabolite-to-parent ratios (RR_{DXT}/RR_{DXM}) at Site A (forest) and Site B (exposed) microclimates

Analyte	Observed Max/Min Range Within Bone Elements	Observed Max/Min Range Within Animals	Max/Min Pooled Bone and All Animals
DXM			
Site A	2.1-22.3	2.7-8.5	22
Site B	1.6-7.9	2.1-5.1	10
DXT			
Site A	2.0-51.5	5.2-14.4	52
Site B	1.4-13.2	3.9-7.6	18
RR_{DXT}/RR_{DXM}			
Site A	2.2-12.4	2.1-6.3	19
Site B	1.7-11.6	3.5-15.7	19

CHAPTER 4

DISCUSSION

4.1 Study Overview

To our knowledge, this is the first study to compare drug responses from bone tissues in skeletonized remains having established microclimatic differences across decomposition sites wherein environmental conditions were measured above the surface of decomposing, drug-positive animals. The rates of decomposition have been shown to be controlled by environmental conditions, largely temperature and moisture content, by dictating the biological and biochemical processes during decay such that the degree and speed of decomposition will differ across microclimates and weather events (19, 65, 67). Observed drug levels in bone tissues have been shown to vary across different decomposition environments (17, 18). The microclimate factors controlling decomposition may also influence the distribution of drugs in bone tissues directly or by limits placed on decomposition processes. Drugs have been found in soil substrates below decomposed remains, in maggots feeding on drug-positive remains and in the bone tissues at the base of positioned remains (18, 24, 76–78). If the degree of insect activity and liquefaction of a decomposing body influences the degree of drug partitioning into bone from decomposing soft tissues, these processes will be dictated by microclimate conditions.

The objectives of this study were to establish environmental differences and assess microclimate and bone element effects on the recovery of DXT and its metabolites from decomposed bone tissues. Because dmDXT standard curve responses could not be validated, quantified results were limited to DXM and its primary metabolite DXT. The results from this study show limited agreement with previous studies from our laboratory. Bone elements and microclimate have shown to be a major influence on distributions of drugs in bone tissues (12, 14, 18, 31). Microclimate and bone elements showed no significant influence on observed DXM or

DXT values, indicating bone as a drug reservoir may behave uniformly for certain drugs across different environments of decomposition.

4.2 Differential Decomposition

The physical condition of rat remains between Sites A and B exhibited distinct patterns of decomposition. Rats at Site B mummified with muscular soft tissues dried and well preserved while Site A animal remains had flattened and partially skeletonized by the end of 3 weeks of outdoor exposure. Typical appearances of rat remains at the conclusion of decomposition are presented below in Figure 4.1. Temperatures during decomposition is shown to be a major influence on decomposition, with observed differences in the conditions of remains and significant temperature differences across Sites A and B. RH% value were also significantly different between the sites, but since relative humidity is a function of temperature as well as water content in the air, the differences in RH% between Sites A and B reflect the differences in temperature. Microclimates during day (sunrise to sunset) and night (sunset to sunrise) were compared between sites by Mann-Whitney *U* tests. Microclimates during the night had no significant differences for recorded measurements. Temperature and RH% during the day were significantly different between sites with $p = 0.00002$ and $p = 0.0001$ for temperature and RH%, respectively. Because the differences were present during daylight hours, variation in microclimates can be attributed to differences in sun exposure. Figure 4.2 presents the distributions of day and night microclimate parameters at Sites A and B. AH, the amount of water vapor in air (g/m^3) measured 3 cm above decomposing remains was not significantly different between sites or between day and night site comparisons. As the atmospheric water content above decomposing remains is similar at both Site A and Site B, variation in decomposition is attributed to temperature differences due to different sun exposure.

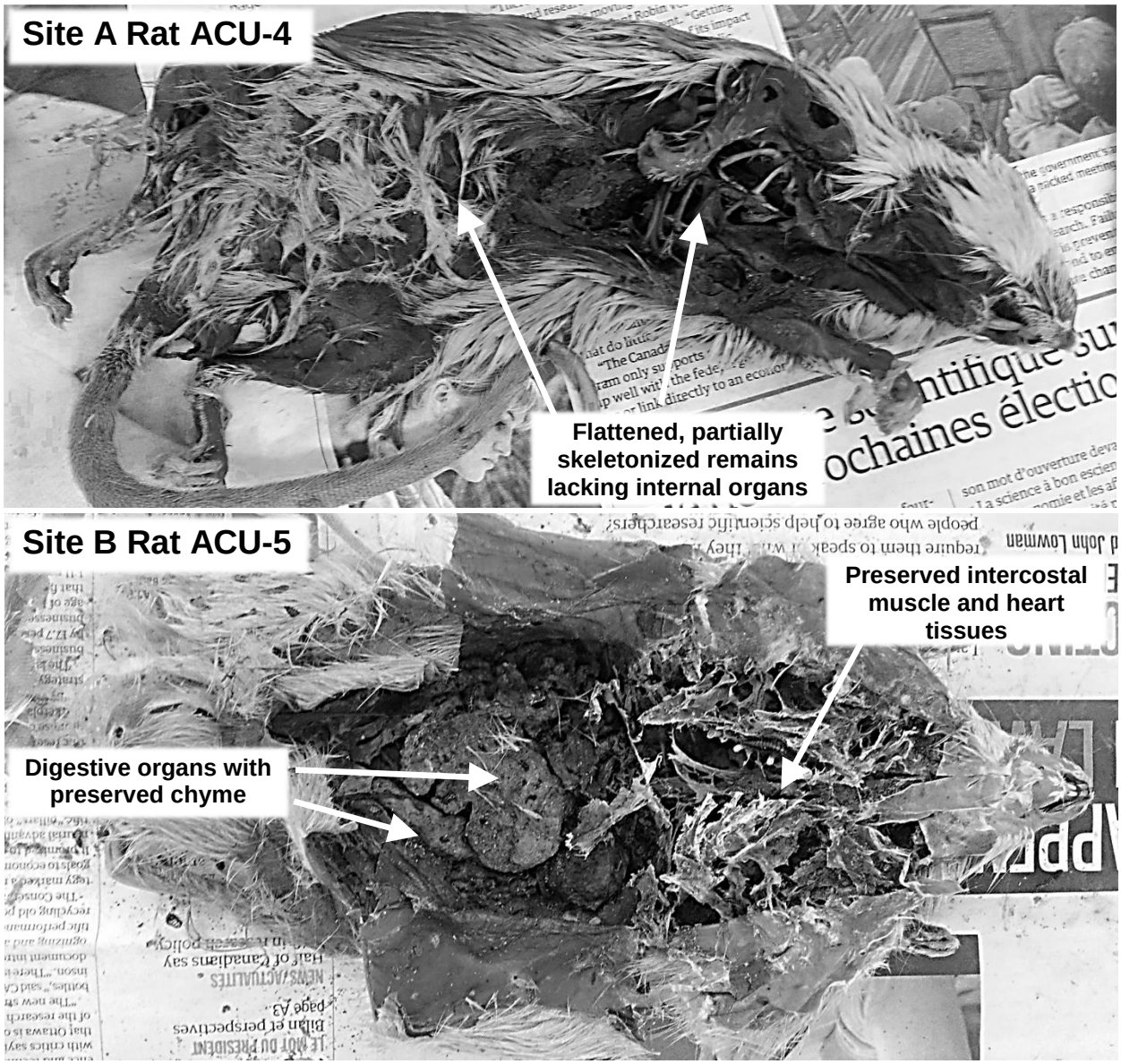

Figure 3.1: Differential conditions of rat remains following decomposition at Site A (forested) and Site B (exposed). Rats at Site A were partially skeletonized and lacked internal organs while Site B rats retained much of their muscle and internal organ tissues. The presence of undigested chyme in Site B rats indicates microbial action by digestive bacteria was supressed early on at Site B.

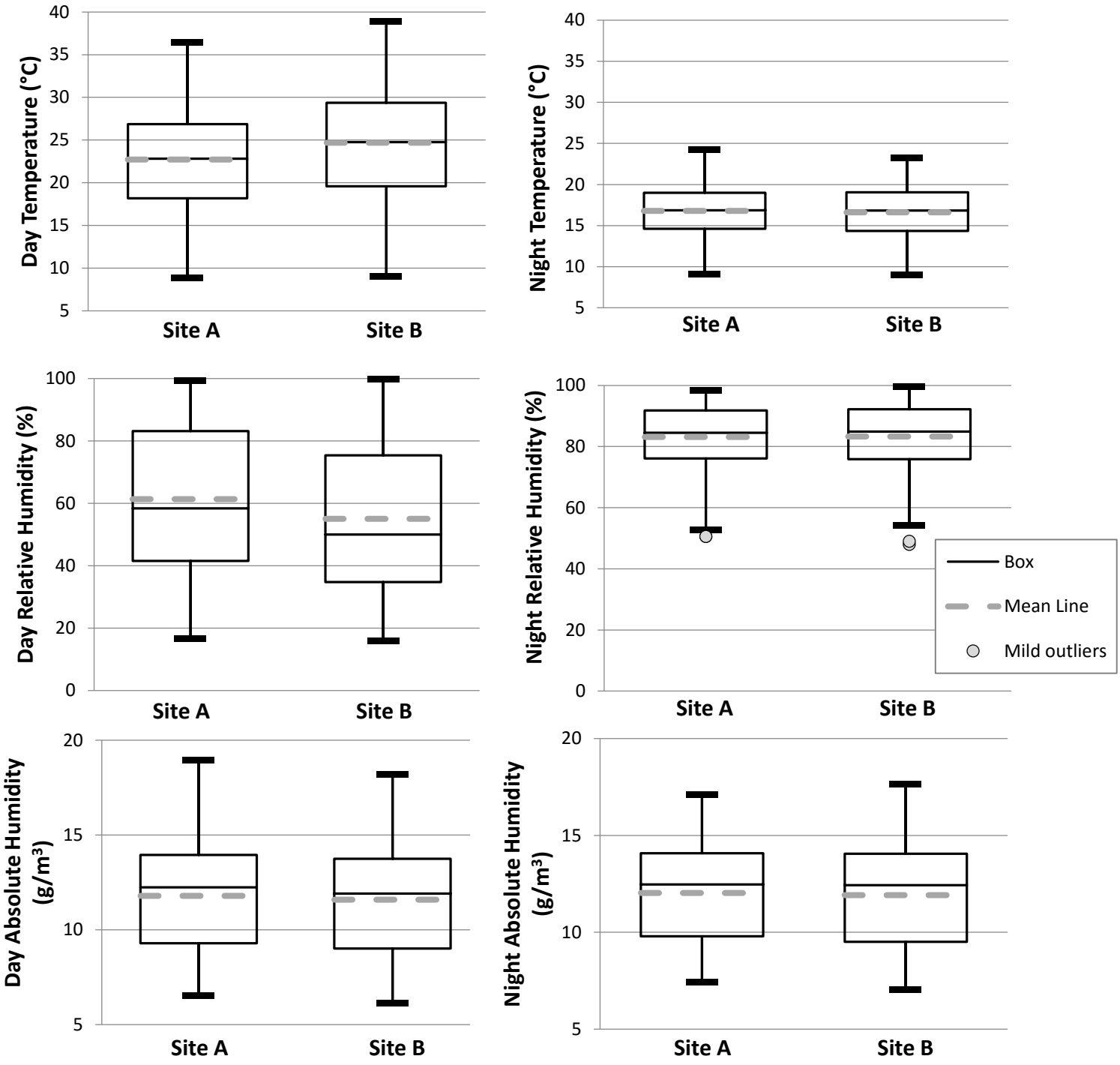

Figure 4.2: Distribution of microclimate parameters during day and night hours. Significant differences were observed between Sites A and B during daylight hours for temperature (p = 0.00002) and relative humidity (p = 0.0001) by MW U test analysis. No significant differences between sites are observed for night (sundown to sunup hours) microclimate measurements.

Differences in insect activity were also noted between microclimate sites. Loss of drugs from soft tissues due to insect activity (76–78) may impact post-mortem redistribution of drugs from liquefied remains on to the surfaces of, or in to, bones. Initial insect activity was higher at Site B than at Site A, the increase in insect activity may be due to rapid bloat and release of early decomposition products that was brought on by higher temperatures and sun exposure. Insect activity at Site B dropped off sharply as the study progressed and remained lesser than the insect action at Site A, especially for maggot presence and activity. The degree of insect activity will be influenced by the temperature and humidity of the environment. An experiment found hour long exposures to RH% and temperatures encountered during this study at Site B lethal to a number of arthropod species (79). If insects are indeed a factor in drug in bone responses, exclusion of insects by environmental conditions will limit any effect insects have on drug levels.

4.3 Comparing Bone and Blood Drug Responses

Some work has been done to establish corollary relationships with bone and blood drug concentrations. To test for this, blood was taken from each animal perimortem from all animals except ACU-A4, which perished prior to blood sampling. Correlations between blood and bone element RR/m values from each animal for DXM and DXT were assessed using Pearson correlation coefficients (R^2). Calculated R^2 values, means, coefficient of variance (CV%) and standard deviations of RR/m values are presented above in Table 3.3. Blood samples of 0.25 mL from each animal were spiked with 200 ng d3-DXM and d3-DXT internal standards and were prepared and extracted using the same methods for bone tissue extractions. As the density of blood is approximately 1.05 g/mL, volume was used to calculate mass normalized response ratios in blood (71). Only one (1/42) correlation of note, Site A DXT scapulae ($R^2 = 0.973$), was observed for all calculated blood to bone Pearson coefficient correlations.

Of all calculated R^2 values, 41/42 showed no significant correlation between blood and bone drug responses. The observed bone to blood correlations in this study reflect previous work (18, 31). The Site A DXT scapula correlation that appears significant may be due to insignificant sample size to achieve statistic validity given the lack of blood from Animal ACU-A4, or perhaps under these experimental conditions, DXT responses in Site A scapula elements approach an actual correlation. The processes that dictate drug sequestration in bone tissues are varied and complex and will be influenced by drug properties, post-mortem environment, variations in individual metabolic rates and other factors yet to be accounted for in drugs in bone studies (3, 4, 8, 10, 12, 14, 16, 17, 28, 29, 80, 81). Because all the factors that influence drug in bone levels have yet to be sufficiently addressed, any correlations made between blood and bone drug responses should be viewed with caution.

4.4 Drug in Bone Responses

Only one comparison, femoral DXM levels, displayed significant differences between microclimate sites (p = 0.047). Within bone element comparisons did not exhibit significant differences between microclimates for remaining DXM values, all DXT responses and all metabolite to drug ratios. Marked differences in microclimates and insect activities did not impact levels of DXM or DXT from bones recovered after differential decomposition. Drug distribution did not differ significantly between bone elements, contrary to what has been observed in previous work from our laboratory (12, 14, 18, 31). Observed drug distributions may reflect post-mortem properties of DXM and DXT, the metabolic rates of the species or individual rats used in this study (48, 80, 81), as well as the specific microclimate conditions encountered.

Estimated bone-drug concentrations were calculated from responses above LOQ values and standard curve plots, and then normalized for bone tissue sample masses. Estimated sample

concentrations are presented below in Table 4.1. Estimated concentrations of drugs in bone at Site A ranged from 399 to 10,474 ng/g for DXM and 142 to 3,045 ng/g for DXT. Site B concentrations ranged from 3,435 to 8,727 ng/g DXM and 133 to 3,668 ng/g DXT. These calculated concentrations are at best estimates given that solid matrices like bone tissues prevent conventional calibration or recovery measurements. All 70 experimental DXM values from both sites were above the LOQ values (25 ng) established during method validation. All DXT responses from Site B were above LOQ values (25 ng), while 29/35 Site A DXT values were above the LOQ. Though no statistically significant differences for any drug responses between sites were observed, the differences in absolute ranges of drug responses between sites A and B, in addition to the 6/35 Site A DXT values below LOQ may speak to some microclimate influences on drug distributions.

Although in previous studies (17, 18) the environment during decomposition has been shown to effect drug distributions in bone tissues, the lack of significant differences across microclimates observed here may be a function of DXM and DXT properties or insufficient numbers of samples used in this study. Patterns of drug-metabolite ratios observed in experiments in acute vs. repeated doses have been useful in discriminating between different drug dosing patterns (7, 82), and have been seen in decomposed bone tissues (12, 14, 18). Metabolite/parent ratios may offset variations in drug and metabolite measurements in different bones. The RR_{DXT}/RR_{DXM} values presented here can go to future work comparing drug-metabolite ratios between different dosing patterns and assessing the role of parent-metabolite ratios in accounting for the wide variations seen in toxicological analyses of drugs from different bone elements.

The results of this study show limited agreement with previous work on drug recoveries from decomposed bone tissues. The effect of environment on drug recoveries from bone has been

shown to have significant impact (17, 18), variations in this study across microclimates are not significant, however this may reflect insufficient sample size used in this study.

The degree of liquefaction of soft tissue remains may be a factor in the distribution of DXM or DXT in bone tissues. Drug presence in bone is hypothesized to reflect high marrow and trabecular bone contents as these offer the highest surface areas for drug into bone partitioning. Certain pharmaceuticals, like tetracycline have been shown to have "bone seeking" properties and can be sequestered in bone while low systemic concentrations are observed. (29). The affinity a given drug has for bone will affect the degree of distribution into bone tissues and potentially drug stability during decomposition and should be considered when interpreting drug responses in bone tissues. Different bone elements appear to be a factor in the distribution of DXM and DXT, though not to the significance seen in previous studies (12, 14, 16, 18, 31). The distribution and variation of drug levels in this study show that at best qualitative interpretations may be made from toxicological analyses of bone at this stage, until the viability of quantitative relationships between drug and metabolite levels may be more systematically investigated.

4.5 Validation Problems of 3-hydroxymorphinan

The recovery of 3-hydroxymorphinan (dmDXT) using the methods of this study was insufficient to meet validation requirements. Pure dmDXT standard in methanolic solutions for use in retention time standards showed substandard peak areas and lacked uniformity while DXM and DXT performed as expected, following previously published studies (9). Glass-drug interaction was suspected given that pure dmDXT drug standard was not appearing adequately in retention time standards. Retention time standard preparation methods were changed to address dmDXT recovery and 1 mL of drug-free, control bone tissue broth was evaporated to dryness to "line" the inside of the retention time test tube before the addition of drug standards and

derivatization. This was tried to test if dmDXT was interacting with and adhering to the glass walls of the test tubes used in the study. Retention time standard analysis benefited from the updated method and dmDXT peak widths and areas somewhat improved.

Recovery of dmDXT was poor in standard curve analyses and the validation of dmDXT was abandoned. However, dmDXT could still be identified by its retention time and mass spectra in experimental samples, though dmDXT peaks were often broad, irregular and sometimes unresolved. At the conclusion of this study, test tubes were silylated to further test for dmDXT-glass interactions. Retention time standards from pure drug standards (DXM, DXT and dmDXT) in standard and silylated tubes were prepared and analyzed by the GC/MS methods used in this study. No improvement in dmDXT peak shape and area were seen using silylated tubes. The results here may indicate that glass wall interactions with dmDXT may not the cause of poor dmDXT analyses. Testing different derivatizing agents may address the poor dmDXT results seen in this study. Given that DXT derivatization of the 3-hydroxy group (shared with dmDXT) gives reproducible results, the derivatization of the secondary amine group on dmDXT using the methods of this study may not be sufficient to provide required volatility for GC methods. For future GC studies, analysis of dmDXT may benefit from testing different derivatization agents.

4.6 Future Work

Without a large database of different drug responses and established standard methods, interpretation of quantitative measurements of drugs from bone tissues is not possible. The interpretation of drug responses in decomposed bone is difficult. Given the heterogeneity in bone morphology and physiology, genetic polymorphisms in metabolism, changes in stability and bone seeking properties across drugs, differences in biological and biochemical decomposition processes and the microclimate conditions present during decomposition, a number of factors

should be considered when interpreting drug responses in bone tissues (19, 27, 29, 67, 80, 81). Substantial variation in drug and metabolite responses may be corrected for by parent-metabolite ratios in some cases (12, 14, 82). It is important to include consideration of as many major metabolites as possible in such investigations. Here, the investigation was limited to the parent drug and only one metabolite, but the results can go to comparing administration patterns of DXM with its major metabolite DXT. Similar studies should be undertaken using larger sample sets to establish statistically sound patterns and trends across different microclimates to allow for the interpretation of drug responses from bone tissue analysis.

The use of new analytical methods should also be explored. Given the issues with dmDXT in this study, liquid chromatography methods with suitable detection instruments may benefit the analysis of DXM and its metabolites from biological samples by reducing sample preparation and eliminating derivatization steps. Recent advancements in analytical chemistry may make quantifying and identifying drugs, metabolites and endogenous compounds from a variety of biological or environmental sample matrices possible in single sample analyses from the atomic masses and mass spectra of analytes using Quadrupole Time-of-Flight (Q-Tof) UPLC/MS methods (83–88). Q-Tof methods may help to establish larger drug and metabolite databases that can aid the interpretation of metabolite-drug ratios from post-mortem tissue samples with regards to drug exposure patterns and potential microclimate effects.

CHAPTER 5

CONCLUSION

To our knowledge, this is the first study to establish closely measured microclimate parameter differences during decomposition for comparison of drug and metabolite distributions in bone tissues. The degree of soft tissue liquefaction may play a role in post-mortem redistribution of some drugs into bones, the environmental conditions during decomposition will determine the degree of liquefaction and insect activity on decaying remains. Significant differences in temperature and relative humidity are attributed to divergent sun exposures at the decomposition sites as microclimate differences are only seen during daylight hours. Environment has been shown to effect recoveries of drugs from bone tissues, though the results of this study contrast previously seen trends. Distributions across different bones and environments may not be a significant factor to consider in drug recoveries for certain drugs, which may reflect a drugs affinity for bone. Future work across distinct microclimates and with different drugs should be undertaken to go towards building a database of drug and metabolite responses to aid in interpretations of drugs and drug exposure patterns in decomposed skeletal remains.

REFERENCES

1. Hoecker, F.E. and Roofe, P.G. (1951) Studies of Radium in Human Bone. *Radiology*, **56**, 89–98.

2. Neuman, W.F., Hursh, J.B., Boyd, J. and Hodge, H.C. (1955) On the Mechanism of Skeletal Fixation of Radium. *Annals of the New York Academy of Sciences*, **62**, 125–136.

3. Rabinowitz, M.B. (1991) Toxicokinetics of Bone Lead. *Environmental Health Perspectives*, **91**, 33.

4. Hu, H., Rabinowitz, M. and Smith, D. (1998) Bone lead as a biological marker in epidemiologic studies of chronic toxicity: conceptual paradigms. *Environmental Health Perspectives*, **106**, 1–8.

5. Noguchi, T.T., Nakamura, G.R. and Griesemer, E.C. (1978) Drug analyses of skeletonizing remains. *Journal of Forensic Sciences*, **23**, 490–492.

6. Kojima, T., Okamoto, I., Miyazaki, T., Chikasue, F., Yashiki, M. and Nakamura, K. (1986) Detection of methamphetamine and amphetamine in a skeletonized body buried for 5 years. *Forensic Science International*, **31**, 93–102.

7. Bynum, N.D., Poklis, J.L., Gaffney-Kraft, M., Garside, D. and Ropero-Miller, J.D. (2005) Postmortem Distribution of Tramadol, Amitriptyline, and Their Metabolites in a Suicidal Overdose. *Journal of Analytical Toxicology*, **29**, 401–406.

8. McGrath, K.K. and Jenkins, A.J. (2009) Detection of drugs of forensic importance in postmortem bone. *The American Journal of Forensic Medicine and Pathology*, **30**, 40–44.

9. Fraser, C.D., Cornthwaite, H.M. and Watterson, J.H. (2015) Analysis of dextromethorphan and dextrorphan in decomposed skeletal tissues by microwave assisted extraction, microplate solid-phase extraction and gas chromatography- mass spectrometry (MAE-MPSPE-GCMS). *Drug Testing and Analysis*, **7**, 708–713.

10. Watterson, J.H. and Botman, J.E. (2009) Detection of Acute Diazepam Exposure in Bone and Marrow: Influence of Tissue Type and the Dose-Death Interval on Sensitivity of Detection by ELISA with Liquid Chromatography Tandem Mass Spectrometry Confirmation*. *Journal of Forensic Sciences*, **54**, 708–714.

11. Lafrenière, N.M. and Watterson, J.H. (2009) Detection of acute fentanyl exposure in fresh and decomposed skeletal tissues. *Forensic Science International*, **185**, 100–106.

12. Desrosiers, N.A., Watterson, J.H., Dean, D. and Wyman, J.F. (2012) Detection of amitriptyline, citalopram, and metabolites in porcine bones following extended outdoor decomposition. *Journal of Forensic Sciences*, **57**, 544–549.

13. Cengiz, S., Ulukan, Ö., Ates, I. and Tugcu, H. (2006) Determination of morphine in postmortem rabbit bone marrow and comparison with blood morphine concentrations. *Forensic Science International*, **156**, 91–94.

14. Watterson, J.H. and Cornthwaite, H.M. (2013) Discrimination Between Patterns of Drug Exposure by Toxicological Analysis of Decomposed Skeletal Tissues. Part II: Amitriptyline and Citalopram. *Journal of Analytical Toxicology*, **37**, 565–572.

15. Cornthwaite, H.M. and Watterson, J.H. (2014) Microwave assisted extraction of ketamine and its metabolites from skeletal tissues. *Analytical Methods*, **6**, 1142–1148.

16. Watterson, J.H., Desrosiers, N.A., Betit, C.C., Dean, D. and Wyman, J.F. (2010) Relative Distribution of Drugs in Decomposed Skeletal Tissue. *Journal of Analytical Toxicology*, **34**, 510–515.

17. Desrosiers, N.A. and Watterson, J.H. (2010) The effects of burial on drug detection in skeletal tissues. *Drug Testing and Analysis*, **2**, 346–356.

18. Cornthwaite, H.M. and Watterson, J.H. (2014) The Influence of Body Position and Microclimate on Ketamine and Metabolite Distribution in Decomposed Skeletal Remains. *Journal of Analytical Toxicology*, **38**, 548–554.

19. Vass, A.A., Barshick, S.-A., Sega, G., Caton, J., Skeen, J.T., Love, J.C., et al. (2002) Decomposition chemistry of human remains: a new methodology for determining the postmortem interval. *Journal of Forensic Sciences*, **47**, 542–553.

20. Jans, M.M.E. (2008) Microbial bioerosion of bone – a review. In Wisshak, M., Tapanila, L. (eds), Current Developments in Bioerosion. Springer Berlin Heidelberg, pp. 397–413. http://link.springer.com/chapter/10.1007/978-3-540-77598-0_20 (16 December 2015).

21. Kudo, K., Sugie, H., Syoui, N., Kurihara, K., Jitsufuchi, N., Imamura, T., et al. (1997) Detection of triazolam in skeletal remains buried for 4 years. *International Journal of Legal Medicine*, **110**, 281–283.

22. Horak, E.L. and Jenkins, A.J. (2005) Postmortem Tissue Distribution of Olanzapine and Citalopram in a Drug Intoxication. *Journal of Forensic Sciences*, **50**, 1–3.

23. Drummer, O.H. (2004) Postmortem toxicology of drugs of abuse. *Forensic Science International*, **142**, 101–113.

24. Wyman, J.F., Dean, D.E., Yinger, R., Simmons, A., Brobst, D., Bissell, M., et al. (2011) The Temporal Fate of Drugs in Decomposing Porcine Tissue*. *Journal of Forensic Sciences*, **56**, 694–699.

25. Winek, C.L., Westwood, S.E. and Wahba, W.W. (1990) Plasma versus bone marrow desipramine: a comparative study. *Forensic Science International*, **48**, 49–57.

26. Guillot, E., de Mazancourt, P., Durigon, M. and Alvarez, J.-C. (2007) Morphine and 6-acetylmorphine concentrations in blood, brain, spinal cord, bone marrow and bone after lethal acute or chronic diacetylmorphine administration to mice. *Forensic Science International*, **166**, 139–144.

27. Wu, D., Otton, S.V., Kalow, W. and Sellers, E.M. (1995) Effects of route of administration on dextromethorphan pharmacokinetics and behavioral response in the rat. *Journal of Pharmacology and Experimental Therapeutics*, **274**, 1431–1437.

28. Bailey, B., Daneman, R., Daneman, N., Mayer, J.M. and Koren, G. (2000) Discrepancy between CYP2D6 phenotype and genotype derived from post-mortem dextromethorphan blood level. *Forensic Science International*, **110**, 61–70.

29. Stepensky, D., Kleinberg, L. and Hoffman, P.A. (2012) Bone as an Effect Compartment. *Clinical Pharmacokinetics*, **42**, 863–881.

30. Manual of Forensic Taphonomy. https://books.google.ca/books/about/Manual_of_Forensic_Taphonomy.html?id=dQfSBQAAQBAJ (15 November 2015).

31. Watterson, J.H., Donohue, J.P. and Betit, C.C. (2012) Comparison of relative distribution of ketamine and norketamine in decomposed skeletal tissues following single and repeated exposures. *Journal of Analytical Toxicology*, **36**, 429–433.

32. Walker, F.O. and Hunt, V.P. (1989) An Open Laboratoryel Trial of Dextromethorphan in Huntington's Disease. [Review]. *Clinical Neuropharmacology*, **12**, 322–330.

33. Bonuccelli, U., Del Dotto, P., Piccini, P., Behgé, F., Corsini, G.U. and Muratorio, A. (1992) Dextromethorphan and parkinsonism. *Lancet (London, England)*, **340**, 53.

34. Fisher, R.S., Cysyk, B.J., Lesser, R.P., Pontecorvo, M.J., Ferkany, J.T., Schwerdt, P.R., et al. (1990) Dextromethorphan for treatment Of complex partial seizures. *Neurology*, **40**, 547–547.

35. Tortella, F.C., Pellicano, M. and Bowery, N.G. (1989) Dextromethorphan and neuromodulation: old drug coughs up new activities. *Trends in Pharmacological Sciences*, **10**, 501–507.

36. Tortella, F.C. and Musacchio, J. (1986) Dextromethorphan and carbetapentane: centrally acting non-opioid antitussive agents with novel anticonvulsant properties. *Brain Research*, **383**, 314–318.

37. Bem, D.J.L. and Peck, R. (2012) Dextromethorphan. *Drug Safety*, **7**, 190–199.

38. Hinsberger, A., Sharma, V. and Mazmanian, D. (1994) Cognitive deterioration from long-term abuse of dextromethorphan: a case report. *Journal of Psychiatry and Neuroscience*, **19**, 375–377.

39. Degkwitz, R. (1964) Dextromethorphan (Romilar) and an Intoxicating Agent. *Der Nervenarzt*, **35**, 412–414.

40. Fleming, P.M. (1986) Dependence on dextromethorphan hydrobromide. *BMJ*, **293**, 597–597.

41. Rammer, L., Holmgren, P. and Sandler, H. (1988) Fatal intoxication by dextromethorphan: A report on two cases. *Forensic Science International*, **37**, 233–236.

42. Logan, B.K., Goldfogel, G., Hamilton, R. and Kuhlman, J. (2009) Five Deaths Resulting from Abuse of Dextromethorphan Sold Over the Internet. *Journal of Analytical Toxicology*, **33**, 99–103.

43. Regenthal, R., Krueger, M., Koeppel, C. and Preiss, R. (1999) Drug Levels: Therapeutic and Toxic Serum/Plasma Concentrations of Common Drugs. *Journal of Clinical Monitoring and Computing*, **15**, 529–544.

44. Dalpe-Scott, M., Degouffe, M., Garbutt, D. and Drost, M. (1995) A comparison of drug concentrations in postmortem cardiac and peripheral blood in 320 cases. *Journal (Canadian Society of Forensic Science)*, **28**, 113–121.

45. Székely, J.I., Sharpe, L.G. and Jaffe, J.H. (1991) Induction of phencyclidine-like behavior in rats by dextrorphan but not dextromethorphan. *Pharmacology Biochemistry and Behavior*, **40**, 381–386.

46. Holtzman, S.G. (1994) Discriminative stimulus effects of dextromethorphan in the rat. *Psychopharmacology*, **116**, 249–254.

47. Nicholson, K.L., Hayes, B.A. and Balster, R.L. (1999) Evaluation of the reinforcing properties and phencyclidine-like discriminative stimulus effects of dextromethorphan and dextrorphan in rats and rhesus monkeys. *Psychopharmacology*, **146**, 49–59.

48. Ishmael, J.E., Franklin, P.H. and Murray, T.F. (1998) Dextrorotatory opioids induce stereotyped behavior in Sprague-Dawley and Dark Agouti rats. *Psychopharmacology*, **140**, 206–216.

49. Newman, A.H., Bevan, K., Bowery, N. and Tortella, F.C. (1992) Synthesis and evaluation of 3-substituted 17-methylmorphinan analogs as potential anticonvulsant agents. *Journal of Medicinal Chemistry*, **35**, 4135–4142.

50. Murray, T.F. and Leid, M.E. (1984) Interaction of dextrorotatory opioids with phencyclidine recognition sites in rat brain membranes. *Life Sciences*, **34**, 1899–1911.

51. Furukawa, H., Singh, S.K., Mancusso, R. and Gouaux, E. (2005) Subunit arrangement and function in NMDA receptors. *Nature*, **438**, 185–192.

52. Vollenweider, F.X. and Kometer, M. (2010) The neurobiology of psychedelic drugs: implications for the treatment of mood disorders. *Nature Reviews Neuroscience*, **11**, 642–651.

53. Reissig, C.J., Carter, L.P., Johnson, M.W., Mintzer, M.Z., Klinedinst, M.A. and Griffiths, R.R. (2012) High doses of dextromethorphan, an NMDA antagonist, produce effects similar to classic hallucinogens. *Psychopharmacology*, **223**, 1–15.

54. Jocelyn Paré, J.R., Bélanger, J.M.R. and Stafford, S.S. (1994) Microwave-assisted process (MAP^{TM}): a new tool for the analytical laboratoryoratory. *Trends in Analytical Chemistry*, **13**, 176–184.

55. Desrosiers, N.A., Betit, C.C. and Watterson, J.H. (2009) Microwave-assisted extraction in toxicological screening of skeletal tissues. *Forensic Science International*, **188**, 23–30.

56. Ganzler, K., Salgó, A. and Valkó, K. (1986) Microwave extraction : A novel sample preparation method for chromatography. *Journal of Chromatography A*, **371**, 299–306.

57. Mandal, V., Mohan, Y. and Hemalatha, S. (2007) Microwave assisted extraction - An innovative and promising extraction tool for medicinal plant research. *Pharmacognosy Reviews*, **1**, 7.

58. Renoe, B.W. (1994) Microwave Assisted Extraction. *American Laboratoryoratory*, **26**, 34–40.

59. Letellier, M. and Budzinski, H. (1999) Microwave assisted extraction of organic compounds. *Analusis*, **27**, 259–270.

60. Introduction to Gas Chromatography (2013) In Forensic Applications of Gas Chromatography. CRC Press, pp. 1–4. http://www.crcnetbase.com/doi/abs/10.1201/b14954-2 (16 December 2015).

61. Bartle, K.D. and Myers, P. (2002) History of gas chromatography. *Trends in Analytical Chemistry*, **21**, 547–557.

62. Welsch, T., Müller, R., Engewald, W. and Werner, G. (1982) Surface modification of glass capillaries by high-temperature silylation. *Journal of Chromatography A*, **241**, 41–48.

63. Levine, B. (2010) Principles of Forensic Toxicology. American Association for Clinical Chemistry, Washington, DC.

64. Regent Technologies (2000) GC Derivatization. June 2000. https://www.chromspec.com/pdf/gc_derivatization_methods.pdf (16 December 2015).

65. Megyesi, M.S., Nawrocki, S.P. and Haskell, N.H. (2005) Using Accumulated Degree-Days to Estimate the Postmortem Interval from Decomposed Human Remains. *Journal of Forensic Sciences*, **50**, 1–9.

66. Michaud, J.-P. and Moreau, G. (2011) A Statistical Approach Based on Accumulated Degree-days to Predict Decomposition-related Processes in Forensic Studies*,†. *Journal of Forensic Sciences*, **56**, 229–232.

67. Vass, A.A. (2011) The elusive universal post-mortem interval formula. *Forensic Science International*, **204**, 34–40.

68. Dabbs, G.R. (2010) Caution! All data are not created equal: The hazards of using National Weather Service data for calculating accumulated degree days. *Forensic Science International*, **202**, e49–e52.

69. Gates, D.M. (1962) Energy exchange in the biosphere. Harper & Row.

70. Scientific Working Group for Forensic Toxicology (SWGTOX) (2013) Standard Practices for Method Validation in Forensic Toxicology. *Journal of Analytical Toxicology*, **37**, 452–474.

71. Wiebe, T. (2013) Differentiation of Acute and Repeated Tramadol Exposures in Skeletal Tissues by Gas Chromatography-Mass Spectrometry. 2013.

72. Greenspan, L. (1977) Humidity fixed points of binary saturated aqueous solutions. *J of Research, National Bureau of Standards*, 1977.

73. Bolton, D. (1980) The Computation of Equivalent Potential Temperature. *Monthly Weather Review*, **108**, 1046–1053.

74. Hall, S.J., Learned, J., Ruddell, B., Larson, K.L., Cavender-Bares, J., Bettez, N., et al. (2015) Convergence of microclimate in residential landscapes across diverse cities in the United States. *Landscape Ecology*, **31**, 101–117.

75. Canada, E. (2011) Historical Climate Data - Environment Canada. October 31, 2011. http://climate.weather.gc.ca/climateData/hourlydata_e.html?timeframe=1&Prov=ON&StationID=49508&hlyRange=2011-08-04|2016-01-17&Year=2015&Month=7&Day=1 (19 January 2016).

76. Gosselin, M., Fernandez, M. del M.R., Wille, S.M.R., Samyn, N., Boeck, G.D. and Bourel, B. (2010) Quantification of Methadone and its Metabolite 2-Ethylidene-1,5-dimethyl-3,3-diphenylpyrrolidine in Third Instar Larvae of Lucilia sericata (Diptera: Calliphoridae) Using Liquid Chromatography-Tandem Mass Spectrometry. *Journal of Analytical Toxicology*, **34**, 374–380.

77. Gunn, J.A., Shelley, C., Lewis, S.W., Toop, T. and Archer, M. (2006) The Determination of Morphine in the Larvae of Calliphora stygia using Flow Injection Analysis and HPLC with Chemiluminescence Detection. *Journal of Analytical Toxicology*, **30**, 519–523.

78. Bourel, B., Tournel, G., Hedouin, V., Deveaux, M., Goff, M.L. and Gosset, D. (2001) Morphine extraction in necrophagous insects remains for determining ante-mortem opiate intoxication. *Forensic Science International*, **120**, 127–131.

79. Edney, E.B. (1951) The Evaporation of Water from Woodlice and the Millipede Glomeris. *Journal of Experimental Biology*, **28**, 91–115.

80. Mortimer, O., Lindstrom, B., Laurell, H., Bergman, U. and Rane, A. (1989) Dextromethorphan: polymorphic serum pattern of the O-demethylated and didemethylated metabolites in man. *British Journal of Clinical Pharmacology*, **27**, 223–227.

81. Pfaff, G., Briegel, P. and Lamprecht, I. (1983) Inter-individual variation in the metabolism of dextromethorphan. *International Journal of Pharmaceutics*, **14**, 173–189.

82. Bailey, D.N. and Shaw, R.F. (1979) Tricyclic Antidepressants: Interpretation of Blood and Tissue Levels in Fatal Overdose. *Journal of Analytical Toxicology*, **3**, 43–46.

83. Chindarkar, N.S., Park, H.-D., Stone, J.A. and Fitzgerald, R.L. (2015) Comparison of Different Time of Flight-Mass Spectrometry Modes for Small Molecule Quantitative Analysis. *Journal of Analytical Toxicology*, **39**, 675–685.

84. Fardet, A., Llorach, R., Martin, J.-F., Besson, C., Lyan, B., Pujos-Guillot, E., et al. (2008) A Liquid Chromatography−Quadrupole Time-of-Flight (LC−QTOF)-based Metabolomic Approach Reveals New Metabolic Effects of Catechin in Rats Fed High-Fat Diets. *Journal of Proteome Research*, **7**, 2388–2398.

85. Paglia, G., Hrafnsdóttir, S., Magnúsdóttir, M., Fleming, R.M.T., Thorlacius, S., Palsson, B.Ø., et al. (2011) Monitoring metabolites consumption and secretion in cultured cells using ultra-performance liquid chromatography quadrupole–time of flight mass spectrometry (UPLC–Q–ToF-MS). *Analytical and Bioanalytical Chemistry*, **402**, 1183–1198.

86. Bijlsma, L., Sancho, J.V., Hernández, F. and Niessen, W.M.A. (2011) Fragmentation pathways of drugs of abuse and their metabolites based on QTOF MS/MS and MSE accurate-mass spectra. *Journal of Mass Spectrometry*, **46**, 865–875.

87. Okada, T., Nakamura, Y., Kanaya, Y., Takano, A., Malla, K.J., Nakane, J., et al. (2009) Metabolome analysis of Ephedra plants with different contents of ephedrine alkaloids by using UPLC-Q-TOF-MS. *Planta medica*, **75**, 1356–1362.

88. Xie, C., Zhong, D., Yu, K. and Chen, X. (2012) Recent advances in metabolite identification and quantitative bioanalysis by LC–Q-TOF MS. *Bioanalysis*, **4**, 937–959.

APPENDIX

Appendix I:

Microclimate Data

Table A1.1 Microclimate Parameters Temperature, Relative Humidity and Absolute Humidity

Date/Time:	Site A Low Temp (°C)	Site B Low Temp (°C)	Site A Low RH (%)	Site B Low RH (%)	Site A Low AH (g/m^3)	Site B Low AH (g/m^3)
2015-07-07 10:00	23.51	23.36	52.1	52.6	11.1	11
2015-07-07 11:00	23.48	23.39	52.7	53.7	11.2	11.2
2015-07-07 12:00	23.7	23.68	50.6	51.6	10.8	11
2015-07-07 13:00	23.75	23.68	50.1	50.6	10.7	10.8
2015-07-07 14:00	23.56	23.53	49.6	50	10.6	10.6
2015-07-07 15:00	17.78	23.34	73.6	48	11.2	10
2015-07-07 16:00	17.07	22.04	72.7	54.7	10.6	10.7
2015-07-07 17:00	16.31	17.12	73.6	70.1	10.3	10.2
2015-07-07 18:00	15.52	16	71.2	70.6	9.5	9.6
2015-07-07 19:00	16.54	17.19	67.1	64	9.3	9.3
2015-07-07 20:00	15.78	16.33	70.7	67.1	9.4	9.3
2015-07-07 21:00	14.75	14.87	68.6	68.1	8.7	8.6
2015-07-07 22:00	12.66	13.15	88.5	78.9	9.8	9.1
2015-07-07 23:00	11.38	10.94	91.8	88.9	9.4	8.9
2015-07-08 0:00	10.92	10.23	92.6	91	9.3	8.7
2015-07-08 1:00	11.16	10.11	93.8	94.2	9.4	9
2015-07-08 2:00	10.77	9.94	95	95.7	9.3	8.9
2015-07-08 3:00	10.06	9.52	95	96.1	9	8.7
2015-07-08 4:00	10.01	9.52	96.5	97.2	9	8.8
2015-07-08 5:00	9.99	8.95	95.7	96.4	8.9	8.5
2015-07-08 6:00	9.45	9.12	96.8	97.2	8.8	8.6
2015-07-08 7:00	10.43	10.55	96.5	96.4	9.4	9.4
2015-07-08 8:00	12.04	13.36	92.2	87.1	9.9	10.1
2015-07-08 9:00	14.4	17.12	79.9	65.6	9.9	9.6
2015-07-08 10:00	16.5	20.57	70.2	58.3	9.8	10.4
2015-07-08 11:00	18.78	22.88	58.4	48.5	9.3	9.9
2015-07-08 12:00	20.38	24.08	45.9	33.8	8	7.4
2015-07-08 13:00	22.07	25.75	36.3	29.9	7.1	7.1
2015-07-08 14:00	23.84	27.15	35.3	29	7.7	7.5
2015-07-08 15:00	27	27.61	26.2	27.1	6.8	7.2
2015-07-08 16:00	29.88	27.93	23	28	6.9	7.6
2015-07-08 17:00	27.98	27.66	25.7	24.4	7	6.5
2015-07-08 18:00	26.07	25.37	28.5	29.9	6.9	6.9
2015-07-08 19:00	23.58	22.62	40.3	42.3	8.6	8.4
2015-07-08 20:00	21.02	20.54	50.1	49	9.1	8.7
2015-07-08 21:00	18.73	18.12	58.4	57.3	9.3	8.9
2015-07-08 22:00	17.02	16.83	69.7	65.6	10.2	9.4
2015-07-08 23:00	16.57	16.24	73.1	68.6	10.2	9.6

Date/Time:	Site A Low Temp (°C)	Site B Low Temp (°C)	Site A Low RH (%)	Site B Low RH (%)	Site A Low AH (g/m^3)	Site B Low AH (g/m^3)
2015-07-09 0:00	15.88	15.3	74.6	73.1	10.2	9.5
2015-07-09 1:00	14.75	14.28	80.9	78	10.3	9.5
2015-07-09 2:00	14.06	13.8	85	82.2	10.3	9.7
2015-07-09 3:00	13.46	13.29	86.3	84	10	9.7
2015-07-09 4:00	12.83	12.76	88	88	9.9	9.9
2015-07-09 5:00	12.4	12.33	90.6	89.3	10	9.6
2015-07-09 6:00	12.16	12.11	91.4	91.8	9.8	9.9
2015-07-09 7:00	12.54	12.83	92.6	90.5	10.2	10.2
2015-07-09 8:00	14.71	16.31	84.5	73.1	10.7	10.2
2015-07-09 9:00	16.69	21.19	68.6	52.6	9.8	9.8
2015-07-09 10:00	18.28	21.64	57.9	48.5	9	9.3
2015-07-09 11:00	19.3	22.4	55.3	46.4	9.2	9.3
2015-07-09 12:00	19.95	24.76	56.3	40.8	9.6	9.3
2015-07-09 13:00	22.98	27.69	38.3	31.9	7.8	8.4
2015-07-09 14:00	24.64	29.05	34.8	29	7.9	8.4
2015-07-09 15:00	27.91	29.2	32.9	28	8.9	8.1
2015-07-09 16:00	29.25	28.65	29.5	30.4	8.5	8.6
2015-07-09 17:00	28.95	30.18	29	27.6	8.4	8.5
2015-07-09 18:00	25.54	26.02	35.3	32.8	8.4	8
2015-07-09 19:00	24.33	24.28	37.3	37.8	8.3	8.4
2015-07-09 20:00	22.38	21.88	53.7	56.3	10.7	10.7
2015-07-09 21:00	20.28	19.47	62.5	64.5	10.9	10.8
2015-07-09 22:00	18.4	17.57	72.7	74.1	11.3	11.1
2015-07-09 23:00	17.52	16.66	76.6	78.9	11.4	11.2
2015-07-10 0:00	16.69	15.78	79.9	84.5	11.4	11.2
2015-07-10 1:00	15.93	14.99	84.1	87.6	11.5	11.1
2015-07-10 2:00	14.78	14.25	88.9	91	11.3	11
2015-07-10 3:00	14.64	13.8	91.8	93.8	11.4	11.1
2015-07-10 4:00	14.3	13.56	91	93.8	11.3	11.1
2015-07-10 5:00	13.82	13.2	91.4	93.8	10.8	10.8
2015-07-10 6:00	13.46	12.59	92.6	94.5	10.7	10.4
2015-07-10 7:00	13.63	13.92	92.6	90.5	11	11
2015-07-10 8:00	15.5	17.16	81.8	75.6	10.9	11
2015-07-10 9:00	17.69	21.93	71.7	54.2	10.7	10.6
2015-07-10 10:00	19.38	24.54	59.9	46.4	10	10.3
2015-07-10 11:00	20.95	27.57	57.3	38.3	10.5	10.1
2015-07-10 12:00	23.1	29.38	54.2	38.8	11.3	11.4
2015-07-10 13:00	26.05	31.22	47.5	35.8	11.5	11.5
2015-07-10 14:00	27.22	32.03	43.4	33.3	11.2	11.2
2015-07-10 15:00	29.85	32.5	36.8	30.4	11.1	10.4
2015-07-10 16:00	32.32	32.42	34.8	32.8	12	11.3

Date/Time:	Site A Low Temp (°C)	Site B Low Temp (°C)	Site A Low RH (%)	Site B Low RH (%)	Site A Low AH (g/m^3)	Site B Low AH (g/m^3)
2015-07-10 17:00	29.93	30.76	40.3	38.3	12.2	12.1
2015-07-10 18:00	28.36	27.76	42.3	43.3	11.7	11.7
2015-07-10 19:00	26.1	25.97	49	50	11.9	12.1
2015-07-10 20:00	24.25	24.16	53.2	54.2	11.8	11.8
2015-07-10 21:00	22.4	22.16	61.5	63	12.3	12.3
2015-07-10 22:00	21.45	20.85	64.1	66.6	12	12.2
2015-07-10 23:00	20.21	19.66	71.2	73.6	12.4	12.6
2015-07-11 0:00	19.23	18.54	75.1	77.5	12.3	12.4
2015-07-11 1:00	18.59	17.88	77.5	81.3	12.4	12.4
2015-07-11 2:00	17.88	17.09	80.9	85.4	12.3	12.5
2015-07-11 3:00	17.21	16.38	85	88.4	12.4	12.3
2015-07-11 4:00	16.85	16.09	87.6	90.5	12.5	12.3
2015-07-11 5:00	16.4	15.66	89.8	93	12.5	12.4
2015-07-11 6:00	16.26	15.54	91.8	94.2	12.8	12.5
2015-07-11 7:00	16.59	16.66	90.2	91.8	12.9	13.1
2015-07-11 8:00	17.73	19.16	85.4	80.8	13	13.2
2015-07-11 9:00	19.64	23.94	77.5	63	13.2	13.7
2015-07-11 10:00	22	27.74	71.7	52.1	14	14.1
2015-07-11 11:00	24.45	30.51	61.5	44.4	13.7	13.7
2015-07-11 12:00	26.63	32.42	55.3	40.3	14	13.8
2015-07-11 13:00	29	34.27	47	34.8	13.6	13.3
2015-07-11 14:00	30.63	33.61	43.4	35.3	13.7	13
2015-07-11 15:00	32.34	33.69	38.3	35.3	13.2	13
2015-07-11 16:00	33.93	33.79	33.3	33.8	12.5	12.4
2015-07-11 17:00	32.03	32.73	38.3	34.8	12.9	12.2
2015-07-11 18:00	30.2	29.73	40.8	42.8	12.6	12.9
2015-07-11 19:00	27.52	27.52	49	49.5	13	13.1
2015-07-11 20:00	25.97	25.68	54.7	55.2	13.3	13.1
2015-07-11 21:00	24.37	23.75	62.5	64	13.9	13.6
2015-07-11 22:00	22.91	21.95	71.7	74.6	14.6	14.5
2015-07-11 23:00	22.02	20.95	73.1	78.4	14.3	14.3
2015-07-12 0:00	21.14	20.02	76.6	82.2	14	14.4
2015-07-12 1:00	20.4	19.19	83.6	87.1	14.9	14.2
2015-07-12 2:00	19.71	18.5	85.9	90.1	14.7	14.4
2015-07-12 3:00	18.92	17.71	87.2	93	14.2	13.9
2015-07-12 4:00	18.69	17.47	91.4	94.5	14.6	14.1
2015-07-12 5:00	17.97	16.95	93	95.3	14.2	13.6
2015-07-12 6:00	17.73	16.78	92.2	95.3	14.1	13.6
2015-07-12 7:00	17.88	17.83	92.6	94.2	14.1	14.4
2015-07-12 8:00	19.66	20.85	89.8	84.5	15.3	15.4
2015-07-12 9:00	21.3	25.49	83.6	66.1	15.6	15.7

Date/Time:	Site A Low Temp (°C)	Site B Low Temp (°C)	Site A Low RH (%)	Site B Low RH (%)	Site A Low AH (g/m^3)	Site B Low AH (g/m^3)
2015-07-12 10:00	23.41	28.85	77.5	54.7	16.1	15.5
2015-07-12 11:00	25.8	32.19	61.5	41.3	14.9	14.2
2015-07-12 12:00	27.74	33.66	54.2	35.3	14.7	13
2015-07-12 13:00	29.65	35.38	44.4	30.9	13.1	12.4
2015-07-12 14:00	31.7	36.37	39.8	28	13.1	12
2015-07-12 15:00	32.75	35.27	37.8	28	13.3	11.2
2015-07-12 16:00	33.17	34.74	46.5	32.3	16.7	12.7
2015-07-12 17:00	31.83	32.73	43.9	36.8	14.8	12.9
2015-07-12 18:00	30.99	29.83	40.3	43.3	13	13.1
2015-07-12 19:00	28.36	27.34	48	45.4	13.3	12
2015-07-12 20:00	26.39	25.93	50.1	50	12.4	12.1
2015-07-12 21:00	24.11	23.99	65.1	62	14.2	13.5
2015-07-12 22:00	21.81	21.61	76.1	75.1	14.5	14.3
2015-07-12 23:00	20.59	20.52	82.7	77	14.8	13.7
2015-07-13 0:00	20.21	19.73	83.6	78.4	14.6	13.4
2015-07-13 1:00	19.54	19.02	84.5	82.7	14.1	13.5
2015-07-13 2:00	18.92	18.5	85.9	85.8	14	13.7
2015-07-13 3:00	18.07	17.88	87.6	89.7	13.4	13.7
2015-07-13 4:00	17.16	17.47	89.8	90.5	13.1	13.5
2015-07-13 5:00	16.59	16.83	90.6	93	12.9	13.3
2015-07-13 6:00	15.85	16.5	90.6	88.9	12.3	12.4
2015-07-13 7:00	16.95	18.04	91.4	86.3	13	13.2
2015-07-13 8:00	18.66	19.76	85	78.4	13.6	13.4
2015-07-13 9:00	20.97	24.3	75.1	62	13.7	13.8
2015-07-13 10:00	22.86	27.57	71.7	52.6	14.6	13.9
2015-07-13 11:00	24.69	29.7	61.5	44.9	14	13.2
2015-07-13 12:00	25.8	30.63	52.7	38.8	12.8	12.2
2015-07-13 13:00	28.13	30.73	43.4	34.3	12	10.8
2015-07-13 14:00	27.76	29.98	42.3	34.3	11.4	10.3
2015-07-13 15:00	28.58	30.2	42.9	38.8	12.1	12
2015-07-13 16:00	29.15	30.15	42.3	38.8	12.2	12
2015-07-13 17:00	27.1	27.74	45.4	42.3	11.8	11.4
2015-07-13 18:00	27.57	26.95	47.5	46.9	12.6	12.1
2015-07-13 19:00	25.2	24.95	54.2	54.7	12.6	12.4
2015-07-13 20:00	23.96	23.96	61	59.9	13.3	13
2015-07-13 21:00	22.14	22.04	67.6	66.1	13.2	12.9
2015-07-13 22:00	20.61	20.95	75.6	75.1	13.5	13.7
2015-07-13 23:00	20.26	20.92	80.4	75.6	14	13.8
2015-07-14 0:00	19.38	20.26	89.3	87.6	14.9	15.3
2015-07-14 1:00	19.11	19.95	91.8	95.7	15	16.3
2015-07-14 2:00	18.57	19.33	93	91.4	14.8	15.3

Date/Time:	Site A Low Temp (°C)	Site B Low Temp (°C)	Site A Low RH (%)	Site B Low RH (%)	Site A Low AH (g/m^3)	Site B Low AH (g/m^3)
2015-07-14 3:00	18.04	18.88	93	93.8	14.2	15.3
2015-07-14 4:00	17.31	18.35	92.6	94.9	13.5	14.8
2015-07-14 5:00	17.4	18.69	95	95.3	14.2	15.2
2015-07-14 6:00	17.5	18.76	94.6	95.3	14.1	15.2
2015-07-14 7:00	17.47	18.76	94.6	94.2	14.1	15
2015-07-14 8:00	19.59	20.73	92.6	86.3	15.5	15.4
2015-07-14 9:00	19.92	20.97	86.7	84.9	14.8	15.5
2015-07-14 10:00	20.68	21.64	85	84	15.2	16
2015-07-14 11:00	22.6	23.75	78	71.1	15.6	15.1
2015-07-14 12:00	23.89	25.51	69.2	65	15.1	15.4
2015-07-14 13:00	20.54	21.35	72.2	70.1	12.9	13.1
2015-07-14 14:00	18.5	19.07	71.2	68.1	11.4	11.1
2015-07-14 15:00	18.02	19.16	68.1	64.5	10.4	10.5
2015-07-14 16:00	18.52	19.9	59.9	55.2	9.6	9.4
2015-07-14 17:00	18.33	19.57	51.1	49	8	8.2
2015-07-14 18:00	18.54	19.04	52.7	52.1	8.4	8.5
2015-07-14 19:00	17.78	18.07	55.3	54.2	8.4	8.3
2015-07-14 20:00	17.28	17.69	55.8	53.7	8.1	8
2015-07-14 21:00	15.83	16.14	58.4	57.3	8	7.8
2015-07-14 22:00	14.35	14.44	63.5	63	7.9	7.8
2015-07-14 23:00	13.34	13.39	64.1	63.5	7.4	7.3
2015-07-15 0:00	12.01	12.42	72.2	70.6	7.8	7.8
2015-07-15 1:00	10.97	11.36	77.1	74.1	7.7	7.6
2015-07-15 2:00	10.7	10.84	76.1	75.6	7.4	7.6
2015-07-15 3:00	10.45	10.31	78	80.8	7.6	7.7
2015-07-15 4:00	9.57	9.37	84.1	85.8	7.6	7.8
2015-07-15 5:00	9.12	8.95	86.3	87.1	7.6	7.7
2015-07-15 6:00	8.88	9.03	88	88	7.8	7.8
2015-07-15 7:00	9.64	10.18	85	83.1	7.9	7.9
2015-07-15 8:00	10.97	12.01	76.6	72.6	7.7	7.8
2015-07-15 9:00	13.24	16.07	68.6	54.2	7.9	7.4
2015-07-15 10:00	15.11	18.76	55.8	45.4	7.3	7.2
2015-07-15 11:00	16.97	21.21	52.7	40.3	7.7	7.5
2015-07-15 12:00	18.83	23.8	49	34.8	7.8	7.4
2015-07-15 13:00	21.19	26.27	41.8	28.5	7.8	7.1
2015-07-15 14:00	23.43	27.74	33.3	25.7	6.9	7
2015-07-15 15:00	26.88	28.18	28.1	24.8	7.1	6.9
2015-07-15 16:00	29.05	28.31	23.9	23	6.9	6.4
2015-07-15 17:00	28.08	29.33	25.7	22.1	7	6.5
2015-07-15 18:00	25.54	26.05	29.5	27.6	7	6.7
2015-07-15 19:00	23	23.17	33.8	31.9	6.9	6.6

Date/Time:	Site A Low Temp (°C)	Site B Low Temp (°C)	Site A Low RH (%)	Site B Low RH (%)	Site A Low AH (g/m^3)	Site B Low AH (g/m^3)
2015-07-15 20:00	20.99	21.88	51.6	34.8	9.4	6.6
2015-07-15 21:00	17.52	19.49	62	48	9.3	8
2015-07-15 22:00	15.83	16.76	72.7	67.6	9.9	9.6
2015-07-15 23:00	16.09	15.54	71.2	70.6	9.7	9.4
2015-07-16 0:00	15.33	14.11	71.2	74.6	9.3	9
2015-07-16 1:00	14.16	13.07	79.4	81.7	9.6	9.2
2015-07-16 2:00	13.03	12.21	84.5	86.3	9.5	9.3
2015-07-16 3:00	12.28	11.53	87.6	91	9.4	9.3
2015-07-16 4:00	11.36	11.36	90.2	92.6	9.2	9.5
2015-07-16 5:00	10.97	11.41	91.8	92.6	9.2	9.5
2015-07-16 6:00	10.53	11.11	94.2	95.7	9.2	9.6
2015-07-16 7:00	11.53	12.95	95.7	94.9	9.8	10.7
2015-07-16 8:00	14.18	16.4	91.8	81.7	11.1	11.4
2015-07-16 9:00	16.69	21.95	80.4	59.4	11.5	11.6
2015-07-16 10:00	19.02	25.56	70.2	47.4	11.5	11.3
2015-07-16 11:00	21.02	29.1	50.6	32.3	9.2	9.3
2015-07-16 12:00	23	30.13	46.5	28	9.5	8.6
2015-07-16 13:00	26.19	30.51	38.3	26.2	9.5	8.1
2015-07-16 14:00	26.98	29.93	33.3	25.3	8.6	7.6
2015-07-16 15:00	29.55	29.65	28.5	25.3	8.4	7.5
2015-07-16 16:00	31.37	29.2	24.8	23.9	8.2	6.9
2015-07-16 17:00	28.11	28.36	27.1	24.8	7.3	6.9
2015-07-16 18:00	26.17	24.66	29	29.9	7.2	6.8
2015-07-16 19:00	22.93	22.28	40.8	40.8	8.3	8
2015-07-16 20:00	20.8	20.71	48.5	48	8.9	8.6
2015-07-16 21:00	18.64	18.95	59.9	57.8	9.6	9.4
2015-07-16 22:00	16.45	16.62	70.7	69.1	9.9	9.9
2015-07-16 23:00	15.83	15.38	74.6	75.6	10.2	9.8
2015-07-17 0:00	14.52	14.85	80.9	81.3	10	10.3
2015-07-17 1:00	13.65	14.4	84.5	84	10	10.4
2015-07-17 2:00	14.25	15.57	83.2	76	10.1	10.1
2015-07-17 3:00	13.96	14.85	81.8	75.6	9.9	9.6
2015-07-17 4:00	13.48	14.23	81.8	76.5	9.5	9.3
2015-07-17 5:00	14.06	14.56	89.8	88.4	10.9	11
2015-07-17 6:00	14.59	15.4	89.3	85.8	11.1	11.2
2015-07-17 7:00	15.33	16.09	85.9	82.7	11.2	11.3
2015-07-17 8:00	15.83	16.66	81.8	78.4	11.1	11.2
2015-07-17 9:00	16.16	16.93	80.9	77	11	11
2015-07-17 10:00	16.64	17.64	81.3	77.5	11.6	11.6
2015-07-17 11:00	16.43	17.04	87.6	84.5	12.2	12.3
2015-07-17 12:00	16	16.45	91	91.8	12.4	12.8

Date/Time:	Site A Low Temp (°C)	Site B Low Temp (°C)	Site A Low RH (%)	Site B Low RH (%)	Site A Low AH (g/m^3)	Site B Low AH (g/m^3)
2015-07-17 13:00	15.52	16.21	94.2	95.3	12.5	13.3
2015-07-17 14:00	15.35	15.83	96.5	97.5	12.5	13.3
2015-07-17 15:00	15.45	15.95	97.2	97.9	12.9	13.3
2015-07-17 16:00	15.81	16.5	97.6	97.9	13	13.6
2015-07-17 17:00	16.09	17.02	97.6	97.9	13.3	14.3
2015-07-17 18:00	16.19	17.04	97.6	97.5	13.3	14.2
2015-07-17 19:00	16.33	17.28	97.6	96.4	13.6	14.1
2015-07-17 20:00	16.33	17.19	97.6	96.4	13.6	14.1
2015-07-17 21:00	16.31	17.07	97.9	97.2	13.6	14.2
2015-07-17 22:00	16.45	17.21	97.9	98.2	13.6	14.3
2015-07-17 23:00	16.47	17.02	97.9	98.2	13.6	14.3
2015-07-18 0:00	16.47	16.97	97.9	97.9	13.6	14.3
2015-07-18 1:00	16.59	16.95	98.3	98.2	14	14
2015-07-18 2:00	16.62	16.9	97.9	97.9	14	14
2015-07-18 3:00	16.59	16.83	97.6	97.9	13.9	14
2015-07-18 4:00	16	15.69	97.6	98.9	13.3	13.2
2015-07-18 5:00	16.04	16.19	98.3	99.9	13.4	13.6
2015-07-18 6:00	16.31	16.62	99	99.6	13.8	14.2
2015-07-18 7:00	16.83	17.14	99	98.6	14.1	14.4
2015-07-18 8:00	17.52	18.5	96.8	96.4	14.4	15.4
2015-07-18 9:00	18.95	22.24	93	83.1	15.2	16.2
2015-07-18 10:00	20.4	25.88	88.5	72.1	15.8	17.5
2015-07-18 11:00	22.26	26.07	84.5	70.1	16.5	17
2015-07-18 12:00	21.95	23.48	85.4	77.5	16.7	16.5
2015-07-18 13:00	21.95	23.63	83.6	77	16.3	16.4
2015-07-18 14:00	22.81	24.47	80.9	74.1	16.5	16.5
2015-07-18 15:00	22.74	24.47	82.2	75.6	16.8	16.8
2015-07-18 16:00	23.68	25.88	78.5	69.6	16.7	16.9
2015-07-18 17:00	23.56	25.1	84.5	74.6	18	17.3
2015-07-18 18:00	24.64	26.02	76.1	70.1	17.3	17
2015-07-18 19:00	23.77	24.83	80.9	76	17.2	17.3
2015-07-18 20:00	22.64	23.29	85.9	82.7	17.1	17.2
2015-07-18 21:00	21.71	21.95	88.5	88.4	16.9	17.2
2015-07-18 22:00	21.07	21.78	93	92.2	17	17.6
2015-07-18 23:00	21.14	21.54	93.8	93.4	17.1	17.8
2015-07-19 0:00	20.42	20.83	94.6	94.5	16.9	17.3
2015-07-19 1:00	19.33	19.57	93.4	93.8	15.6	15.7
2015-07-19 2:00	17.76	18.04	93.8	97.2	14.3	14.8
2015-07-19 3:00	17.09	17.43	95.7	98.2	14	14.7
2015-07-19 4:00	16.71	17.52	96.5	99.6	13.8	14.9
2015-07-19 5:00	16.85	17.26	97.2	99.3	13.9	14.5

Date/Time:	Site A Low Temp (°C)	Site B Low Temp (°C)	Site A Low RH (%)	Site B Low RH (%)	Site A Low AH (g/m^3)	Site B Low AH (g/m^3)
2015-07-19 6:00	16.64	17.43	96.8	99.9	13.8	14.9
2015-07-19 7:00	17.81	18.47	99	99.3	15.1	15.5
2015-07-19 8:00	19.35	20.85	98.3	91.8	16.4	16.8
2015-07-19 9:00	21.45	23.75	89.3	81.3	16.7	17.3
2015-07-19 10:00	22.62	26.53	84.1	72.6	16.8	18
2015-07-19 11:00	24.01	29.65	81.3	57.8	17.7	17.1
2015-07-19 12:00	25.97	31.19	73.6	51.1	17.9	16.4
2015-07-19 13:00	27.49	32.14	57.3	43.3	15.2	14.6
2015-07-19 14:00	27.39	30.23	54.7	42.8	14.5	13.2
2015-07-19 15:00	26.93	28.6	52.1	44.9	13.2	12.7
2015-07-19 16:00	28.58	29.93	45.4	39.8	12.8	12
2015-07-19 17:00	26.83	29.18	41.3	34.8	10.5	10
2015-07-19 18:00	27.66	27.17	36.8	37.8	9.7	9.8
2015-07-19 19:00	25.12	25	41.3	41.8	9.6	9.7
2015-07-19 20:00	23.41	23.27	43.9	43.3	9.1	9
2015-07-19 21:00	21.61	20.57	48.5	52.1	9.3	9.3
2015-07-19 22:00	18.85	17.62	67.6	66.1	10.8	9.9
2015-07-19 23:00	17.52	17.07	71.7	68.6	10.7	10
2015-07-20 0:00	17.95	17.04	75.6	79.4	11.5	11.6
2015-07-20 1:00	17.31	16.24	79	84	11.5	11.7
2015-07-20 2:00	16.74	15.71	83.2	88	11.9	11.7
2015-07-20 3:00	16.31	15.26	84.1	89.7	11.7	11.7
2015-07-20 4:00	15.85	14.9	85.4	90.5	11.6	11.5
2015-07-20 5:00	15.33	14.4	88.9	93.4	11.6	11.6
2015-07-20 6:00	14.92	14.78	92.6	94.9	11.8	12.1
2015-07-20 7:00	15.76	16.24	91.8	91.4	12.2	12.7
2015-07-20 8:00	17.38	18.66	87.6	83.1	13.1	13.3
2015-07-20 9:00	20.07	24.45	79.4	60.9	13.9	13.5
2015-07-20 10:00	22.07	28.03	74.1	50.6	14.5	13.7
2015-07-20 11:00	25	31.11	61.5	40.8	14.3	13.1
2015-07-20 12:00	25.44	28.88	56.3	44.9	13.4	12.7
2015-07-20 13:00	26.29	27.98	52.7	45.4	13.1	12.3
2015-07-20 14:00	29.43	32.78	44.4	36.3	13.1	12.7
2015-07-20 15:00	26.85	29.28	52.1	44.9	13.2	13
2015-07-20 16:00	27	28.16	54.2	49.5	14	13.7
2015-07-20 17:00	23.72	24.66	76.1	75.1	16.2	17.1
2015-07-20 18:00	24.83	24.64	59.9	60.9	13.6	13.8
2015-07-20 19:00	24.28	23.92	60.5	62.5	13.5	13.6
2015-07-20 20:00	23.12	22.93	62	63.5	12.9	12.9
2015-07-20 21:00	21.52	21.23	70.2	70.1	13.1	13.1
2015-07-20 22:00	20.33	19.38	75.1	78	13.1	13

Date/Time:	Site A Low Temp (°C)	Site B Low Temp (°C)	Site A Low RH (%)	Site B Low RH (%)	Site A Low AH (g/m^3)	Site B Low AH (g/m^3)
2015-07-20 23:00	19.3	18.12	76.1	80.8	12.7	12.6
2015-07-21 0:00	18.28	16.83	77.5	83.1	12.1	11.8
2015-07-21 1:00	17.26	15.95	79.4	84.5	11.6	11.5
2015-07-21 2:00	16.07	15.38	83.2	84.9	11.3	11
2015-07-21 3:00	15.45	14.47	86.3	89.3	11.5	11.1
2015-07-21 4:00	15.71	15.33	85.9	88.9	11.4	11.6
2015-07-21 5:00	15.19	14.47	87.6	91	11.4	11.3
2015-07-21 6:00	15.19	15.02	85	87.1	11.1	11.1
2015-07-21 7:00	15.3	15.16	82.7	84.9	10.8	11
2015-07-21 8:00	15.83	16.45	76.1	77.5	10.4	10.8
2015-07-21 9:00	16.4	18.31	72.2	65	10.1	10.1
2015-07-21 10:00	18.4	20.42	63	54.7	9.8	9.8
2015-07-21 11:00	19.95	25.27	54.7	40.3	9.3	9.4
2015-07-21 12:00	21.95	28.36	45.4	30.4	8.9	8.4
2015-07-21 13:00	24.33	28.33	38.8	30.4	8.6	8.4
2015-07-21 14:00	26.46	30.25	32.9	25.3	8.2	7.8
2015-07-21 15:00	27.12	29.38	30.9	25.3	8	7.5
2015-07-21 16:00	24.93	26.44	36.3	30.4	8.3	7.5
2015-07-21 17:00	24.62	26.56	45.9	34.8	10.4	8.8
2015-07-21 18:00	24.23	25.8	36.8	33.3	8.2	8.1
2015-07-21 19:00	23.22	23.99	36.8	33.8	7.7	7.4
2015-07-21 20:00	22.14	22.69	35.8	35.3	7	7.2
2015-07-21 21:00	20.21	19.85	37.3	38.8	6.5	6.6
2015-07-21 22:00	17.95	17.19	50.6	48	7.7	7
2015-07-21 23:00	16.78	15.88	52.7	54.2	7.5	7.4
2015-07-22 0:00	15.42	14.52	62.5	60.9	8.1	7.6
2015-07-22 1:00	14.49	13.68	65.1	66.1	8.1	7.8
2015-07-22 2:00	14.18	13.39	69.7	71.6	8.4	8.3
2015-07-22 3:00	13.48	12.95	76.6	78.9	8.9	8.9
2015-07-22 4:00	13.68	13.39	76.1	78.4	9	9.1
2015-07-22 5:00	14.11	13.96	73.1	74.1	8.9	9
2015-07-22 6:00	14.71	14.85	69.7	69.1	8.9	8.8
2015-07-22 7:00	14.32	14.3	72.7	73.1	9	9.1
2015-07-22 8:00	15.04	16	69.7	67.6	8.9	9.2
2015-07-22 9:00	16.71	22	66.1	46.4	9.4	9
2015-07-22 10:00	18.31	23.22	57.9	43.3	9	9
2015-07-22 11:00	19.66	23.34	53.2	42.3	9.1	8.8
2015-07-22 12:00	22	26.36	47	35.3	9.2	8.8
2015-07-22 13:00	24.28	28.23	37.3	28	8.3	7.7
2015-07-22 14:00	25.58	28.4	32.9	27.1	7.8	7.5
2015-07-22 15:00	26.85	29.1	30	25.3	7.6	7.3

Date/Time:	Site A Low Temp (°C)	Site B Low Temp (°C)	Site A Low RH (%)	Site B Low RH (%)	Site A Low AH (g/m^3)	Site B Low AH (g/m^3)
2015-07-22 16:00	25	25.93	33.3	30.4	7.7	7.4
2015-07-22 17:00	23.89	25.08	36.3	32.8	7.9	7.6
2015-07-22 18:00	23.72	24.3	37.8	34.8	8	7.7
2015-07-22 19:00	22.72	23.1	34.8	35.3	7.1	7.4
2015-07-22 20:00	21.57	21.69	36.3	36.3	6.9	6.9
2015-07-22 21:00	19.47	19.61	48	43.8	8	7.3
2015-07-22 22:00	16.28	16	63	60.4	8.8	8.2
2015-07-22 23:00	14.95	14.37	71.2	72.6	9	9
2015-07-23 0:00	13.89	13.41	75.1	72.1	8.9	8.3
2015-07-23 1:00	13.53	13.05	78	84	9.2	9.5
2015-07-23 2:00	12.35	11.67	78.5	84.9	8.4	8.9
2015-07-23 3:00	12.79	12.13	82.2	84.9	9.3	9.1
2015-07-23 4:00	13.34	13.56	79.4	74.6	9.2	8.8
2015-07-23 5:00	12.69	12.47	81.3	78	9	8.6
2015-07-23 6:00	12.11	11.65	84.5	83.6	9.1	8.8
2015-07-23 7:00	13.56	13.94	79.9	77.5	9.5	9.4
2015-07-23 8:00	15.04	16.62	77.5	69.6	9.8	9.9
2015-07-23 9:00	17.14	19.76	71.7	56.8	10.5	9.7
2015-07-23 10:00	19.33	26.85	57.3	35.8	9.6	9.1
2015-07-23 11:00	22	29.33	39.8	25.7	7.8	7.6
2015-07-23 12:00	23.72	30.91	31.9	21.7	6.8	6.8
2015-07-23 13:00	26.61	32.47	26.7	18.3	6.8	6.3
2015-07-23 14:00	27.32	32.55	26.2	18.7	6.8	6.4
2015-07-23 15:00	31.57	34.19	20	16.2	6.6	6.1
2015-07-23 16:00	31.01	32.57	21.7	19.1	7	6.7
2015-07-23 17:00	27.44	29.5	25.3	22.1	6.7	6.5
2015-07-23 18:00	29.03	28.75	23	22.6	6.6	6.4
2015-07-23 19:00	26.8	26.88	26.7	26.2	6.8	6.6
2015-07-23 20:00	24.08	24.08	37.3	37.3	8.1	8.1
2015-07-23 21:00	21.5	21.04	45.9	43.3	8.6	7.9
2015-07-23 22:00	19.71	19.04	50.6	49	8.6	8
2015-07-23 23:00	18.73	17.92	56.3	55.2	9	8.4
2015-07-24 0:00	17.26	16.26	63.5	64	9.3	8.9
2015-07-24 1:00	16.35	15.42	66.6	70.1	9.3	9.1
2015-07-24 2:00	15.14	14.08	74.1	76.5	9.6	9.3
2015-07-24 3:00	14.61	13.53	77.5	80.8	9.6	9.6
2015-07-24 4:00	14.59	13.68	78	82.2	9.7	9.7
2015-07-24 5:00	14.04	12.76	83.2	86.7	10.1	9.8
2015-07-24 6:00	13.48	12.37	84.1	87.6	9.7	9.7
2015-07-24 7:00	13.75	13.72	85.4	84.5	10.1	10
2015-07-24 8:00	15.83	16.9	78	73.6	10.6	10.5

Date/Time:	Site A Low Temp (°C)	Site B Low Temp (°C)	Site A Low RH (%)	Site B Low RH (%)	Site A Low AH (g/m^3)	Site B Low AH (g/m^3)
2015-07-24 9:00	18.07	25	71.7	44.4	10.9	10.3
2015-07-24 10:00	20.33	28.95	61	35.3	10.7	10.2
2015-07-24 11:00	23.24	32.11	50.1	28.5	10.4	9.6
2015-07-24 12:00	25.71	33.66	38.8	21.7	9.2	8
2015-07-24 13:00	30.05	34.74	28.1	19.5	8.5	7.6
2015-07-24 14:00	30.48	35.33	26.7	18.3	8.2	7.3
2015-07-24 15:00	32.96	35.94	20.8	16.6	7.3	7
2015-07-24 16:00	36.4	35.62	16.6	15.8	7.1	6.5
2015-07-24 17:00	33.27	34.69	19.5	17	7	6.7
2015-07-24 18:00	31.78	31.14	24.4	23	8.2	7.4
2015-07-24 19:00	26.76	26.73	45.4	44.9	11.5	11.4
2015-07-24 20:00	24.83	25.05	53.7	53.7	12.2	12.5
2015-07-24 21:00	23.48	23.82	59.9	58.9	12.8	12.5
2015-07-24 22:00	22.31	22.72	65.6	65	13.1	13.2
2015-07-24 23:00	20.92	21.21	72.7	72.6	13.3	13.5
2015-07-25 0:00	19.42	19.76	79	78.9	13.2	13.5
2015-07-25 1:00	18.5	18.8	83.6	83.1	13.3	13.3
2015-07-25 2:00	17.64	18.02	86.3	86.7	12.9	13.2
2015-07-25 3:00	18.31	19.09	85.4	84	13.3	13.7
2015-07-25 4:00	18.35	19.26	88	86.3	13.7	14.4
2015-07-25 5:00	18.78	19.49	86.3	84	13.8	14
2015-07-25 6:00	18.26	18.88	90.6	89.3	14.1	14.6
2015-07-25 7:00	18.28	19.19	91.8	87.1	14.3	14.2
2015-07-25 8:00	18.99	19.71	89.3	86.3	14.6	14.7
2015-07-25 9:00	19.14	19.95	93	93	15.2	15.9
2015-07-25 10:00	18.78	19.57	95.7	95.7	15.3	16
2015-07-25 11:00	17.85	18	99.3	99.9	15.2	15.2
2015-07-25 12:00	19.73	20.52	100	98.2	17.1	17.5
2015-07-25 13:00	22.57	24.18	98.6	79.9	19.7	17.4
2015-07-25 14:00	22.64	24.01	93	79.9	18.5	17.4
2015-07-25 15:00	26.07	28.13	77.5	66.6	18.8	18.4
2015-07-25 16:00	28.85	30.2	58.9	53.1	16.6	16.4
2015-07-25 17:00	28.4	30.76	53.7	46.4	14.8	14.6
2015-07-25 18:00	26.02	27.66	58.9	53.1	14.3	14.1
2015-07-25 19:00	26.05	26.12	53.7	53.7	13	13
2015-07-25 20:00	24.37	24.83	63	58.9	14	13.4
2015-07-25 21:00	21.9	21.83	77.5	68.6	14.8	13.1
2015-07-25 22:00	19.61	19.66	83.6	77.5	14	13.2
2015-07-25 23:00	18.45	18.69	87.2	82.7	13.6	13.2
2015-07-26 0:00	17.54	18.14	91	90.1	13.6	14.1
2015-07-26 1:00	17.12	17.57	93	89.3	13.6	13.3

Date/Time:	Site A Low Temp (°C)	Site B Low Temp (°C)	Site A Low RH (%)	Site B Low RH (%)	Site A Low AH (g/m^3)	Site B Low AH (g/m^3)
2015-07-26 2:00	17.81	17.66	89.8	88	13.7	13.1
2015-07-26 3:00	16.88	16.76	91.8	91	13.1	13
2015-07-26 4:00	16.5	16.47	92.6	92.2	12.9	12.8
2015-07-26 5:00	16.04	15.97	93.8	92.2	12.8	12.6
2015-07-26 6:00	15.95	15.59	94.2	93.8	12.8	12.5
2015-07-26 7:00	16.4	16.59	95	94.9	13.2	13.5
2015-07-26 8:00	17.9	19.28	92.2	85.4	14.1	14.3
2015-07-26 9:00	19.85	25.61	84.1	59.9	14.4	14.2
2015-07-26 10:00	21.97	28.78	74.6	48	14.5	13.6
2015-07-26 11:00	24.45	31.67	68.6	42.3	15.3	13.9
2015-07-26 12:00	26.32	33.48	54.2	37.3	13.4	13.7
2015-07-26 13:00	29.6	34.29	41.8	32.3	12.3	12.4
2015-07-26 14:00	30.96	35.01	40.3	30.4	13	11.9
2015-07-26 15:00	31.75	34.72	39.8	31.4	13.4	12.3
2015-07-26 16:00	31.9	33.01	36.3	33.3	12.2	12
2015-07-26 17:00	29.95	30.99	38.3	34.3	11.5	11
2015-07-26 18:00	26.68	27.42	49	48	12.4	12.7
2015-07-26 19:00	25.54	26.71	52.7	50	12.5	12.7
2015-07-26 20:00	24.04	24.25	57.3	59.9	12.5	13.3
2015-07-26 21:00	22.12	22.28	80.9	83.6	15.8	16.3
2015-07-26 22:00	20.16	20.64	90.2	86.3	15.8	15.4
2015-07-26 23:00	18.95	19.88	91.8	85.8	15	14.7
2015-07-27 0:00	18.66	19.26	92.6	87.6	14.8	14.6
2015-07-27 1:00	18.88	18.78	90.2	90.5	14.7	14.5
2015-07-27 2:00	18.4	18.04	89.8	92.2	14	14.1
2015-07-27 3:00	17.66	17.45	91.8	93.8	13.7	14
2015-07-27 4:00	17.16	16.85	93.4	94.5	13.6	13.5
2015-07-27 5:00	17.04	16.66	93.4	94.9	13.6	13.5
2015-07-27 6:00	16.76	16.26	94.6	96.8	13.5	13.5
2015-07-27 7:00	17.02	17.31	95.7	95.7	14	14
2015-07-27 8:00	18.57	20.02	93	87.6	14.8	15.3
2015-07-27 9:00	20.68	26.44	84.5	62	15.1	15.4
2015-07-27 10:00	23	30.2	75.6	49.5	15.4	15.3
2015-07-27 11:00	24.93	32.39	68.1	41.8	15.5	14.4
2015-07-27 12:00	27.02	34.4	60.5	39.3	15.7	15.1
2015-07-27 13:00	30.48	35.92	45.9	29	14.1	11.9
2015-07-27 14:00	30.05	33.69	43.4	33.8	13.1	12.4
2015-07-27 15:00	33.25	35.49	35.8	29.5	12.9	11.8
2015-07-27 16:00	31.09	32.03	50.6	33.3	16.3	11.2
2015-07-27 17:00	34.27	35.92	25.7	21.7	9.9	8.9
2015-07-27 18:00	32.68	32.81	28.5	27.6	10	9.7

Date/Time:	Site A Low Temp (°C)	Site B Low Temp (°C)	Site A Low RH (%)	Site B Low RH (%)	Site A Low AH (g/m^3)	Site B Low AH (g/m^3)
2015-07-27 19:00	30.91	31.24	33.3	32.8	10.5	10.6
2015-07-27 20:00	28.6	28.55	44.9	44.9	12.7	12.7
2015-07-27 21:00	26.22	25.49	54.2	56.3	13.4	13.4
2015-07-27 22:00	24.21	23.22	61.5	63.5	13.4	13.2
2015-07-27 23:00	21.95	22.33	75.1	66.1	14.6	13.2
2015-07-28 0:00	20.97	21.11	77.5	73.6	14.1	13.4
2015-07-28 1:00	20.85	20.99	79	77	14.4	14.1
2015-07-28 2:00	20.11	19.88	80.9	80.8	14.1	13.8
2015-07-28 3:00	19.59	19.68	84.1	84	14	14.3
2015-07-28 4:00	19.26	19.3	86.3	84.5	14.4	14.1
2015-07-28 5:00	19.09	18.95	87.2	87.1	14.2	14.2
2015-07-28 6:00	18.78	18.54	88.9	88.4	14.2	14.1
2015-07-28 7:00	19.35	19.49	88	88.4	14.7	14.8
2015-07-28 8:00	20.57	22.88	85.9	75.6	15.3	15.4
2015-07-28 9:00	22.79	29.03	81.8	50.6	16.7	14.6
2015-07-28 10:00	25.27	32.88	67.1	42.3	15.6	14.9
2015-07-28 11:00	27.66	35.65	59.9	35.3	15.9	14.5
2015-07-28 12:00	29.53	36.73	53.7	33.3	15.8	14.3
2015-07-28 13:00	33.45	38.07	40.3	31.9	14.8	14.6
2015-07-28 14:00	34.16	38.52	39.3	29.5	14.7	13.8
2015-07-28 15:00	36.13	38.94	32.4	26.2	13.6	12.6
2015-07-28 16:00	38.82	39.08	27.6	26.2	13.2	12.8
2015-07-28 17:00	36.08	38.29	28.1	23.9	11.8	11.2
2015-07-28 18:00	34.53	34.53	32.4	32.8	12.4	12.6
2015-07-28 19:00	31.06	30.99	40.8	40.8	13.1	13.1
2015-07-28 20:00	29.03	28.85	47.5	49	13.7	13.8
2015-07-28 21:00	26.76	26.07	55.8	54.7	14.1	13.3
2015-07-28 22:00	24.23	24.49	67.6	60.4	15	13.4
2015-07-28 23:00	22.5	23.07	74.6	68.6	14.9	14.3
2015-07-29 0:00	22.93	22.55	69.7	70.6	14.2	14.1
2015-07-29 1:00	21.54	21.59	79	75.6	15.1	14.4
2015-07-29 2:00	20.85	20.95	81.8	78.4	14.9	14.3
2015-07-29 3:00	20.71	21.11	84.1	79.9	15	14.6
2015-07-29 4:00	20.23	20.8	85.4	81.3	14.9	14.8
2015-07-29 5:00	19.47	20.38	88	84.9	14.7	14.8
2015-07-29 6:00	18.45	19.3	88.9	87.6	13.9	14.6
2015-07-29 7:00	19.68	20.35	88.5	86.3	15.1	15.1
2015-07-29 8:00	20.42	22.86	84.5	75.1	15.1	15.3
2015-07-29 9:00	22.81	27.39	71.7	52.1	14.6	13.8
2015-07-29 10:00	25.22	32.03	62.5	41.3	14.5	13.9
2015-07-29 11:00	27.74	33.53	54.7	38.3	14.8	14.1

Date/Time:	Site A Low Temp (°C)	Site B Low Temp (°C)	Site A Low RH (%)	Site B Low RH (%)	Site A Low AH (g/m^3)	Site B Low AH (g/m^3)
2015-07-29 12:00	29.45	34.03	49	36.3	14.5	13.6
2015-07-29 13:00	32.7	34.53	39.8	32.8	14	12.6
2015-07-29 14:00	33.27	34.32	37.8	32.3	13.6	12.4
2015-07-29 15:00	33.59	33.93	33.8	29.9	12.4	11.2
2015-07-29 16:00	33.98	33.95	30	30.4	11.3	11.4
2015-07-29 17:00	29.15	29.65	39.8	39.3	11.5	11.6
2015-07-29 18:00	27.29	27.69	49.6	48.5	12.8	12.8
2015-07-29 19:00	25.41	25.93	61	60.4	14.5	14.7
2015-07-29 20:00	20.64	21.21	96.5	96.4	17.2	18
2015-07-29 21:00	20.45	21.11	96.8	93.4	17.3	17
2015-07-29 22:00	19.61	20.14	97.2	96.4	16.2	16.8
2015-07-29 23:00	19.19	19.28	97.6	95.3	15.9	15.9
2015-07-30 0:00	17.9	18	95.4	91.4	14.6	14
2015-07-30 1:00	17.28	17.24	93.8	94.5	13.7	13.8
2015-07-30 2:00	16.69	16.59	96.5	95.7	13.8	13.6
2015-07-30 3:00	16.26	16.21	95.7	93.8	13.3	13.1
2015-07-30 4:00	15.73	16	96.1	93	12.8	12.7
2015-07-30 5:00	15.04	16.12	96.1	91.4	12.2	12.4
2015-07-30 6:00	15.16	16.04	97.6	92.6	12.7	12.6
2015-07-30 7:00	16.12	17.47	97.2	88.9	13.2	13.3
2015-07-30 8:00	17.62	20.14	90.6	78.9	13.5	13.8
2015-07-30 9:00	19.3	23.77	87.2	66.6	14.6	14.2
2015-07-30 10:00	20.99	26.63	76.1	57.3	13.9	14.5
2015-07-30 11:00	22.5	28.48	71.2	50	14.2	13.8
2015-07-30 12:00	23.31	28.18	59.9	46.4	12.5	12.8

Appendix II:

Drug Responses

Table A2.1 Control Animal Drug Responses

Bone Type:	Animal:	Mass (g):	DXM	d3-DXM	DXT	d3-DXT	DXT 150	d3-DXT 153	dmDXT
VERT	Ctrl A-1	0.204	1716	141471	0	134236	7752	126979	0
VERT	Ctrl A-2	0.2039	2859	142945	681	130315	13610	122677	0
FEMUR	Ctrl A-1	0.198	1417	89769	850	74467	15701	166445	0
FEMUR	Ctrl A-2	0.196	1799	85927	1221	78447	7930	170960	0
RIB	Ctrl A-1	0.2106	1388	41603	265	42254	8416	100956	0
RIB	Ctrl A-2	0.2119	231	39920	1449	53576	6261	121141	291
TIBIA	Ctrl A-1	0.2193	6726	128861	0	141158	38142	196543	0
TIBIA	Ctrl A-2	0.2003	1036	61853	0	55397	9720	162383	0
PELVIS	Ctrl A-1	0.1988	9962	177824	0	98787	10820	293815	0
PELVIS	Ctrl A-2	0.2146	6715	210354	0	151053	17044	362615	0
SKULL	Ctrl A-1	0.2085	12815	52128	0	73730	8737	85990	322
SKULL	Ctrl A-2	0.2135	17078	80559	0	103659	9455	136468	626
SCAPULA	Ctrl A-1	0.121	0	177737	0	79168	16547	344016	0
SCAPULA	Ctrl A-2	0.1095	632	132160	0	83693	10507	267657	0
BLOOD	Ctrl A-1	0.25	1217	56380	1489	27364	15397	62930	0
BLOOD	Ctrl A-2	0.25	268	51307	177	15592	19450	43460	0
VERT	Ctrl B-1	0.2078	0	299658	0	382241	98874	457512	0
VERT	Ctrl B-2	0.2129	0	292104	0	320780	116680	442971	0
FEMUR	Ctrl B-1	0.2013	2307	149603	2267	163701	25845	238543	0
FEMUR	Ctrl B-2	0.1922	8751	171750	3249	178190	36796	235336	0
RIB	Ctrl B-1	0.1935	2186	57660	747	54622	5980	108505	796
RIB	Ctrl B-2	0.2101	3704	89193	356	80747	5010	165391	510
TIBIA	Ctrl B-1	0.1982	3950	170589	0	235366	95684	402045	0
TIBIA	Ctrl B-2	0.2132	0	188437	0	204345	18192	272166	0
PELVIS	Ctrl B-1	0.2024	13510	469176	0	169363	42288	465028	0
PELVIS	Ctrl B-2	0.2108	10077	200758	0	486259	101643	221136	0
SKULL	Ctrl B-1	0.2087	78154	96782	4152	336561	139654	223332	2720
SKULL	Ctrl B-2	0.2111	12919	317376	3238	108946	27711	470982	2237

Bone Type:	Animal:	Mass (g):	DXM	d3-DXM	DXT	d3-DXT	DXT 150	d3-DXT 153	dmDXT 315
SCAPULA	Ctrl B-1	0.1129	312	102255	0	428484	60710	197889	0
SCAPULA	Ctrl B-2	0.1052	4823	200745	0	56910	11731	294651	0
BLOOD	Ctrl B-1	0.25	906	64615	417	14530	5735	52130	0
BLOOD	Ctrl B-2	0.25	561	43841	327	29061	5225	82352	0

Table A2.2: Drug Responses Following Acute DXM (75 mg/kg) Administrations

Bone Type:	Animal:	Mass (g):	DXM	d3-DXM	DXT	d3-DXT	DXT 150	d3-DXT 153	dmDXT
VERT	Acu A-1	0.2003	1783727	384820	282935	327484	387763	392702	381235
VERT	Acu A-2	0.2081	2339929	330909	193846	390081	483373	359498	312805
VERT	Acu A-3	0.2053	580940	338067	177453	455348	172959	463850	328313
VERT	Acu A-4	0.213	838039	269173	56590	313240	75678	398862	70184
VERT	Acu A-5	0.2324	2766437	360644	1061047	323231	1079752	413445	650164
FEMUR	Acu A-1	0.1979	651196	285612	76710	290977	127852	394005	22298
FEMUR	Acu A-2	0.2163	700739	246434	125029	280497	161624	527395	40643
FEMUR	Acu A-3	0.1933	214142	146762	28494	164532	107391	328588	2549
FEMUR	Acu A-4	0.1981	857382	292203	16609	243366	81202	381523	5210
FEMUR	Acu A-5	0.2049	738954	231726	7289	235869	143027	329193	31356
RIB	Acu A-1	0.2007	936395	177348	n/a	217159	290799	356757	142291
RIB	Acu A-2	0.2099	2322787	268094	834387	368328	1041087	649098	210042
RIB	Acu A-3	0.1977	275337	379817	n/a	399640	85117	596569	74759
RIB	Acu A-4	0.205	1064064	283732	n/a	322834	48062	512533	65798
RIB	Acu A-5	0.1953	916555	162771	518117	216219	821118	471682	384480
TIBIA	Acu A-1	0.2025	1794655	270662	n/a	239603	248482	345625	66446
TIBIA	Acu A-2	0.2138	592501	151913	n/a	121745	146248	270256	27223
TIBIA	Acu A-3	0.1993	790670	249553	133564	268326	228844	567462	n/a
TIBIA	Acu A-4	0.2089	1931559	307369	n/a	339134	107238	493320	n/a
TIBIA	Acu A-5	0.1971	922853	207367	139554	232471	183956	393234	n/a
PELVIS	Acu A-1	0.2014	744165	163603	n/a	381993	241347	244301	106361
PELVIS	Acu A-2	0.2	657135	246855	n/a	463485	224634	568979	106760
PELVIS	Acu A-3	0.2053	629080	393950	108105	152340	188451	469978	10443
PELVIS	Acu A-4	0.1919	276843	234192	n/a	107120	27499	358016	4820
PELVIS	Acu A-5	0.2099	944679	140456	110769	159117	388140	224225	84932
SKULL	Acu A-1	0.208	573181	114575	101493	81602	282505	155631	13106
SKULL	Acu A-2	0.206	784699	157421	113970	116738	339391	147183	35801
SKULL	Acu A-3	0.2114	78986	189464	34969	89294	28234	344909	8207

Bone Type:	Animal:	Mass (g):	DXM	d3-DXM	DXT	d3-DXT	DXT 150	d3-DXT 153	dmDXT
SKULL	Acu A-4	0.2026	251780	181755	29555	86355	18113	336996	1455
SKULL	Acu A-5	0.1998	1018929	152349	119577	177430	509390	186575	60567
SCAPULA	Acu A-1	0.1986	1249376	154054	n/a	320103	629983	322563	63053
SCAPULA	Acu A-2	0.1978	4951878	619299	n/a	723840	1522410	909889	172348
SCAPULA	Acu A-3	0.1914	207664	580031	174588	282793	88861	636992	22508
SCAPULA	Acu A-4	0.2113	1350696	262835	n/a	311795	141005	174843	48066
SCAPULA	Acu A-5	0.2016	754332	89911	138743	285034	458481	446409	113540
BLOOD	Acu A-1	0.25	135366	139258	21194	37940	14524	92825	0
BLOOD	Acu A-2	0.25	95136	93494	38949	43776	23671	88389	0
BLOOD	Acu A-3	0.25	208053	126661	75534	39417	57159	109329	0
BLOOD	Acu A-4	0.25	n/a	n/a	n/a	n/a	n/a	n/a	n/a
BLOOD	Acu A-5	0.25	184582	96583	24461	14729	26957	73213	0
VERT	Acu B-1	0.2098	865708	302552	196605	259389	274661	349234	142246
VERT	Acu B-2	0.2134	1196231	291283	241133	305102	363508	318474	300999
VERT	Acu B-3	0.2093	1113701	283265	225557	261721	296580	359569	282985
VERT	Acu B-4	0.2144	553159	219478	211559	242253	286562	328965	157631
VERT	Acu B-5	0.2098	1361103	550570	1431363	587629	n/a	n/a	363373
FEMUR	Acu B-1	0.2153	1525833	213460	185634	230710	287170	425702	23371
FEMUR	Acu B-2	0.2069	1107747	299408	209514	341588	301016	517806	25608
FEMUR	Acu B-3	0.2152	587507	213242	25603	211804	64204	281332	945
FEMUR	Acu B-4	0.203	1693874	393745	241555	351557	331523	621697	21595
FEMUR	Acu B-5	0.2057	3660702	445623	1444719	471938	1883994	820923	194274
RIB	Acu B-1	0.2094	656936	141693	122643	134498	327790	285414	54594
RIB	Acu B-2	0.2146	1182467	244346	723675	265236	1298916	624451	134235
RIB	Acu B-3	0.2069	603789	270080	n/a	261705	182497	467891	71558
RIB	Acu B-4	0.1965	622771	245645	214521	290359	349157	563360	102566
RIB	Acu B-5	0.2088	4319499	463922	2002519	584577	3214070	977086	424249
TIBIA	Acu B-1	0.2083	1257227	216983	137996	239464	186983	430489	n/a
TIBIA	Acu B-2	0.2089	1848061	269575	n/a	276860	280389	439671	40061

Bone Type:	Animal:	Mass (g):	DXM	d3-DXM	DXT	d3-DXT	DXT 150	d3-DXT 153	dmDXT
TIBIA	Acu B-3	0.1995	555707	196259	n/a	175181	49921	279424	n/a
TIBIA	Acu B-4	0.2057	681325	201498	n/a	164086	119839	277699	n/a
TIBIA	Acu B-5	0.2048	622016	220892	n/a	228761	130053	306632	n/a
PELVIS	Acu B-1	0.2093	1005620	617426	n/a	404585	1109819	600458	98473
PELVIS	Acu B-2	0.2152	948966	690394	n/a	690225	700001	649111	133323
PELVIS	Acu B-3	0.2084	731166	250231	n/a	606255	235496	509894	76469
PELVIS	Acu B-4	0.2068	666907	318844	n/a	367222	998584	598571	60791
PELVIS	Acu B-5	0.2057	4875872	575259	n/a	n/a	975948	1128382	141866
SKULL	Acu B-1	0.2135	674648	149632	n/a	389322	234764	305448	92051
SKULL	Acu B-2	0.2124	669373	120002	69581	165690	295042	116372	46719
SKULL	Acu B-3	0.2081	197347	181077	59519	71287	98835	218002	22055
SKULL	Acu B-4	0.2093	1357662	316213	46206	164369	112151	216461	22400
SKULL	Acu B-5	0.2113	1011550	214585	n/a	516566	611561	437150	135079
SCAPULA	Acu B-1	0.1917	875039	643986	n/a	189461	648223	405892	42122
SCAPULA	Acu B-2	0.1978	929246	362563	n/a	503424	n/a	750788	169675
SCAPULA	Acu B-3	0.2078	284271	312654	n/a	91792	80099	434066	2391
SCAPULA	Acu B-4	0.2019	823891	228258	64117	415567	337332	274521	64333
SCAPULA	Acu B-5	0.2076	1203727	166809	175437	374032	673663	275812	36499
BLOOD	Acu B-1	0.25	128071	113298	47431	42803	33575	92050	352
BLOOD	Acu B-2	0.25	38300	53651	15616	42525	16666	79323	408
BLOOD	Acu B-3	0.25	165734	104535	24597	47844	22031	83405	345
BLOOD	Acu B-4	0.25	254293	145460	90915	46948	56647	132452	716
BLOOD	Acu B-5	0.25	128824	83354	21920	25198	17778	61303	297

Appendix III:

Mass Normalized Drug Responses

Table A3.1 Mass Normalized Response Ratios (RR/m) and Metabolite-Parent Ratios (DXT/DXM)

Sample:	A DXM RR/m:	B DXM RR/m:	A 150 DXT RR/m:	B 150 DXT RR/m:	A DXT/DXM:	B DXT/DXM:
VERT 1	23.141	13.638	4.930	3.749	0.213	0.275
VERT 2	33.980	19.244	6.461	5.349	0.190	0.278
VERT 3	8.370	18.785	1.816	3.941	0.217	0.210
VERT 4	14.617	11.755	0.891	4.063	0.061	0.346
VERT 5	33.007	11.783	11.238	n/a	0.340	n/a
FEMUR 1	11.521	33.201	1.640	3.133	0.142	0.094
FEMUR 2	13.146	17.882	1.417	2.810	0.108	0.157
FEMUR 3	7.548	12.803	1.691	1.060	0.224	0.083
FEMUR 4	14.812	21.192	1.074	2.627	0.073	0.124
FEMUR 5	15.563	39.936	2.120	11.157	0.136	0.279
RIB 1	26.308	22.141	4.061	5.485	0.154	0.248
RIB 2	41.277	22.550	7.641	9.693	0.185	0.430
RIB 3	3.667	10.805	0.722	1.885	0.197	0.174
RIB 4	18.294	12.902	0.457	3.154	0.025	0.244
RIB 5	28.832	44.592	8.914	15.754	0.309	0.353
TIBIA 1	32.744	27.816	3.550	2.085	0.108	0.075
TIBIA 2	18.243	32.817	2.531	3.053	0.139	0.093
TIBIA 3	15.897	14.193	2.023	0.896	0.127	0.063
TIBIA 4	30.082	16.438	1.041	2.098	0.035	0.128
TIBIA 5	22.579	13.750	2.373	2.071	0.105	0.151
PELVIS 1	22.585	7.782	4.905	8.831	0.217	1.135
PELVIS 2	13.310	6.387	1.974	5.011	0.148	0.785
PELVIS 3	7.778	14.021	1.953	2.216	0.251	0.158
PELVIS 4	6.160	10.114	0.400	8.067	0.065	0.798
PELVIS 5	32.043	41.205	8.247	4.205	0.257	0.102
SKULL 1	24.051	21.118	8.727	3.600	0.363	0.170
SKULL 2	24.198	26.262	11.194	11.937	0.463	0.455
SKULL 3	1.972	5.237	0.387	2.179	0.196	0.416
SKULL 4	6.837	20.514	0.265	2.475	0.039	0.121
SKULL 5	33.474	22.309	13.665	6.621	0.408	0.297
SCAPULA 1	40.836	7.088	9.834	8.331	0.241	1.175
SCAPULA 2	40.424	12.957	8.459	n/a	0.209	n/a
SCAPULA 3	1.871	4.375	0.729	0.896	0.390	0.205
SCAPULA 4	24.321	17.878	3.817	6.086	0.157	0.340
SCAPULA 5	41.616	34.760	5.094	11.765	0.122	0.338
BLOOD 1	3.888	4.522	0.626	1.459	0.161	0.323
BLOOD 2	4.070	2.855	1.071	0.840	0.263	0.294
BLOOD 3	6.570	6.342	2.091	1.057	0.318	0.167
BLOOD 4		6.993		1.711		0.245
BLOOD 5	7.644	6.182	1.473	1.160	0.193	0.188

Appendix IV:

Validation Standard Curves

Table A4.1 Standard Curve 1 Drug Responses

Concentration (ng/ml)	DXT	d3-DXT	DXM	d3-DXM	dmDXT	DXT 150	d3-DXT 153
0	0	0	394	0	0	5687	1111
0	877	135	1687	0	0	4090	1611
0	388	140	1473	81	0	4495	1803
10	4427	121671	2244	97637	0	23389	244684
10	7728	171565	4680	126162	0	31677	353911
10	44438	169235	31861	123704	0	75033	337419
25	19604	174316	8910	108813	0	41216	280976
25	18867	152076	7101	102844	0	47686	270563
25	24917	152573	14613	101628	0	38959	254931
50	46511	164233	23963	102360	0	75679	260418
50	51969	194090	24548	129328	0	70687	266819
50	30863	113679	14840	95637	0	63071	214889
100	88658	136700	46823	109248	0	135488	297753
100	94170	159086	43977	106175	0	152676	268988
100	101168	180809	46615	117791	0	159658	319484
250	174719	113975	78542	82968	0	291453	240287
250	223201	140430	90565	93734	0	281794	248972
250	234216	166436	130816	110495	0	260032	271478
500	451835	153125	210091	98773	219	626177	321177
500	399882	145206	215725	104349	303	662158	299613
500	373497	111409	208405	100168	205	534736	253112
1000	829825	156422	455084	113519	1080	1386060	389285
1000	780260	163519	435695	117842	10251	1319385	285520
1000	817504	159400	506047	123442	14794	1342692	389938
2000	1602285	192562	1376784	167206	31855	2108231	458873
2000	3026665	295542	2470394	250962	45509	2733563	570074
2000	2417366	254196	2416984	220418	50562	2541760	535887
Accuracy x1	371284	175937	200992	156196	2367	642230	396684
Accuracy x2	278692	159792	173199	169379	6015	474079	303067
Accuracy x3	280347	144099	181945	155517	3139	527920	308742
Accuracy y1	1174820	223524	841512	184641	14807	1900270	494284
Accuracy y2	766519	142489	560621	121849	23075	1291052	343141
Accuracy y3	1028406	194662	1157229	224932	31094	1423304	413048

Table A4.2 Standard Curve 2 Drug Responses

Concentration (ng/ml)	DXT	d3-DXT	DXM	d3-DXM	dmDXT	DXT 150	d3-DXT 153
0	0	0	0	0	0	8244	899
0	1774	329	2431	92	0	6615	1778
0	968	225	2289	106	0	5267	3073
10	12246	131734	13537	162972	0	34738	267900
10	10304	107071	8405	113281	0	26408	255517
10	9966	145312	8991	132745	0	31427	292137
25	26368	114964	20127	138505	0	57003	277072
25	23369	125508	16305	130527	0	60151	256891
25	23331	139067	19047	173171	0	68584	311966
50	51129	141972	29414	109026	0	123315	324374
50	40514	130279	38278	170136	0	103811	280673
50	18237	92162	21976	128793	0	55193	199040
100	90401	115981	51484	125349	0	187097	283745
100	77653	116740	56887	127487	0	165013	254392
100	83566	111292	48578	117924	0	167349	259589
250	197454	139036	194195	160434	0	423121	292854
250	207147	187564	228270	209423	0	410244	295145
250	230316	186016	257508	235360	0	444686	285659
500	392762	186983	463704	182028	1504	763672	377694
500	468192	190652	478911	223572	4549	1019863	424045
500	414995	172525	479045	227297	7426	721886	324605
1000	677407	170069	760177	176095	9476	856730	298163
1000	1991500	344478	1934879	359235	14279	2431301	704597
1000	952860	204775	1063834	220655	10858	1300169	396997
2000	3542259	358676	2690369	294911	45139	6095702	1138312
2000	3368761	330494	2122312	276730	56013	5683214	948383
2000	3574607	322280	2405499	267962	50891	5792391	904219
Accuracy x1	116637	182333	123902	209312	0	242388	378260
Accuracy x2	113260	242617	136297	251269	0	264976	390579
Accuracy x3	103922	163503	102276	219567	0	210314	307656
Accuracy y1	1209777	227450	1352695	235455	8764	1756022	515378
Accuracy y2	2799497	387554	2153159	361511	19797	3005863	755312
Accuracy y3	3016189	459478	2270787	404953	24650	4663484	1013363

Table A4.3 Standard Curve 3 Drug Responses

Concentration (ng/ml)	DXT	d3-DXT	DXM	d3-DXM	dmDXT	DXT 150	d3-DXT 153
0	1352	0	1456	0	0	4018	774
0	0	0	144	0	0	1960	325
0	497	0	1702	0	0	1661	574
10	4311	87174	5195	64611	0	13286	186898
10	6988	131067	5563	86962	0	16627	223275
10	5727	147143	3947	81670	0	20403	264085
25	15251	131888	8701	88465	0	33459	257979
25	13892	103595	12074	82662	0	28316	205080
25	29804	207089	13712	112892	0	54397	397168
50	20699	75158	17362	69511	0	40320	141403
50	29211	102029	14308	75453	0	57597	230979
50	33270	145055	17481	85770	0	71410	278860
100	116716	185008	69755	141245	0	208634	366115
100	78941	145392	44273	93073	0	131310	269172
100	127150	210470	61208	115537	0	158846	392287
250	252339	186298	88684	68311	0	361940	350662
250	215377	155115	94303	84213	0	364232	324706
250	146685	129851	76485	88185	0	275162	282124
500	432231	190991	148804	71494	11341	589598	323825
500	481960	194952	177429	92562	4301	863055	432416
500	529367	168612	236811	105221	9654	836294	401579
1000	786400	197729	227195	63124	18607	1524491	448451
1000	1101798	245721	283209	80687	39287	1725261	602362
1000	848796	211121	359819	85421	33879	1671713	511183
2000	1858750	250052	397295	56985	85220	2514408	592072
2000	1693812	216401	492005	62400	59660	2196732	505445
2000	2027298	281467	444472	60203	85875	2551419	632008
Accuracy x1	427901	310316	162759	160529	5424	749163	593437
Accuracy x2	212262	159020	134210	107268	8644	389363	312332
Accuracy x3	229064	188448	209572	167509	8641	491606	345108
Accuracy y1	1191353	269335	662509	140624	30717	2227432	616866
Accuracy y2	1324834	283035	403407	76545	41751	2334031	599565
Accuracy y3	968830	202867	446069	86178	35145	1710484	472266

Table A4.4 Standard Curve Mean Relative Responses (RR) and Coefficient of Variance (CV%)

	Concentration (ng/ml)	Mean DXT 150 RR	DXT-150 CV(%)	Mean DXT RR	DXT CV(%)	Mean DXM RR	DXM CV(%)	Mean dmDXT RR	dmDXT CV(%)
Curve 1	0	3.38	44.4	n/a	n/a	n/a	n/a	n/a	n/a
	10	0.09	4.6	0.11	111.8	0.11	124.2	0	n/a
	25	0.16	9.8	0.13	20.0	0.10	40.7	0	n/a
	50	0.28	5.6	0.27	2.9	0.19	20.5	0	n/a
	100	0.51	11.2	0.60	7.5	0.41	4.0	0	n/a
	200	1.10	11.8	1.51	6.2	1.03	12.8	0	n/a
	500	2.09	6.3	3.02	10.1	2.09	1.5	0	19.0
	1000	3.87	16.7	5.07	5.4	3.94	5.4	0.07	78.6
	2000	4.71	2.2	9.36	10.4	9.68	14.2	0.20	12.7
	Accuracy X	1.63	4.5	1.93	9.5	1.16	11.4	0.02	44.9
	Accuracy Y	3.68	5.7	5.31	1.2	4.77	6.9	0.14	40.2
Curve 2	0	4.87	79.3	n/a	n/a	n/a	n/a	n/a	n/a
	10	0.11	12.4	0.09	17.6	0.07	10.3	0	n/a
	25	0.22	6.5	0.19	16.3	0.13	14.0	0	n/a
	50	0.34	16.5	0.34	10.4	0.25	12.8	0	n/a
	100	0.65	1.2	0.73	8.1	0.42	4.8	0	n/a
	200	1.46	5.8	1.25	12.6	1.13	6.0	0	n/a
	500	2.22	8.6	2.32	8.3	2.27	10.8	0.02	59.7
	1000	3.20	9.2	4.81	18.9	4.84	11.0	0.05	15.1
	2000	5.92	8.9	10.39	6.1	8.59	9.3	0.18	14.1
	Accuracy X	0.67	3.5	0.58	17.0	0.53	11.9	0	n/a
	Accuracy Y	4.00	15.0	6.37	15.2	5.77	3.0	0.05	24.1
Curve 3	0	4.71	34.5	n/a	n/a	n/a	n/a	n/a	n/a
	10	0.07	4.2	0.05	15.8	0.06	25.0	0	n/a
	25	0.13	3.4	0.13	10.9	0.12	19.6	0	n/a
	50	0.26	7.2	0.26	11.5	0.21	14.7	0	n/a
	100	0.49	16.9	0.59	7.6	0.50	5.5	0	n/a
	200	1.04	7.1	1.29	10.9	1.10	19.8	0	n/a
	500	1.97	6.8	2.62	17.4	2.08	8.0	0.10	57.0
	1000	3.18	8.8	4.16	6.8	3.77	10.1	0.39	24.5
	2000	4.21	3.7	7.49	4.2	7.41	6.2	1.29	22.7
	Accuracy X	1.31	7.5	1.31	6.5	1.17	11.7	0.06	42.7
	Accuracy Y	3.71	4.3	4.63	3.9	5.05	5.9	0.39	42.0

Figure A4.1 Standard Curves Validation Plots

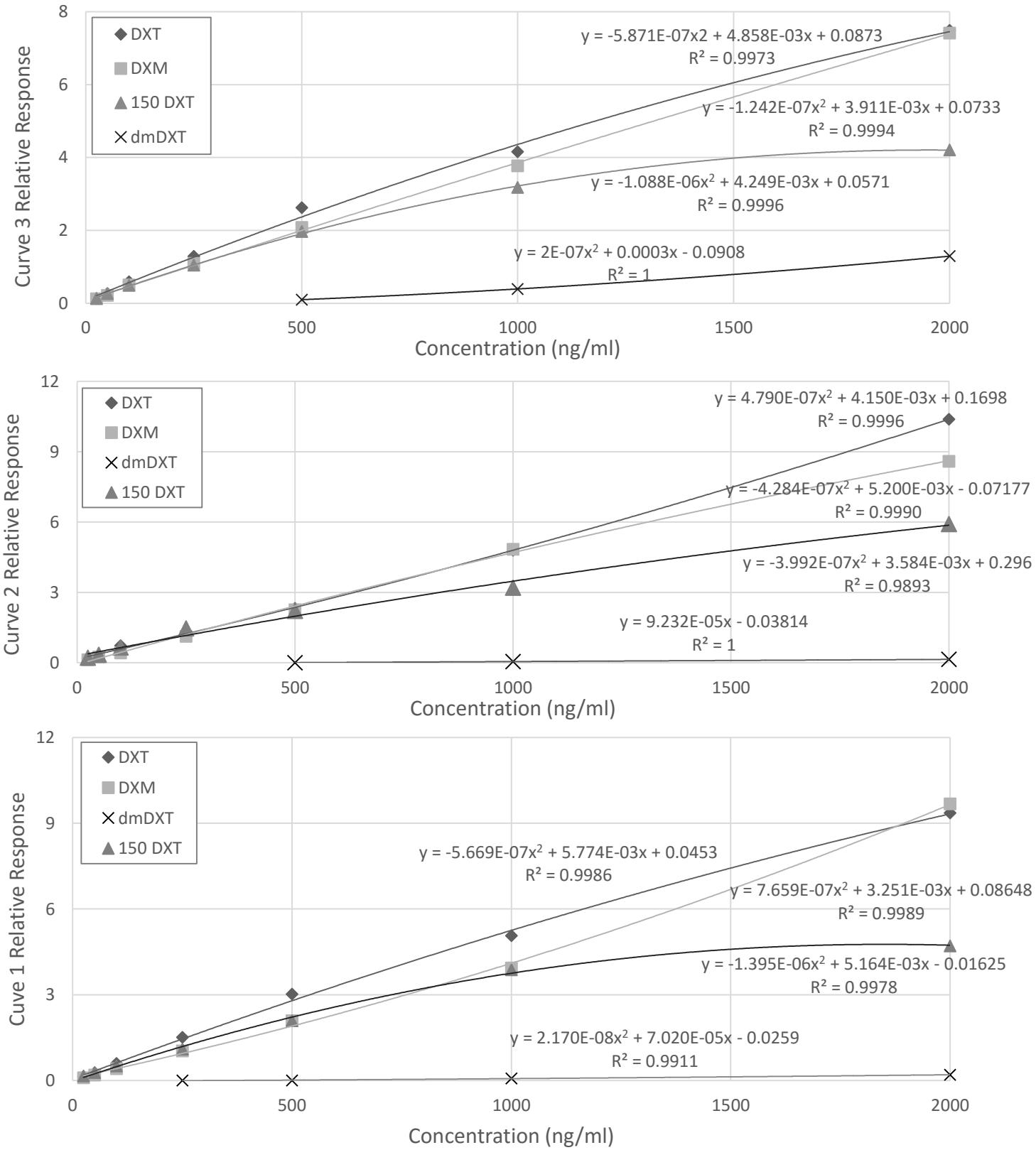

Appendix V:

Relative Humidity Sensor Validation

Figure A5.1 Saturated Binary Salt Solution Relative Humidity Measurements.

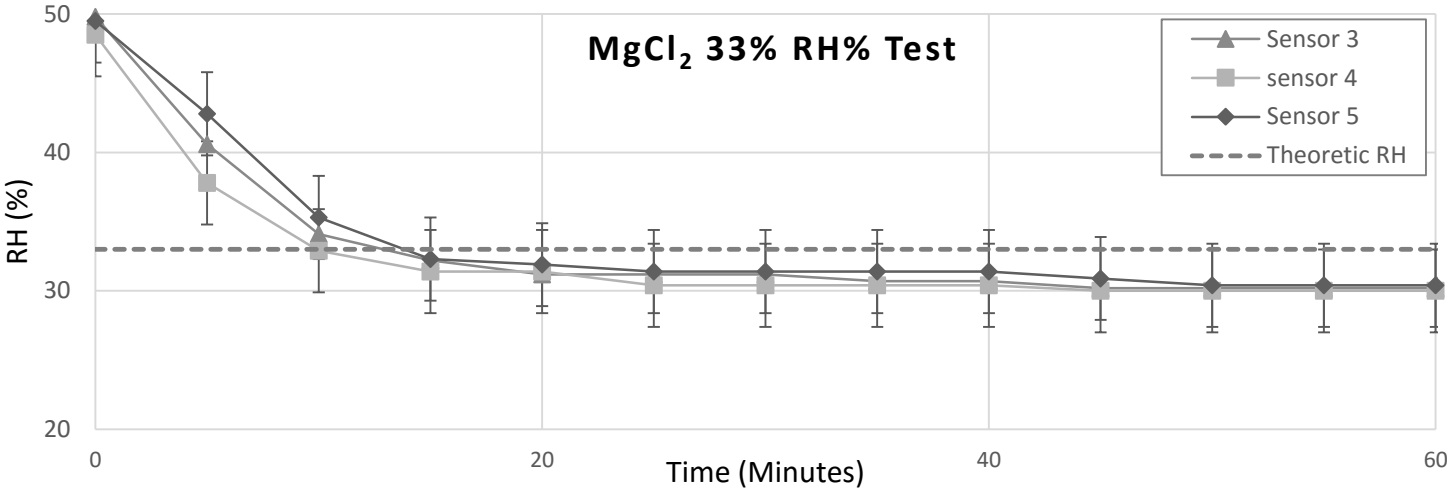

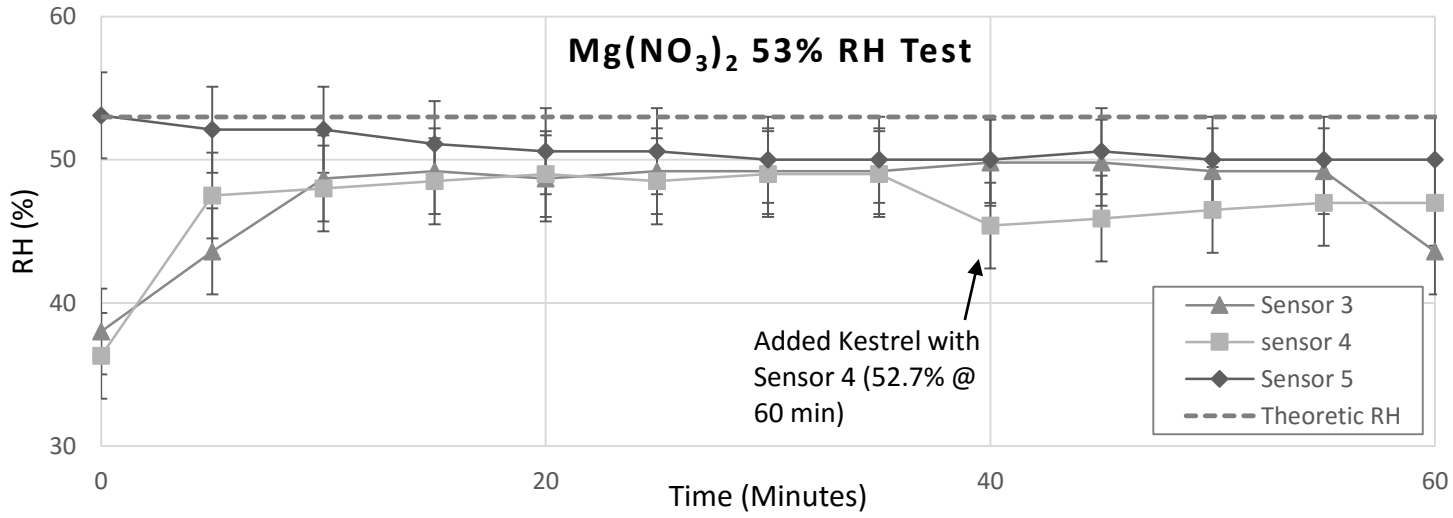

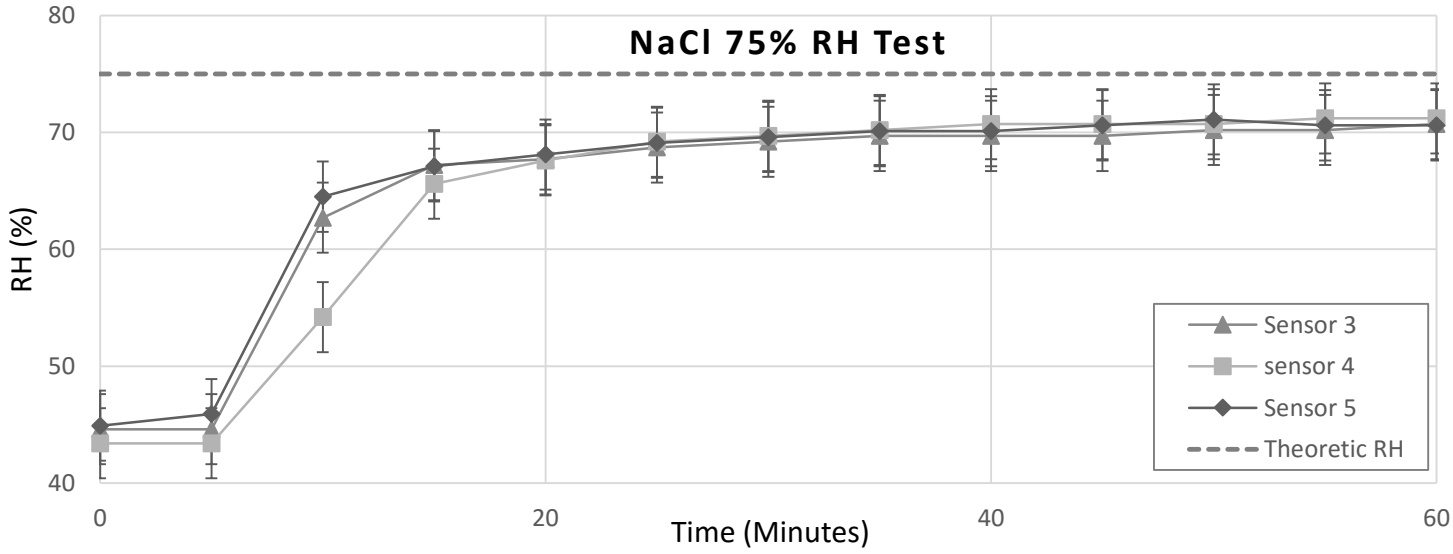

Appendix VI:

Daily Decomposition Site Notes

Table A6.1 Site A Decomposition Site Daily Notes

Date:	Time:	Stage of Decomposition:	Insect Activity:	Notes:
08-Jul		Fresh	Yes	Rats appear fresh. No odor. 2-3 Green bottle flies present.
09-Jul	Morning	Fresh	Yes	Rats are fresh. Dark discolouration on open organs going from pink to brown. A few bottle flies present.
	Evening	Fresh/Bloat	Yes	Rats beginning to exhibit abdominal distention, bloat becoming evident. A mild odor of decomposition noted. Bottle flies present.
10-Jul	Morning	Bloat	Yes	Continued distention of abdomen and bloat. Bottle flies present.
	Noon	Bloat	Yes	As above, odor more evident.
11-Jul	Morning	Bloat/Active	Yes	Rats exhibit transition from bloat to active decay, open abdomens, bodies begin to flatten. Bottle flies and maggots evident, a single Silphidae (carrion beetle) observed approaching carcasses.
12-Jul	Morning	Bloat/Active	Yes	Some open rat carcasses with extensive maggot activity. Bottle flies and maggots most prevalent, decomposition appears to outpace Site B at this time.
13-Jul	Morning	Active	Yes	Notable odor approaching site. Decomposition proceeding well, maggots less evident, perhaps moving into carcasses from open abdomens. Maggots and small bottle flies present.
14-Jul	Morning	Active	Yes	Odour noted approaching site, becoming stronger closer to rats. Little fly activity, a few flies noted at site, maggots active but appearing in less numbers than previous visits. Carcasses exhibit some early flattening and open abdomens. Skin appearing dark brown. Transition from active to dry?
15-Jul	Morning	Active	Yes	Odour noted 10 m from site, closer and less strong than previous two visits. Little fly activity, maggot activity subdued, appears to have less maggots present in rats. Active to dry transition?
16-Jul	Morning	Active	Yes	Decreased odor noted approaching site. Little bug activity, a few bottle flies present. Remains are mostly open, late active (?) with brown skin sloughing some fur, mostly still white.
17-Jul	Morning	Active	Yes	Little insect activity after rain yesterday. Rats wet, beginning to appear dry/late active transition, odor noted when close to site.
18-Jul	Morning	Active	Yes	Similar to previous day.
19-Jul	Morning	Late Active	Yes	Rat remains are open, flattening somewhat; bottle flies and siliphidae beetles present. Mild odor present at site.

Date:	Time:	Stage of Decomposition:	Insect Activity:	Notes:
20-Jul	Morning	Late Active	Yes	A few flies at site, mild odor. Rats are open and flattening, some ribs poking through. Late active/dry transition?
21-Jul				
22-Jul	Morning	Late Active	Yes	Beetles noted at site. Faint odor, brown tissues and skin among bone tissue becoming exposed.
23-Jul				
24-Jul				
25-Jul	Afternoon	Late Active/Dry	No	After hard rain earlier today, no observed insect activity. Rats wetted by precipitation, condition appearing late active/dry; some partial skeletonization, some soft tissues remain besides fragile appearing skin.
26-Jul	Morning	Late Active/Dry	Yes	Some small “cheese skipper” and bottle flies with segmented black insects. Body conditions are as previous day, flattening, with some exposed bone tissue
27-Jul	Morning	Dry	Yes	Cheese skipper and black, segmented insects present. Bodies appearing more flat, bones more exposed; some skin and muscle tissues present. Hot day, 31° today, 34° forecasted tomorrow
28-Jul	Morning	Dry	Yes	Remains are flattening, partially skeletonized remains are present; exposed bone tissues and skin, some other tissue remains present. A few “cheese skipper” flies and segmented bugs present at site.
29-Jul	Morning	Dry	No	Flattening remains appear transitioning more fully into dry. No observed insect activity.
30-Jul				RATS COLLECTED

Table A6.2 Site B Decomposition Site Daily Notes

Date:	Time:	Stage of Decomposition:	Insect Activity:	Notes:
08-Jul		Fresh	Yes	Rats are fresh, no odor. 1 green bottle fly present.
09-Jul	Morning	Fresh/Bloat	Yes	Rats appear generally fresh, exhibit beginning stages of bloat with presentation of some abdominal distension. Many bottle flies present, audible hum of activity noted approaching the site.
	Evening	Bloat	Yes	Bloat is now evident, distension of carcasses greater than at Site A. Decomposition odor is noted.
10-Jul	Morning	Bloat	Yes	Greater degree of abdominal distension than in Site A, bottle fly activity greater than at Site A, as noted above.
	Noon	Bloat	Yes	Swollen, balloon-like abdomens, numerous bottle flies and maggots present in open abdomen of Repeated #1
11-Jul	Morning	Bloat/Active	Yes	Transition from Bloat to Active, some open sides on rat carcases as bodies begin to open and flatten. Strong odor noted at site.
12-Jul	Morning	Blot/Active	Yes	Some open rat carcasses with extensive maggot activity. Bottle flies and maggots most prevalent. Site B decomposition appears to lag Site A at this time, reversing initial appearance with fewer rats transitioning to Active appearance, some remaining in full bloat.
13-Jul	Morning	Active	Yes	Odor is less notable than during past visits. Bottle flies and maggots are present. Rats central within the cage appear to decompose faster, active decay with open, flattening carcasses. Rats on margins appear delayed, stagnant in bloat… drier conditions? Hidden maggots?
14-Jul	Morning	Active	Yes	Little odor at site. Very little fly activity, only a couple of small bottle flies identified. Maggot activity seen, but less than during previous visits. Rats central in cage open carcasses, losing hair, skin appearing brown. Rats on margins appear behind in decomposition.
15-Jul	Morning	Late Active	Yes	Odor subdued, noted only 2-3 m upwind of site. Little fly activity, maggots present but less prevalent than earlier visits. Central rats are open, skin losing fur appearing dark brown and leathery. Rats on margins of cage appear “fresher”, white fur, carcasses appear more competent, lacking open abdomens and flattening of central rats.
16-Jul	Morning	Late Active	n/a	Carcasses beginning to appear to dry; brown, leathery skin with muscle tissue present. Most rats appear late active to dry.
17-Jul	Morning	Late Active/Dry	Yes	A few bottle flies present, 1 large sarcophagidae seen. Rats wet from previous days precipitation, appear late active/dry, skin drawn and leathery, some rats competent while others open, subject to more early insect activity?

Date:	Time:	Stage of Decomposition:	Insect Activity:	Notes:
18-Jul	Morning	Late Active/Dry	Yes	similar to previous day
19-Jul	Morning	Late Active/Dry	Yes	flies audible at site, flesh flies among bottle flies present. Remains appear to be drying, little insect and no active maggots seen.
20-Jul	Morning	Dry	Yes	Little fly activity at site. Carcasses more competent than Site A, maggot activity seems to have ceased w/in last few days; dry skin, loss of fur, leathery remains over partially decomposed and more complete remains.
21-Jul				
22-Jul	Morning	Dry	Yes	Numerous small to medium bottle flies at scene. Odor down wind, more evident than at Site A today. Skin appearing dry, from brown to greyish white in colour. Brown tissue remains on remains which appear more whole than at Site A
23-Jul				
24-Jul				
25-Jul	Afternoon	Dry	No	As site A, wetted by precip; bodies more competent than other site. No observed insect activity.
26-Jul	Morning	Dry	Yes	A few bottle flies and a carrion beetle observed. Bodies remain pseudo-competent, skin losing fur, skin appearing brownish to light grey.
27-Jul	Morning	Dry	Yes	Hot at site. Only 2 small bottle flies observed. Remains appearing mummified almost, competent to partially decomposed. Those exhibiting more advanced decomposition appearing flatter than other, more whole rats.
28-Jul	Morning	Dry	No	No observed insect activity. Papery appearing skin, some "partial skeletonization" with exposed ribs and other bone tissues, generally remains are more competent with near to complete appearing remains.
29-Jul	Morning	Dry	No	No insect activity observed (1 flesh eater fly seen at leaving of site on cage margin) Dry, papery skin appearing whitish brown, condition of remains indicative of less insect activity past bloat(?) than at Site A; remains partially mummified/desiccated?
30-Jul				RATS COLLECTED